The Cambrian Conundrum: Early Divergence and Later Ecological Success in the Early History of Animals

Douglas H. Erwin,[1,2]* Marc Laflamme,[1] Sarah M. Tweedt,[1,3] Erik A. Sperling,[4] Davide Pisani,[5] Kevin J. Peterson[6]*

Diverse bilaterian clades emerged apparently within a few million years during the early Cambrian, and various environmental, developmental, and ecological causes have been proposed to explain this abrupt appearance. A compilation of the patterns of fossil and molecular diversification, comparative developmental data, and information on ecological feeding strategies indicate that the major animal clades diverged many tens of millions of years before their first appearance in the fossil record, demonstrating a macroevolutionary lag between the establishment of their developmental toolkits during the Cryogenian [(850 to 635 million years ago Ma)] and the later ecological success of metazoans during the Ediacaran (635 to 541 Ma) and Cambrian (541 to 488 Ma) periods. We argue that this diversification involved new forms of developmental regulation, as well as innovations in networks of ecological interaction within the context of permissive environmental circumstances.

When Charles Darwin published *The Origin of Species* (*1*), the sudden appearance of animal fossils in the rock record was one of the more troubling facts he was compelled to address. He wrote: "There is another and allied difficulty, which is much graver. I allude to the manner in which numbers of species of the same group, suddenly appear in the lowest known fossiliferous rocks" (p. 306). Darwin argued that the incompleteness of the fossil record gives the illusion of an explosive event, but with the eventual discovery of older and better-preserved rocks, the ancestors of these Cambrian taxa would be found. Studies of Ediacaran and Cambrian fossils continue to expand the morphologic variety of clades, but the appearance of the remains and traces of bilaterian animals in the Cambrian remains abrupt (Fig. 1 and tables S1 and S2).

The fossil record is now supplemented with geochemical proxies of environmental change; a precise temporal framework allowing for correlation of rocks in different areas of the world and evaluation of rates of evolutionary and environmental change; an increasingly rigorous understanding of the phylogenetic relationships between various living and fossil metazoan clades and their dates of origin, based largely on molecular sequences; and growing knowledge of the evolution of developmental processes through comparative studies of living groups. Collectively, these records allow an understanding of the environmental potential, genetic and developmental possibility, and ecological opportunity that existed before and during the Cambrian. Here, we provide an updated synthesis (*2*, *3*) of these records and thereby a macroevolutionary framework for understanding the Cambrian explosion.

Pattern of Animal Diversification

The Cambrian fossil record. The beginning of the Cambrian Period dated at 541 ± 0.13 million years ago (Ma) (*4*) is defined by the first appearance of the trace fossil *Treptichnus pedum* (*5*) in the rock record, representing the first appearance of bilaterian animals with the ability to make complex burrows both horizontally (Fig. 2A) and vertically (*6*). The earliest skeletal fossils occur in the latest Ediacaran, but the first appearance of an array of plates, spines, shells, and other skeletal elements of bilaterian affinity begins during the early Cambrian Fortunian Stage (541 to ~530 Ma) (*7*, *8*) (Fig. 3). Most of these are disarticulated elements larger than 2 mm in size, but some complete scleritomes (Fig. 2B) have been recovered. They reveal a fauna with considerable morphologic and phylogenetic diversity and are collectively referred to as the "small shelly fauna" (SSF). The earliest SSF are largely of lophotrochozoan affinities; only in Cambrian Stage 3 do biomineralized ecdysozoans and deuterostomes appear (*8*). Many of the SSF elements are preserved as phosphate minerals, and their diversity peaks in abundant phosphate deposits (*9*). Although Ediacaran phosphate deposits are common, they lack SSF, suggesting that bilaterian clades acquired skeletons during the Cambrian.

The pattern seen from the skeletal and trace fossil record is mirrored by soft-bodied fossils found in exceptionally preserved Cambrian faunas in China, Greenland, Australia, Canada (Fig. 2C), and elsewhere. Although many new groups have been described over the past decade, the pattern of diversification of both body fossils and trace fossils has remained largely robust: A recompilation (SOM text 1 and table S1) of the first occurrences of all metazoan phyla, classes, and stem-classes (extinct clades) of equivalent morphologic disparity (Fig. 2, D and E) shows their first occurrences in the latest Ediacaran (by 555 Ma), with a dramatic rise over about 25 million years in the first several stages of the Cambrian, and continuing into the Ordovician (Figs. 1 and 3 and table S3). However, from the early Paleozoic onward there is little addition of new phyla and classes (Fig. 1), and those that are added are largely artifactual, as they represent occurrences of taxa with little or no preservation potential (*10*).

The molecular record. Given the clear signal for an explosive appearance of animal fossils in the early Cambrian (Figs. 1 and 3), most paleontologists favor a near literal reading of the fossil record, supporting a rapid (~25-million-year) evolutionary divergence of most animal clades near the base of the Cambrian [e.g., (*11*)]. But teasing apart the mechanisms underlying the Cambrian explosion requires disentangling evolutionary origins from geological first appearances, and the only way to separate the two is to use a molecular clock (*12*). Many earlier problems with molecular divergence estimates have been addressed, allowing confident estimates of the robustness of the known geologic record (*13*, *14*).

Building upon a previously assembled data set (*14*) and a generally accepted phylogenetic tree, we estimated divergence times for >100 species of animals (alignment available as database S1), encompassing all major metazoan clades (Fig. 1, SOM text 2, table S4, figs. S1 to S4, and database S2). Although much of the topology is well accepted, including the tripartite division of bilaterians into lophotrochozoans, ecdysozoans, and deuterostomes and the paraphyletic nature of "diploblasts" with respect to triploblasts (*15*–*17*), the paraphyletic nature of sponges is more controversial (*15*, *17*). However, the estimated divergence times (SOM text and figs. S5 to S10) do not depend on this presumption; they are also robust to the choice of the root prior, the molecular clock model, subsampling of the calibration points, and relaxation of the bounds of the calibration point intervals themselves (table S4). Although acoelomorphs have figured prominently in discussions about the reconstruction of ancestral bilaterians (*18*, *19*), they are not included in

[1]Department of Paleobiology, MRC-121, National Museum of Natural History, Post Office Box 37012, Washington, DC 20013–7012, USA. [2]Santa Fe Institute, 1399 Hyde Park Road, Santa Fe, NM 87501, USA. [3]Behavior, Ecology, Evolution and Systematics, University of Maryland, College Park, MD 20742, USA. [4]Department of Earth and Planetary Sciences, Harvard University, Cambridge, MA 02138, USA. [5]Department of Biology, The National University of Ireland, Maynooth, Kildare, Ireland. [6]Department of Biology, Dartmouth College, Hanover, NH 03755, USA.

*To whom correspondence should be addressed. E-mail: erwind@si.edu (D.H.E); kevin.j.peterson@dartmouth.edu (K.J.P.)

the analysis owing to their incomplete gene sampling and very long branches; moreover, a recent analysis (*20*) indicates that they may be derived deuterostomes, and thus their only contribution to this analysis would be to demonstrate the extent of character loss among some bilaterian clades (see below).

These molecular estimates suggest that the origin and earliest diversification of animals occurred during the Cryogenian Period. We estimate that the last common ancestor of all living animals arose nearly 800 Ma and that the stem lineages leading to most extant phyla had evolved by the end of the Ediacaran (541 Ma). Most phylum-level crown group divergences occurred coevally between the end of the Ediacaran and the end of the Cambrian (Figs. 1 and 3, large colored circles). This is the case both for taxa with robust fossil records (e.g., echinoderms, molluscs, arthropods) and those with sparse fossil records (e.g., nemerteans, nematodes). For

Fig. 1. The origin and diversification of animals as inferred from the geologic and genetic fossil records. The dramatic rise in the number of animal fossils (see scale on left) in the Cambrian relative to the Ediacaran conveys the impact of the Cambrian explosion of animal life. Little high-level morphological innovation occurred during the subsequent 500 million years in that much of animal disparity, as measured by the Linnean taxonomic ranking, was achieved early in the radiation. Overlying the geologic record is the pattern of animal origination as inferred from the molecular clock. Seven different housekeeping genes from 118 taxa were used to generate this chronogram (see SOM 2 for methodological details and database S1). Twenty-four calibrations (open circles) were used and treated as soft bounds. Divergence times for key nodes and their 95% highest posterior intervals are reported in database S2. All estimates appear to be robust to numerous experimental manipulations performed to assess whether the results were dependent on the parameters used in the analyses (Materials and Methods, SOM Text 2, and figs. S5 to S10). There is general concordance of bilaterian phylum-level crown groups (colored circles; the color of each circle is the same as the corresponding taxonomic bar and label on the far right), with the first appearance of most animal groups at the Ediacaran-Cambrian boundary. In contrast, the origins of the demosponge (dark blue) and cnidarian (yellow) as well as the bilaterian (black) and metazoan (gray) crown groups are deep in the Cryogenian. Geological period abbreviations: Є, Cambrian; O, Ordovician; S, Silurian; D, Devonian; C, Carboniferous; P, Permian; Tr, Triassic; J, Jurassic; K, Cretaceous; Pe, Paleogene; N, Neogene. A high-resolution image is available in the SOM.

taxa with robust fossil records, these coeval origination estimates are concordant with their first appearances in the rock record (Fig. 3), supporting both the general accuracy of our relaxed molecular clock analysis and the intuition of many paleontologists who argued that the known fossil record for crown groups of bilaterian phyla is largely robust (*11*).

Our divergence estimates suggest that crown-group demosponges (Figs. 1 and 3, dark blue circle) and crown-group cnidarians (yellow circle) have deep origins, both at nearly 700 Ma. These could represent artifacts, although the former is corroborated by Cryogenian-age fossil molecules (biomarkers) of demosponges (*21*) and possible sponge body fossils reported from the Cryogenian (*22*). The deep divergence of the cnidarian crown group is less easily explained, but the degree of molecular divergence among cnidarian classes is roughly equal to the protostome-deuterostome divergence (*23*), which is consistent with our results.

The Neoproterozoic fossil record. The unavoidable conclusion from the molecular record is that precambrian animals are largely stem lineages leading to extant phyla, and that these lineages originated in the Ediacaran (Figs. 1 and 3). Numerous eukaryotic taxa, including the first example of multicellularity with complex development (*24*), are represented in rocks assigned to the later (i.e., <580 Ma) Ediacaran Period. Among these fossils should be organisms that can be unambiguously assigned to the Metazoa and to more inclusive lineages (e.g., Bilateria), but mostly these fossils are enigmatic and lineages with diagnostic bilaterian apomorphies have not been identified.

The Ediacaran-aged Doushantuo Formation of South China has yielded a suite of fossilized, multicellular structures of diverse morphology (Fig. 2F), which have been interpreted by some as the early cleavage states of metazoan embryos (*25*). Although some of these forms have been assigned to bilaterian clades (*26*) or described as metazoan resting stages (*27*), it is likely that few (if any) actually represent crown-group metazoans, especially given the absence of any evidence for gastrulation, a metazoan-specific feature (*28*).

More typical of this age is the Ediacara macrobiota (579 to 541 Ma). Emerging consensus is that these fossils represent multiple independent clades of macroscopic organisms (*29*), to which a new framework for Ediacaran phylogeny and classification, highlighting six clades and three likely clades, is proposed (Materials and Methods, SOM text 3, and tables S5 and S6). These clades emphasize a greater amount of higher-order disparity than previously appreciated for these fossils, in contrast to previous analyses that grouped all Ediacara macrofossils as a single extinct clade (*30*) or phylogenetic schemes that emphasize a metazoan-only ancestry (*31*). The proposed framework allows for a direct comparison with higher-order classification in Cambrian metazoans. Three distinct biostratigraphic zones have been recognized (*32*). The Avalon assemblage (579 to ~560 Ma) is largely found in Newfoundland and England. This fauna is dominated by the Rangeomorpha (*33*), a clade (SOM text 3) of modular organisms built from repetitively branched ("fractal") units (Fig. 2G), and it also includes potential macroscopic sponges (*34*). The White Sea assemblage (~560 to ~550 Ma) is widespread and faunally diverse (Fig. 2H) with more than three times the genera of the Avalon assemblage (SOM text 3), marking an expansion in ecospace occupation (*35*) and behavioral complexity as reflected by diverse trace fossils. The youngest assemblage, the Nama (~550 to 541 Ma), is dominated by the Erniettomorpha (Fig. 2I and table S6) and includes evidence of predation in the form of boreholes in the oldest undisputed macroscopic biomineralizing organisms (*36*). Collectively, these three faunas show that assemblages expanded and diversified through the Ediacaran. However, Ediacara macrofossils are not known from the Phanerozoic and evidently went extinct by the Cambrian (*8*, *37*, *38*).

Aside from putative sponges (*34*), of the nine likely clades of Ediacaran organisms that we recognize (table S6), only two can confidently be assigned to the crown Metazoa. The Kimberellomorpha (Fig. 2H1) are centimeter-sized bilaterally symmetrical fossils with a crenulated margin interpreted as a frill surrounding a muscular foot, and a proboscis (*39*, *40*). These bilaterians, and possible molluscs, are commonly associated with radiating trace fossils that may represent feeding on microbial mats (Fig. 2H2). The Dickinsoniomorpha also may have had metazoan affinities. These superficially segmented animals are associated with distinct feeding traces and are possibly stem placozoans or stem eumetazoans (*24*, *41*).

Definitive evidence for the presence of bilaterian animals in the Ediacaran comes from surficial trace fossils. Putative trace fossils have been reported from 565 Ma (*42*), but otherwise most are found in rocks <560 Ma (*6*, *43*). Trace fossils increase in diversity and complexity toward the Cambrian, when the oldest vertical burrows reveal the presence of a hydrostatically resistant coelom in an organism larger than ~1 cm in diameter. This would seem to provide a strong constraint on the evolution of larger bilaterians (*11*, *44*), but the molecular clock ages suggest that coelomic bilaterians (e.g., ambulacrarian

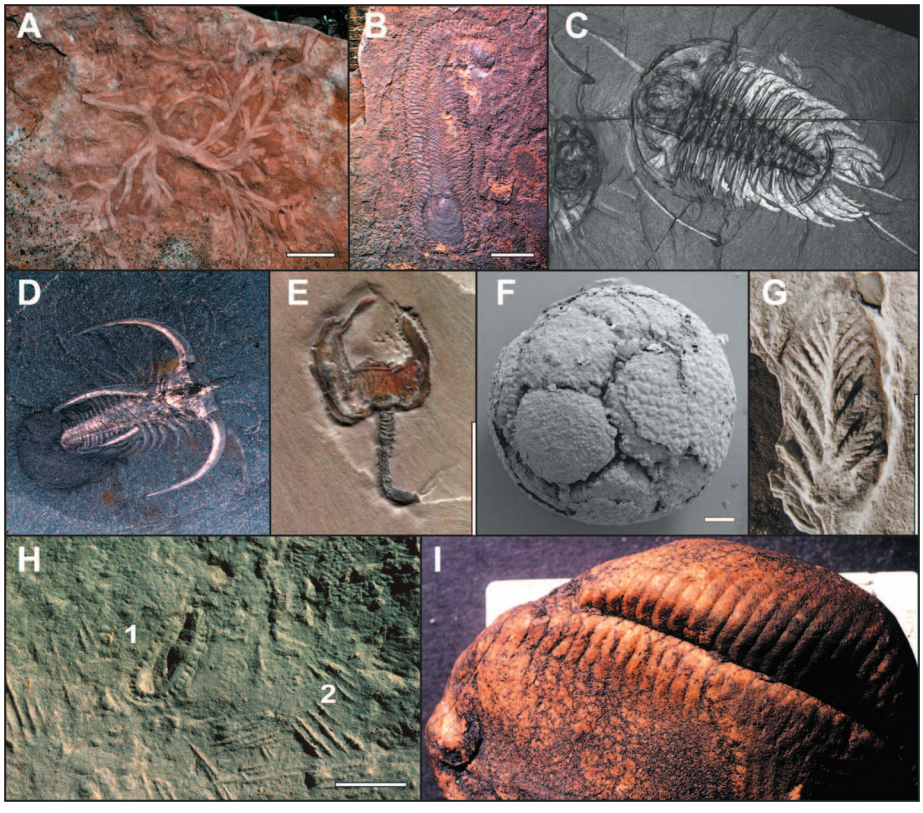

Fig. 2. Fossil diversity during the Ediacaran and Cambrian. (**A**) Early Cambrian complex burrow. (**B**) Scleritome of the small shelly fossil *Halkieria*. (**C**) Mid-Cambrian Burgess Shale trilobite *Olenoides*. (**D**) Stem-group arthropod *Marrella* from the Burgess Shale. (**E**) The stem-group echinoderm *Cothurnocystis* from the mid-Cambrian of Utah. (**F**) Late-stage Doushantuo assemblage of cells (*Tianzhushania*). (**G**) *Avalofractus*, an Ediacaran Rangeomorpha with repetitive branching modularity. (**H**) *Kimberella* (1) with associated *Radulichnus* (2) rasping traces. (**I**) *Pteridinium*, an Ediacaran Erniettomorpha with hollow tubular modular units. Scale bars: (A) 100 μm; (B to I) 1 cm. [Photos: (A), (C), (D), (H), and (I), copyright Smithsonian Institution; (B) provided by J. Vinther; (F) provided by S. Xiao]

deuterostomes) evolved at least 25 million years earlier (Figs. 1 and 3).

In sum, geologic evidence and molecular clock estimates suggest that early animals, notably crown-group demosponges and cnidarians, originated during the Cryogenian. Although bilaterian clades diversified in the Ediacaran, many phylum-level crown groups were not present, appearing first in the Cambrian.

Environmental Potential

Very large geochemical changes have been documented through the Cryogenian and Ediacaran (*45*–*47*), which have been interpreted as indicating substantial changes in redox. Changes in molybdenum abundance in black shales (*48*), the iron chemistry of deep-water sediments (*49*), and potentially other proxies (*46*) have been interpreted as a global signal of increased oxygenation during the Ediacaran. The extent to which these signals are truly global, as well as the magnitude of oxidation, remains uncertain. Animals require oxygen to fuel their metabolism, and these geochemical proxies and their interpretation as markers of redox conditions have been invoked to explain the lag between the origin of animals and the Cambrian radiation itself (*2*). In this view, low oxygen in the oceans and diffusive oxygen transport constrained animals to small size, and only with an increase in oxygen levels could organisms evolve larger, three-dimensional body sizes (*24*, *50*), greatly facilitating their eventual paleontological detection. Thus, although a permissive environment does not explain innovations in metazoan architecture, it might facilitate the appearance of large and ecologically diverse animals in the fossil record.

Genetic and Developmental Possibility

Two findings from comparative genomics and studies of developmental patterning have dramatically changed our understanding of the early evolution of animals. First, whole-genome sequencing of dozens of metazoans has demonstrated that any animal requires only about 20,000 protein-coding genes for the production of its essential morphologic architecture (*51*). Second, much of this protein-coding repertoire—especially the developmental toolkit—is conserved throughout all metazoans and is even found today among single-celled opisthokonts (*24*, *52*–*54*). The distribution of these genes in extant organisms (SOM text 3) implies that this toolkit evolved in a two-step pattern (Fig. 4, left): an initial diversification occurring at the base of the Metazoa before the split between sponges and eumetazoans deep in the Cryogenian (and possibly earlier), followed by a pronounced expansion at least in some families at the base of the Eumetazoa during the late Cryogenian (database S3). Thus, the last common ancestor of metazoans, and especially eumetazoans, was a genetically complex animal possessing all of the families of protein-coding genes used during development, save for the potential absence of *Hox* complex genes (*55*) needed to build the plethora of morphological structures found throughout the crown group.

Consequently, the morphological simplicity of basal animals, and the great differences in morphology between sponges and arthropods or vertebrates, cannot be due to the absence of these protein-coding gene families but instead must involve differences in the temporal and spatial deployment of these genes and their regulation. By extension, this includes the construction of developmental gene regulatory networks (dGRNs) specific to particular characters (for example, the gut, heart, or appendages). At the core of these networks are extremely conserved, highly refractory and recursively wired suites of genes that are crucial for the specification of many of the characteristic morphologies of major clades (*56*, *57*), and ultimately defining the "developmental morphospace" (*57*)

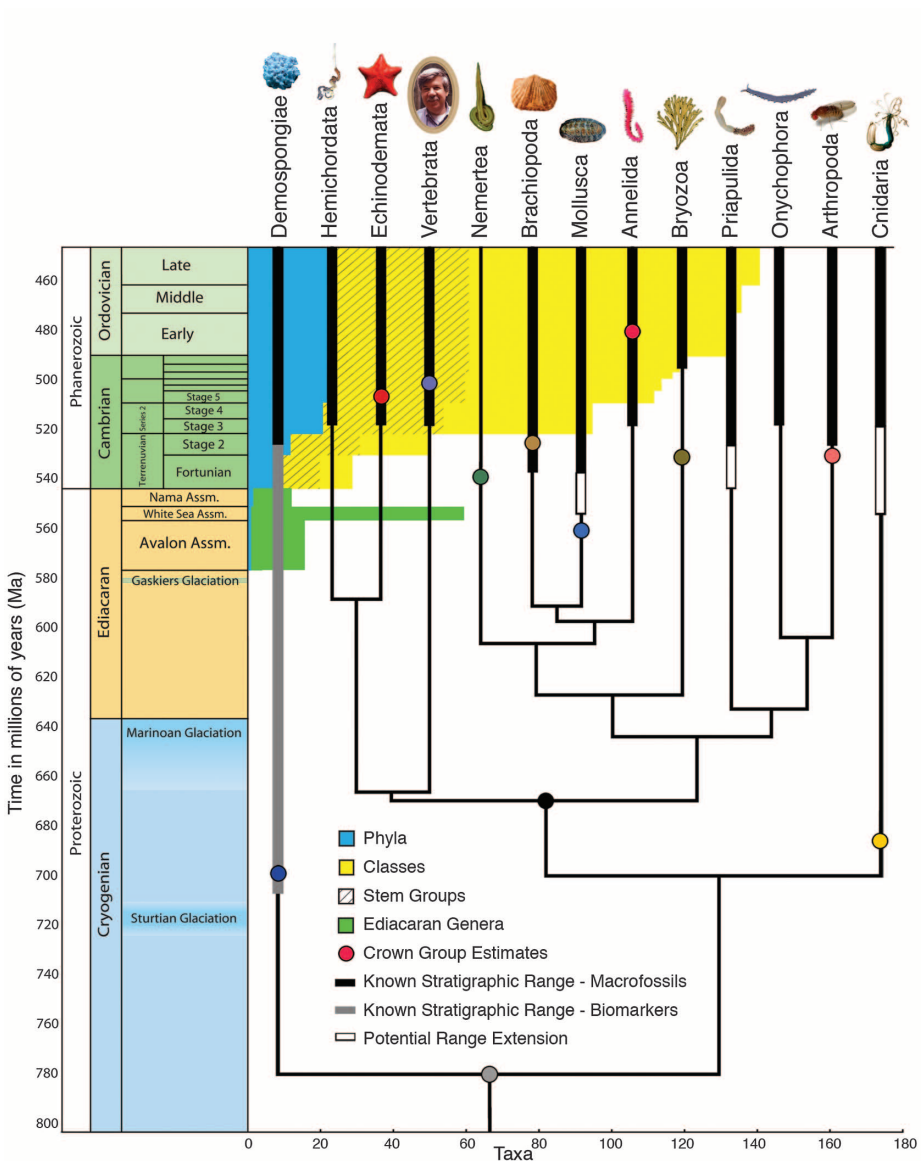

Fig. 3. Detailed stage-level depiction of the animal fossil record as compared to the molecular divergence estimates for 13 different animal lineages. Shown in yellow and blue is the known fossil record of animals at the class and phylum levels, respectively (hatching indicates "stem" lineages, i.e., lineages that belong to a specific phylum but not to any of its living classes); shown in green is the generic record of macroscopic Ediacara fossils (see scale at bottom). Shown in thick black lines are the known fossil records of each of these 13 lineages through the Cryogenian-Ordovician (table S1); most lineages make their first appearance in the Cambrian, consistent with the known fossil record of all animals (yellow and blue). Further, the extent of these stratigraphic ranges closely mirrors the molecular estimates for the age of each of the respective crown groups (colored circles) (see also Fig. 1), highlighting the general accuracy of the molecular clock. Only cnidarians have an unexpectedly deep crown-group origination as estimated by the molecular clock, as the deep demosponge divergence is apparent from taxon-specific biomarkers (gray bar) (*21*).

accessible to a clade. Such networks are likely to have evolved via intercalary evolution in which developmental genes providing spatial, temporal, and homeostatic control were inserted into preexisting simpler dGRN subcircuits (*58*). One example of genetic intercalation into these dGRNs is the continual evolutionary addition of microRNAs (miRNAs). miRNAs encode ~22-nucleotide noncoding regulatory RNAs that affect the translation of target mRNAs, ultimately contributing to the maintenance of cellular homeostasis and cellular identity (*59*) and to the robustness of developmental programs (*60*). Unlike the mRNA toolkit, which was largely established before the evolution of bilaterians (Fig. 4, left), miRNAs (database S4) seem to have been continuously added to eumetazoan genomes through time with very little secondary loss in most taxa (Fig. 4, right) (*60*). When loss did occur, it seems to have been associated with morphological simplification (*20*). For example, each of the extant animals put forth as putative biological models for late precambrian animals, including lophotrochozoan flatworms, acoel flatworms, and *Xenoturbella* (*61*), are characterized by extensive secondary loss of their miRNA complements as compared to more typical invertebrates like ambulacrarian deuterostomes, crustacean arthropods, and polychaete annelids (*60*). In contrast, large expansions in the number of miRNA families correlate to increases in the number of cell types and morphological complexity of animals, as seen, for example, at the base of the bilaterians and at the base of the vertebrates (*60*) (Fig. 4, right).

Whereas there is little difference in the mRNA toolkit between humans and sea anemones (Fig. 4, left), there is a dramatic difference in the miRNA toolkit between these two taxa (Fig. 4, right). The increasing morphologic complexity and developmental stability of bilaterian lineages then likely reflects, at least in part, an increase in the diversity and number of dGRN subcircuits, including the continued and hierarchical incorporation of miRNAs into these networks in a lineage-specific manner (*60*). Other potentially noteworthy aspects of regulatory control that may be important in bilaterian diversification are other forms of RNA regulation, alternative splicing of transcripts (*62*), and combinatorial control of enhancers, but we lack sufficient comparative data to evaluate their role in the diversification of bilaterian animals. Because the signaling pathways and transcription factors important for bilaterian development first appeared among basal metazoan clades that originated in the Cryogenian, the advent of elements of the metazoan developmental toolkit was a necessary but not sufficient component of the Cambrian explosion. A subtle but critical change from the views of a decade ago is that the primary developmental contribution to the origin of bilaterians lay with the construction and elaboration of patterns of developmental control (*56*, *57*), not additions to the mRNA developmental toolkit. The temporal lag between the initial construction of these networks and the eventual appearance of bilaterian fossils suggests that the solution to the dilemma of the Cambrian explosion lies not solely with this genomic and developmental potential, but instead must also be found in the ecology of the Cambrian radiation itself.

Ecological Opportunities

Evolutionary radiations are often described as the invasion of "empty" ecological space, but the transition from the Ediacaran to the Cambrian involved far-reaching changes in benthic and neritic ecosystems and the de novo construction of complex metazoan ecological networks (*63*, *64*). Standard models of adaptive radiation (*65*) involve diversification from a single clade and cannot explain the polyphyletic nature, morphological and ecological breadth, or the extended duration of this event. Rather, we identify a suite of processes that facilitated the construction of biodiversity through positive feedback: ecosystem engineering of the environment, particularly by Cryogenian-Ediacaran sponges and later by burrowing bilaterians, and the formation of new ecological linkages including the evolution of zooplankton, which connected pelagic and benthic systems (*64*), and the advent of metazoan predation.

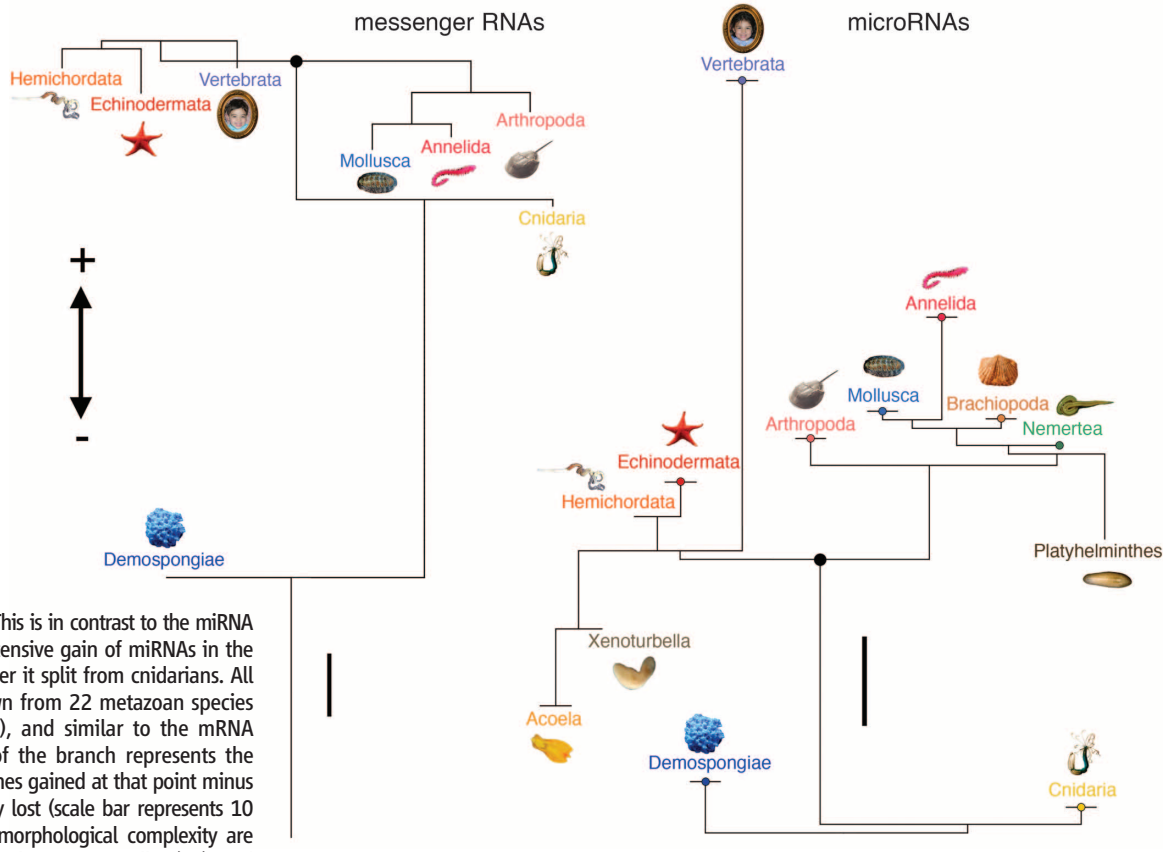

Fig. 4. Acquisition and secondary loss of messenger RNAs (mRNAs, **left**) and microRNAs (miRNAs, **right**) in selected taxa. One hundred and thirty-one representative transcription factors and signaling ligands were coded for eight metazoan taxa (database S3) and mapped onto a widely accepted metazoan topology (*15*, *16*). The length of the branch represents the total number of mRNA genes acquired minus those that were lost (scale bar represents 10 genes total). Much of the developmental mRNA toolkit was acquired before the last common ancestor of cnidarians and bilaterians. This is in contrast to the miRNA repertoire that displays extensive gain of miRNAs in the bilaterian stem lineage after it split from cnidarians. All 139 miRNA families known from 22 metazoan species were coded (database S4), and similar to the mRNA figure (left), the length of the branch represents the total number of miRNA genes gained at that point minus those that were secondarily lost (scale bar represents 10 genes total). Increases to morphological complexity are correlated with increases to the miRNA toolkit (*60*), and secondary simplifications in morphology correlate with a relatively high level of secondary miRNA loss (*20*).

Ecosystem engineering occurs when the activities of one or more species modify the physical and/or chemical environment(s), affecting the flow of energy, nutrients, and other resources through a network of species (*66*, *67*). This often has important ecological and evolutionary consequences (*68*). The engineering activities with the greatest evolutionary implications are those that affect resource availability. For example, sponges remove dissolved organic matter and bacteria from the water column (*34*) and when abundant can transfer large volumes of carbon to the sediment, thus changing the geochemistry of the water column. The advent of vertical burrowing in the early Cambrian enhanced the oxygenation of the sediment and microbial primary productivity, providing food for benthic metazoans (*69*).

Predation was an important component of the growth of these ecological networks. The first appearance of predatory traces, and body fossils of predators, occurs near the Ediacaran-Cambrian transition (*70*). Animals evolved in response to predation pressures by developing novel defensive mechanisms such as biomineralized shells or developing new structures or capabilities that allowed movement into new habitats. The origin of predation can be assessed by mapping feeding modes onto the time-calibrated phylogeny (Fig. 3). Given the similarities between the sponge feeding cell (choanocyte) and choanoflagellates, the metazoan last common ancestor (LCA) was likely a microphagous suspension feeder, irrespective of whether sponges are monophyletic or not. Cnidarians are potential late Cryogenian predators, and the estimated age of their crown group (~687 Ma) is also the minimal estimate for the evolution of the cnidocyte, the stinging cells that enable cnidarians to prey on other animals. However, the ~150-million-year gap between the appearance of the cnidocyte and the estimated origin of pancrustaceans (Fig. 1), their primary modern prey, raises questions about the nature of early Cryogenian food webs. Cnidarians may have preyed on benthic micrometazoans, and the correlative innovation of true endomesoderm in bilaterians and the cnidocyte in their immediate sister group, the cnidarians, may suggest a coevolutionary response between these two lineages at this relatively early stage in animal evolution.

Feeding modes along the eumetazoan stem are difficult to polarize (*41*), but these organisms are unlikely to have been predators, especially upon other animals, as bona fide predation does not appear to be primitive for any of the three great clades of bilaterians. The deuterostome LCA almost certainly filter-fed using gill slits, as the Chordata, Echinodermata, and Hemichordata each have filter-feeding representatives in their basal branches. Within Ecdysozoa, current phylogenetic analyses suggest that the predominantly detritivorous cycloneuralian worms form a paraphyletic assemblage at the base of the clade (*71*, *72*), so detritus feeding was likely primitive for this group. The diversity of feeding strategies among the Lophotrochozoa make it difficult to reconstruct the basal strategy, but because carnivorous molluscs and annelids are derived within each respective phylum, their LCA was unlikely to have been carnivorous either. The only protostome phyla whose crown-group ancestor was likely carnivorous are the chaetognaths and the nemerteans, and both the fossil record (*73*) and molecular clock results (Fig. 3) suggest that their ancestor appeared in the late Ediacaran to early Cambrian. Thus, we see no evidence for a carnivorous lifestyle during the Cryogenian to mid-Ediacaran for any bilaterian lineage. Given that ecology and the physical environment are closely linked, it may be that the origin of animal carnivory, a metabolically expensive feeding strategy, was driven by increased oxygenation.

Outlook

Our emerging understanding of early animal history shows that evolution is not always relentlessly opportunistic, taking advantage of evolutionary novelties as soon as they arise. Rather, the Cambrian explosion involved the construction of historically unique, and uniquely complex, feedbacks between biological potential and eco-environmental context, including the oxygenation of the ocean's waters. These feedbacks relied on networks of gene regulatory interaction that were established long before the construction of metazoan ecosystems. Because of this long lag between the origin and eventual ecological dominance of clades, data on taxonomic occurrences alone are insufficient to understand evolutionary dynamics and must be accompanied by data on abundances and ecological impact, in addition to accurate and precise estimates of both evolutionary origin and geological first appearances. Macroevolutionary lags such as that which preceded the Cambrian explosion were not unique to animals, as similar dynamics seem to underlie plant evolution as well (*24*). Understanding both early animal and plant evolution requires an understanding of the processes that generate biodiversity and the expansion of ecological networks through deep time.

References and Notes

1. C. Darwin, *On the Origin of Species by means of Natural Selection* (John Murray, London, 1859).
2. A. H. Knoll, S. B. Carroll, *Science* **284**, 2129 (1999).
3. J. W. Valentine, D. Jablonski, D. H. Erwin, *Development* **126**, 851 (1999).
4. S. A. Bowring *et al.*, *Am. J. Sci.* **307**, 1097 (2007).
5. E. Landing, *Geology* **22**, 179 (1994).
6. S. Jensen, M. L. Droser, J. G. Gehling, in *Neoproterozoic Geobiology and Paleobiology,* S. Xiao, A. J. Kaufman, Eds. (Springer, Berlin, 2006), pp. 115–157.
7. A. C. Maloof *et al.*, *Geol. Soc. Am. Bull.* **122**, 1731 (2010).
8. A. Kouchinsky *et al.*, *Geol. Mag.* 1 (2011).
9. S. M. Porter, *Palaios* **19**, 178 (2004).
10. D. H. Erwin, J. W. Valentine, J. J. Sepkoski Jr., *Evolution* **41**, 1177 (1987).
11. G. E. Budd, S. Jensen, *Biol. Rev. Camb. Philos. Soc.* **75**, 253 (2000).
12. B. Runnegar, *Lethaia* **15**, 199 (1982).
13. K. J. Peterson *et al.*, *Proc. Natl. Acad. Sci. U.S.A.* **101**, 6536 (2004).
14. K. J. Peterson, J. A. Cotton, J. G. Gehling, D. Pisani, *Philos. Trans. R. Soc. Lond. B Biol. Sci.* **363**, 1435 (2008).
15. H. Philippe *et al.*, *Curr. Biol.* **19**, 706 (2009).
16. K. M. Halanych, *Annu. Rev. Ecol. Syst.* **35**, 229 (2004).
17. E. A. Sperling, K. J. Peterson, D. Pisani, *Mol. Biol. Evol.* **26**, 2261 (2009).
18. J. Baguñà, M. Riutort, *Bioessays* **26**, 1046 (2004).
19. A. Hejnol, M. Q. Martindale, *Philos. Trans. R. Soc. Lond. B Biol. Sci.* **363**, 1493 (2008).
20. H. Philippe *et al.*, *Nature* **470**, 255 (2011).
21. G. D. Love *et al.*, *Nature* **457**, 718 (2009).
22. A. C. Maloof *et al.*, *Nat. Geosci.* **3**, 653 (2010).
23. N. H. Putnam *et al.*, *Science* **317**, 86 (2007).
24. A. H. Knoll, *Annu. Rev. Earth Planet. Sci.* **39**, 217 (2011).
25. S. H. Xiao, Y. Zhang, A. H. Knoll, *Nature* **391**, 553 (1998).
26. J. Y. Chen *et al.*, *Science* **305**, 218 (2004).
27. P. A. Cohen, A. H. Knoll, R. B. Kodner, *Proc. Natl. Acad. Sci. U.S.A.* **106**, 6519 (2009).
28. J. W. Hagadorn *et al.*, *Science* **314**, 291 (2006).
29. S. H. Xiao, M. Laflamme, *Trends Ecol. Evol.* **24**, 31 (2009).
30. A. Seilacher, *Lethaia* **22**, 229 (1989).
31. J. G. Gehling, *Mem. Geol. Soc. India* **20**, 181 (1991).
32. B. M. Waggoner, *Integr. Comp. Biol.* **43**, 104 (2003).
33. G. M. Narbonne, *Science* **305**, 1141 (2004).
34. E. A. Sperling, K. J. Peterson, M. Laflamme, *Geobiology* **9**, 24 (2011).
35. A. M. Bush, R. K. Bambach, D. H. Erwin, in *Quantifying the Evolution of Early Life,* M. Laflamme, J. D. Schiffbauer, S. Q. Dornbos, Eds. (Springer Science, 2011), pp. 111–133.
36. S. Bengtson, Y. Zhao, *Science* **257**, 367 (1992).
37. J. E. Amthor *et al.*, *Geology* **31**, 431 (2003).
38. G. M. Narbonne, *Annu. Rev. Earth Planet. Sci.* **33**, 421 (2005).
39. A. Y. Ivantsov, *Paleontol. J.* **43**, 601 (2009).
40. M. A. Fedonkin, A. Simonetta, A. Y. Ivantsov, in *The Rise and Fall of the Ediacaran Biota,* P. Vickers-Rich, P. Komarower, Eds. (Geological Society, London, 2007), pp. 157–179.
41. E. A. Sperling, J. Vinther, *Evol. Dev.* **12**, 201 (2010).
42. A. G. Liu, D. McIlroy, M. D. Brasier, *Geology* **38**, 123 (2010).
43. S. Jensen, M. L. Droser, J. G. Gehling, *Palaeogeogr. Palaeoclimatol. Palaeoecol.* **220**, 19 (2005).
44. J. W. Valentine, D. H. Erwin, in *Development as an Evolutionary Process,* R. A. Raff, Ed. (Liss, New York, 1987).
45. J. P. Grotzinger, D. A. Fike, W. W. Fischer, *Nat. Geosci.* **4**, 285 (2011).
46. G. Shields-Zhou, L. Och, *GSA Today* **21**, 4 (2011).
47. D. A. Fike, J. P. Grotzinger, L. M. Pratt, R. E. Summons, *Nature* **444**, 744 (2006).
48. C. Scott *et al.*, *Nature* **452**, 456 (2008).
49. D. E. Canfield, S. W. Poulton, G. M. Narbonne, *Science* **315**, 92 (2007).
50. B. Runnegar, *Alcheringa* **6**, 223 (1982).
51. D. H. Erwin, *Philos. Trans. R. Soc. Lond. B Biol. Sci.* **364**, 2253 (2009).
52. A. Sebé-Pedrós, A. de Mendoza, B. F. Lang, B. M. Degnan, I. Ruiz-Trillo, *Mol. Biol. Evol.* **28**, 1241 (2011).
53. G. S. Richards, B. M. Degnan, *Cold Spring Harb. Symp. Quant. Biol.* **74**, 81 (2009).
54. M. Srivastava *et al.*, *Nature* **466**, 720 (2010).
55. J. F. Ryan *et al.*, *Genome Biol.* **7**, R64 (2006).
56. E. H. Davidson, D. H. Erwin, *Science* **311**, 796 (2006).
57. E. H. Davidson, D. H. Erwin, *Cold Spring Harb. Symp. Quant. Biol.* **74**, 65 (2009).
58. E. H. Davidson, D. H. Erwin, *J. Exp. Zool. B (Mol. Dev. Evol.)* **314B**, 182 (2010).
59. E. V. Makeyev, T. Maniatis, *Science* **319**, 1789 (2008).
60. K. J. Peterson, M. R. Dietrich, M. A. McPeek, *Bioessays* **31**, 736 (2009).

61. C. R. Marshall, J. W. Valentine, *Evolution* **64**, 1189 (2010).
62. A. Kalsotra, T. A. Cooper, *Nat. Rev. Genet.* **12**, 715 (2011).
63. D. H. Erwin, J. W. Valentine, *The Cambrian Explosion: The Construction of Animal Biodiversity* (Roberts, Greenwood, CO, 2012).
64. N. J. Butterfield, *Paleobiology* **23**, 247 (1997).
65. J. B. Losos, *Am. Nat.* **175**, 623 (2010).
66. C. G. Jones, J. H. Lawton, M. Shachak, *Ecology* **78**, 1946 (1997).
67. J. P. Wright, C. G. Jones, *Bioscience* **56**, 203 (2006).
68. D. H. Erwin, *Trends Ecol. Evol.* **23**, 304 (2008).
69. A. M. Lohrer, S. F. Thrush, M. M. Gibbs, *Nature* **431**, 1092 (2004).
70. S. Bengtson, *Paleontol. Soc. Pap.* **8**, 289 (2002).
71. O. Rota-Stabelli *et al*., *Proc. R. Soc. B* **278**, 298 (2011).
72. L. I. Campbell *et al*., *Proc. Natl. Acad. Sci. U.S.A.* **108**, 15920 (2011).
73. H. Szaniawski, *Acta Palaeontol. Pol.* **47**, 409 (2002).

Acknowledgments: This work was supported by a NASA National Astrobiology Institute grant (D.H.E and K.J.P) supporting M.L., S.M.T., and E.A.S., and a Smithsonian Institution Fellowship (M.L). E.A.S is also supported by an Agouron Geobiology Fellowship. K.J.P. is also supported by the NSF. D.P. is supported by a Science Foundation Ireland Research Frontier Programme grant (08/RFP/EOB1595). All molecular analyses were performed with the computing infrastructures provided by the Irish Center for High End Computing and the National University of Ireland Maynooth High Performance Computing facility. All data used in the paper are included as files in the SOM. We appreciate technical assistance from L. Campbell and comments from P. Donoghue, G. Edgecombe, G. Narbonne, B. Runnegar, two anonymous reviewers, and the Bio 28 Class of Dartmouth College (2011).

Supporting Online Material

www.sciencemag.org/cgi/content/full/334/6059/1091/DC1
Materials and Methods
SOM Text
Figs. S1 to S10
Tables S1 to S6
Databases S1 to S4
References (*74*–*169*)

9 June 2011; accepted 5 October 2011
10.1126/science.1206375

地球上の動物の命（Animal Life on Earth）

化石の記録は、カンブリア紀の初期にあたる約5億4000万年前に動物が非常に多様化したことを明らかにしているが、この出来事のそもそもの起源はダーウィンの時代から謎のままである。最近の化石の発見や向上した年代測定の結果に基づき、Erwin たちは（p.1091）、初期の動物の関連や発生時期の分子的な見積もりを示した。主要な動物のクレードは、カンブリア紀の何千万年も前に分岐したらしく、分化が起きる前の動物の共通祖先が最後に存在したのは約8億年前と思われる。カンブリア紀初期の環境の変動により新たな生態系の出現が可能となった際に、おそらく多様化には新しい形の遺伝子調節が関与していたであろう。（Sk,KU,nk）

【訳注】クレード：共通祖先から進化した生物種

Supporting Online Material for

The Cambrian Conundrum: Early Divergence and Later Ecological Success in the Early History of Animals

Douglas H. Erwin,* Marc Laflamme, Sarah M. Tweedt, Erik A. Sperling, Davide Pisani, Kevin J. Peterson*

*To whom correspondence should be addressed. E-mail: erwind@si.edu (D.H.E); kevin.j.peterson@dartmouth.edu (K.J.P.)

Published 25 November 2011, *Science* **334**, 1091 (2011)
DOI: 10.1126/science.1206375

This PDF file includes:

Other Supporting Online Material for this manuscript includes the following:
(available at www.sciencemag.org/cgi/content/full/334/6059/1091/DC1)

Databases S1 to S4 as archive files

Table of Contents

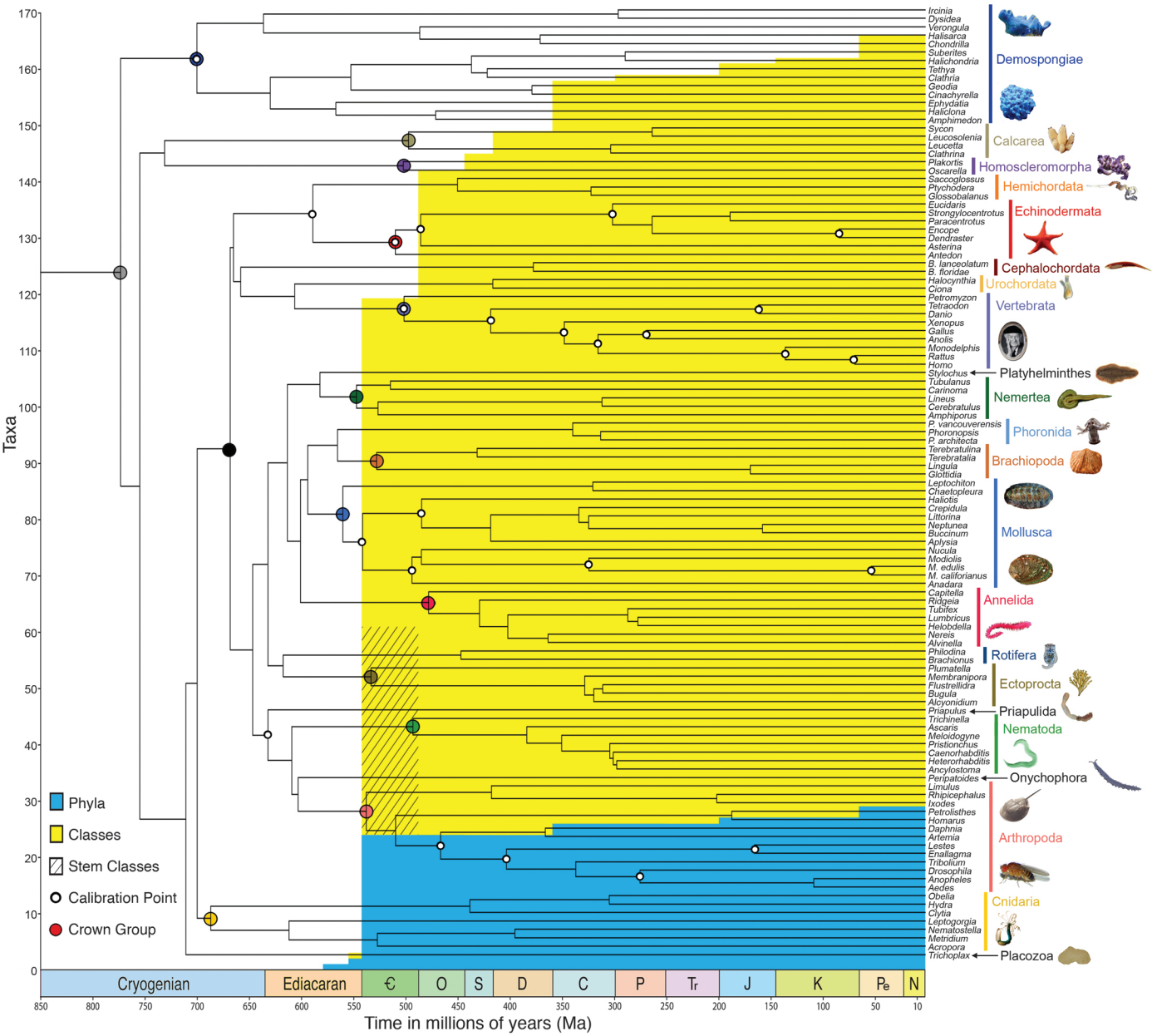
Taxa
Time in millions of years (Ma)
Phyla
Classes
Stem Classes
Calibration Point
Crown Group
Cryogenian
Ediacaran
Є
O
S
D
C
P
Tr
J
K
Pe
N
Demospongiae
Calcarea
Homoscleromorpha
Hemichordata
Echinodermata
Cephalochordata
Urochordata
Vertebrata
Platyhelminthes
Nemertea
Phoronida
Brachiopoda
Mollusca
Annelida
Rotifera
Ectoprocta
Priapulida
Nematoda
Onychophora
Arthropoda
Cnidaria
Placozoa

Materials and Methods

1. The Phanerozoic Fossil Record

First occurrences compilation

Origin of major morphological innovation may be explored indirectly by examining the appearance of the more inclusive Linnaean taxonomic rankings of phyla, classes and orders, but to date there has been no systematic compilation of the patterns of origination of higher clades since 1987 (*10*). Though the diversification of animal life, and particularly the Ediacaran–Cambrian metazoan 'explosion', has continued to be the subject of substantial research, many studies have still utilized family and generic compilations drawn from the exhaustive, yet dated, Sepkoski compendia (*74, 75*) of the mid to late 1990s. In the span of two decades our understanding of metazoan phylogeny has been revolutionized by molecular phylogenetic approaches, new clades and taxa have been described, and the stratigraphic and temporal framework for the Ediacaran and Cambrian has been heavily revised. Li et al. (2007) (*76*) recently compiled data on Cambrian generic diversity of the Chengjiang fossils of south China, but there currently exists no comparable global compendium, nor one that extends beyond the early Cambrian.

We conducted an extensive review of the primary literature and from this compiled a new database of the first appearances of valid genera for all marine metazoan phyla, classes and equivalent stem groups (see discussion of stem groups below) through the entire Phanerozoic, with a particular focus upon the Ediacaran-Cambrian (579-490 Ma) and Ordovician (Table S1). Systematics were updated based on the most recent analyses for each group, and all Cambrian occurrences were correlated to the ten stages of the newly revised Cambrian stratigraphic framework (*77*, *78*). Not all of these stages have been formally defined, but the basis of stage boundaries has been established, allowing for provisional correlation. Where correlations were uncertain we selected the conservative, younger origination alternative.

The first-appearing genera, origination periods and stages, and associated references for all phyla and classes are reported in Table S1. Although the Paleobiology Database (www.paleodb.org) has become an increasingly indispensible tool for studying fossil diversity, it was not originally established to track first occurrences, and its temporal bins average 10 Ma in duration – longer than the revised Cambrian stages. We have thus used the PBDB as a source but whenever possible checked the original publications; PBDB reference ID numbers are listed in Table S1 following their associated primary publication. Other secondary sources utilized include the South China compilation (*76*) and, when necessary, Sepkoski's original generic compendium (*75*). All references not already entered in the PBDB are listed in full within the Additional References section.

Stem group classification

The rise of phylogenetic systematics in paleontology has resulted in the recognition of a large number of stem lineages – those that diverge before the last common ancestor of crown groups – particularly in the Cambrian. Although the focus on tree topography has greatly increased our understanding of phylogenetic patterns in the fossil record, this poses a problem for the compilation of morphological diversity by

tallies of Linnaean rankings. For example, many classes within the Phylum Echinodermata were established decades ago for morphologically distinct, short-lived groups known only from the Cambrian or Ordovician periods; today, these clades would be recognized as unranked stem groups within the phylum, as exemplified by the categorization of newly-recognized panarthropod clades of equally distinctive morphology as stem-groups rather than extinct classes (*79*). Such phylogenetic demarcation in no way changes the groups' morphological distinctiveness or the unique developmental programs likely required to produce these morphologies, but rather reflects the evolution of taxonomic bookkeeping. We thus employed the following strategy for capturing the morphological distinctiveness of unranked stem-groups in our compilation, focusing on the Cambrian period: 1. Clades attributable to a phylum but not to a particular class are considered class-level stem-groups, and are included in class tallies (see below); and 2. Classes which are now recognized as stem lineages are included in counts of stem-groups (see below), but are still included in the class-level tallies.

First Occurrences by Geologic Period

Phyla and class originations were tallied across the Phanerozoic and binned into accepted Early, Middle (if applicable) and Late time bins. For classes, we noted whether first-occurring genera possessed readily fossilizable hard parts to account for preservational differences between groups. Raw counts are depicted in Table S2; the cumulative number of phyla and classes across the Phanerozoic is illustrated in Figure 1. Cambrian occurrences were additionally resolved to the new ten stages, and included in these finer-resolution tallies are the numbers of first-occurring Cambrian stem-groups: stem lineages of a roughly class-level degree of morphological distinctiveness were counted as a subset of total class originations. These data are reported in raw form in Table S3, and are also illustrated in the bar chart of Figure 3.

2. The Molecular Record

Molecular dataset assembly

The alignments used for our phylogenetic and molecular clock analyses are derived from a modification of that from (*80*) and includes 113 metazoans and six eukaryotic outgroups. As in (*80*) our new alignments include the seven nuclear housekeeping genes of (*13, 14*): aldolase, methionine adensolytransferase, ATP synthase beta chain, catalase, elongation factor 1 alpha, triosephosphate isomerase and phosphofructokinase. To this basic protein alignment, which was used for all molecular clock analyses, we concatenated sequences for the 5.8S, 18S and 28S ribosomal genes to generate the alignment used for our phylogenetic analyses. Ribosomal sequences were aligned using the well-curated alignment of (*81*) as a template, and then concatenated with our protein alignment, see also (*80*).

When compared to (*80*), our new alignment includes 20 new species. The ectoprocts *Membranipora sp., Flustrellidra sp. and Bugula sp.* were purchased from the Marine Biological Laboratory (Woods Hole, MA), the rotifer *Philodina roseola* was kindly provided by D. Mark Welch and P. Dutta (Brown University), the cephalochordate *Branchiostoma lanceolatum* was kindly provided by M. Schubert (Lyon), and the amino

acid sequences for the 7 housekeeping genes were sequenced following the protocol of (*82*). Protein sequences for the onychophoran *Peripatoides novaezealandiae* (which was commercially purchased) were obtained as part of a transcriptome-wide cDNA library generated using Illumina technology at TrinSeq (Trinity College Dublin, Institute of Molecular Medicine, Genome Sequencing Laboratory). Protein sequences for *Trichoplax*, the ectoprocts *Plumatella* and *Alcyonidium*, the rotifer *Brachionus*, all seven nematode species, both urochordates, and the cephalochordate *Branchiostoma floridae* were downloaded from Genbank. For all new taxa, nucleotide sequences for the 5.8S, 18S and 28S ribosomal genes that were available in the NCBI Genbank database were downloaded, aligned and added to the (*80*) alignment. Our final data set scores 119 taxa, 2049 amino acids (for the seven nuclear housekeeping genes), and 4680 nucleotides (for the three ribosomal genes).

Phylogenetic analyses

Our complete (amino acids plus nucleotides) alignment was analysed using mixed models in MrBayes v.3 (*83*). We set up two runs of four chains that used two unlinked GTR + Γ models. These were an amino acid GTR + Γ model (which was applied to the amino acid partition), and a nucleotide GTR + Γ model (which was applied to the rDNA partition). For both partitions, the shape of the Gamma distribution was estimated using four rate categories. The analyses were run until convergence was reached. We tested for convergence by plotting the likelihood of the trees saved (and evaluating whether they reached a plateau) and monitoring the average standard deviation of the split frequencies (as in other studies – e.g. (*80*, *82*, *17*, *14*); see also the MrBayes wikipage (*84*)).

Molecular clock analyses

Relaxed molecular clock analyses were performed to estimate divergence times among the major metazoan lineages. We used the topology recovered by our Bayesian analyses (Fig. S1) to anchor our relaxed molecular clock analyses. Although the majority of the nodes in our Bayesian phylogeny (Fig. S1) are resolved according to current knowledge (see also Supplementary Results), an inspection of this figure immediately shows that this is not the case for the Deuterostomia, as the Cephalochordata are recovered as the sister group of Ambulacraria and not as a member of the Chordata (*20*). In addition, contrary to many recent studies (e.g. *17, 15*, *85*) the Placozoa are recovered as the sister group of Bilateria instead of Eumetazoa. Because the aim of this study is dating the metazoan radiation, not disentangling the metazoan relationships, we did not perform further analyses (as, for example, in (*17*, *80*, *85*) to clarify the relationships among the taxa in Fig. S1. Instead, we integrated phylogenetic uncertainty in our molecular clock analyses by dating four alternative tree topologies: Fig. 1, S1 (see also S2), S3, and S4, which display alternative arrangements for taxa of uncertain relationships.

The topology of Fig. 1 was used to derive what we consider to be our optimal divergence times. Fig. 1 is a modification of the tree in Fig. S1 in which the Cephalochordata and the Placozoa are resolved according to current knowledge: the Cephalochordata as in (*20*), and the Placozoa as in (*17*, *15*, *85*). The tree obtained from our MrBayes analyses (Fig. S1) was also dated. Results obtained using the tree in Fig. S1

(see Fig. S2) illustrate the effect of phylogenetic uncertainty with reference to Placozoa and Cephalochordata on our estimated divergence times.

Both Fig. 1 and S1 resolve the three sponge classes in our dataset (Homoscleromorpha, Calcarea and Demospongiae) as a paraphyletic assemblage. More precisely, Demospongiae is resolved as the sister group of all the other Metazoa, whilst a monophyletic Calcarea plus Homoscleromorpha is resolved as the sister group of the Eumetazoa plus Placozoa. However, it is still unclear whether the sponges are monophyletic or paraphyletic (compare (*17*, *82*, *86*) with (*15*, *85*, *87*)), and whether Calcarea plus Homoscleromorpha represent a monophyletic assemblage in trees displaying the paraphyly of sponges (contrast (*17*) and Fig. S1). To integrate phylogenetic uncertainty on sponge relationships in our results, we estimated divergence times on two more topologies (Fig. S3 and S4). Fig. S3 is the same of Fig. 1 but with the sponge classes resolved as in (*17*). That is, Fig. S3 displays a paraphyletic Porifera in which the Homoscleromorpha are more closely related to the Eumetazoa (a clade named Epitheliozoa – (*82*)) than they are to the Calcarea. Fig. S4 is the same as Fig. 1 but with the sponges grouped in a monophyletic Porifera as in (*15*, *85*, *87*).

All molecular clock analyses were performed using the software Phylobayes 3.3b (*88*). Because of limitations in the current implementation of Phylobayes, which does not allow using mixed (nucleotides and amino acids) data sets, we followed (*80*) and used only the 7 nuclear housekeeping genes to estimate divergence times for the nodes in Fig.1 and S2-4. For all molecular clock analyses, branch lengths were re-estimated using the site heterogeneous CAT-GTR + Γ model, which we have previously shown to best fit our amino acid alignment (*17*). Two alternative molecular clock models were used in our analyses: the autocorrelated-rates CIR model of (*89*), and the uncorrelated-rates Uncorrelated Gamma Multipliers (UGM) model of (*90*). We previously showed that the autocorrelated-rates model CIR best fits our data set (*86*). However, even though the uncorrelated-rates UGM model is not an optimal fit to the dataset, it is important to estimate divergence times under this model to evaluate the extent to which our results might be model-dependent.

To calibrate our molecular clock analyses we used a set of 24 calibrations, see Table S4 and (*80*). All calibrations (both minima and maxima) were treated as soft. Experiments were performed using relaxation levels of 5% (the default level in Phylobayes), 10%, 20% and 50% (i.e. up to 50% of the prior probability density of each calibration point was allowed to lie outside the min-max interval defined by the provided calibration). For all molecular clock analyses the outgroup used was the Fungi (see also Database S1), and we set the prior root age for the Fungi-Holozoa split to be 1000 million years (Ma) ago (see also *14*, *80*, *86*). The Standard Deviation (SD) around the root age was set to 100 Ma. We tested the effect of using this root prior on our results by performing analyses using a significantly deeper prior root age (1600 Ma with an SD = 400 Ma). A large SD was used for the root age prior in this analysis to allow testing whether the 1600 Ma prior root age was appropriate, or whether it represented either a gross overestimate or a gross underestimate of the true age of divergence between the Holozoa and the Fungi. Analyses performed using the 1600 Ma prior root age were only performed using the CIR model, the topology in Fig. 1 and an intermediate (20%) soft bound relaxation level (see also Results for justifications of these settings).

To estimate the effect of our fossil calibrations and evaluate whether they biased our results by constraining too strictly (or in any other improper way) our estimated divergence times we performed analyses under the prior. These analyses showed that "composite priors" (*91*) do not seem to improperly bias our results. Further, we performed a 50% Calibrations-Jackknife analysis. For this analysis 50 repetitions were performed and in each repetition 12 (i.e. 50% of the calibrations in Table S4) were randomly deleted. The Jackknife analysis was only performed under the CIR model, using a relaxation level of 20% and the topology of Fig. 1 (see results for further justifications of the settings used for this analysis). For the nodes in Fig. 1 Jackknifed divergence times (and their SD) were estimated across the 50 repetitions.

3. The Neoproterozoic Fossil Record

Higher level groupings of Ediacaran Organisms

The most contentious issue for Ediacara macrofossils is their phylogenetic affinities. In the past, the Ediacara biota were originally characterized as crown Metazoa (*31*), or more controversially as Vendozoa/Vendobionta (*30*, *92*) distinct from Metazoa. It is now recognized that Ediacarans consist of a number of separate groups rather than a single clade, thus shifting the debate to discussions of stem+crown animals, stem clades outside of Metazoa, and even macroscopic algae (*29*). Ediacara macrofossils have been found in a variety of different sediment types and environmental settings. As the preservational complexities of the fossils have become better understood (*38*), the relationships between various morphotypes have become clearer.

Building on this work, we propose a new classification for Ediacara macrofossils. This classification utilizes features of branching or segment architecture, body symmetry, associated trace fossils, and growth parameters, while restricting direct comparisons with modern taxa unless they share undoubted synapomorphies. Where possible we have identified unique synapomorphies of particular clades, although the phylogenetic placement of these clades is difficult to pinpoint, especially where synapomorphies are not shared with metazoan or other eukaryotic clades. We recognize six clades (Rangeomorpha, Erniettomorpha, Dickinsoniomorpha, Arboreomorpha, Triradialomorpha, Kimberellomorpha), three likely clades (Bilaterialomorpha, Tetraradialomorpha, Pentaradialomorpha), and paraphyletic Porifera. The Rangeomorphs, Arboreomorphs, and Triradialomorphs (in addition to the likely sponge *Thectardis* (*34*)) first appear in the Avalon assemblage and continue into the White Sea assemblage, which sees the first appearance of Erniettomorphs, Dickinsoniomorphs, Kimberellomorphs, Bilaterialomorphs, Tetraradialomorphs, and Pentaradialomorphs. The Nama assemblage is presently restricted to Rangeomorphs, Arboreomorphs, Erniettomorphs, and sponges, although this most likely represents a taphonomic bias due to the predominance of Nama-type 3D preservation, which seemingly preferentially preserves these groups (*38*). All groupings consist of multiple species, with the exception of the Tetraradialomorphs and Pentaradialomorphs, and several include distinct morphotypes exhibiting different ecologies. This diversity of morphotypes reduces the likelihood that shared morphology reflects adaptive convergence as was likely for an older grouping, the Petalonamae (fronds (*93*)).

This novel classification of Ediacara macrofossils is discussed in the SOM text below, and is summarized in Table S5. First fossil occurrences and ranges for individual taxa were largely drawn from a 2007 compilation (*94*), and were revised/updated based upon primary literature (e.g. *95-97*). This classification scheme includes conceptual definitions as proposed by (*98-101*).

SOM Text

1. The Phanerozoic Fossil Record

Results: Patterns of fossil origination

The pattern of first appearances confirms earlier suggestions for an abrupt, asymmetric pattern of morphological innovation during the early Cambrian. Two definitively metazoan phyla (Porifera and probable Mollusca) appear in the fossil record in the latest Ediacaran, followed by a dramatic rise in novel phyla in the first stages of the early Cambrian (Tables S2, S3; Figs. 1, 3); in fact, it is very likely that no new phyla appear after the Cambrian, since phyla that appear in the later Paleozoic (Entoprocta, Rotifera, Platyhelminthes) are represented by taxa with little or no preservation potential, indicating that these later first appearances are largely artifactual.

Classes also exhibit this dramatic rise in first occurrences beginning in the early Cambrian and continuing into the Ordovician (Table S2, S3; Figs. 1, 3). From the early Paleozoic onward there is very little addition of new classes, and again, many of these later class appearances are of soft-bodied classes with poor preservation potential, suggesting earlier cryptic originations.

As discussed (and elaborated below), all but two phylum-level crown group molecular divergences occurred coevally between the end of the Ediacaran and the end of the Cambrian (Figs. 1, 3) for both taxa with high and low preservational potential. This illustrates a reciprocal reinforcement of both fossil and molecular signals of rapid morphological innovation in the Cambrian.

2. The Molecular Record

Results: Phylogenetic analyses

Phylogenetic analyses were performed on our new data set and their results are reported in Fig. S1. Most of the nodes in Fig. S1 are highly supported and resolved according to current knowledge. Three areas of the tree, though, require special consideration. The first is the relationships of the sponges, for which there is no current consensus and which is an area of active debate. In agreement with (*14*, *17*, *82, 86*), our results (see Fig. S1) do not support the monophyly of sponges. However, differently from (*14*, *17*, *82, 86*) which found the Homoscleromorpha to be the sister group of the Eumetazoa plus Placozoa, our new data set found the Homoscleromorpha and the Calcarea to be reciprocally monophyletic sister groups, with the Demospongiae representing the sister group of all the other metazoans (Fig. S1). The relationships among the sponge classes are still uncertain (compare (*17, 82, 86*) with (*15, 85, 87*) and Fig. S1), and thus we conjecture that with reference to these taxa the relationships in Fig. S1 (and Fig. 1) might be correct, albeit in need of further validation.

The remaining two areas concern the position of Placozoa and the position of Cephalochordata within Deuterostomia. Within Deuterostomia, results of our Bayesian analyses are at odds with current understanding of deuterostome phylogeny (*20*), as they do not support the monophyly of Chordata. Instead, our results found Cephalochordata as the sister group of the Ambulacraria (Fig S1). Finally, analyses of our data set found the Placozoa to be the sister group of the Bilateria. This result is at odds with most current studies (e.g. *15*, *17*, *85*), but see (*87*) for a different opinion. We suspect that the tree in Fig. S1 is likely to be inaccurate with reference to the relationships of both the Placozoa

and the Cephalochordata, and reflects the difficulty of correctly resolving all nodes in the metazoan tree in a single analysis.

Results: Molecular clock analyses

The aim of this study is timing the metazoan radiation, not disentangling the relationships among the animal phyla. Accordingly, rather than performing further phylogenetic analyses (e.g. (*17*, *80*, *85*)) to better evaluate the relationships among the taxa in Fig. S1 – particularly the Deuerostomia and the Placozoa – we integrated phylogenetic uncertainty in our analyses by dating four alternative topologies: Fig. 1, Fig. S1 (see also S2), Fig. S3 and Fig. S4; see Methods for details.

We consider our optimal divergence times to be those derived using the tree in Fig 1. This tree is a modification of the one in Fig. S1, see Methods for details. To date the nodes in the tree in Fig. 1 the CAT-GTR + G model was used to re-estimate branch lengths, the autocorrelated CIR model was used to relax the clock, a soft-bound relaxation level of 5% was used for all calibration points, and a prior root age of 1000 Ma with a SD of 100 Ma was placed on the Holozoa-Fungi split. The results of the analyses performed using these settings are discussed in the main text, and will not be repeated here.

In this section we shall discuss results of the validation analyses we performed to test whether the results in Fig. 1 are robust. To test the sensitivity of our results, we performed analyses to evaluate the extent to which they depend on: soft bound relaxation level, phylogenetic uncertainty, calibration points used, the depth of the prior root age, and choice of molecular clock model. The results of all these analyses, as well as of our optimal divergence times, are presented in Database S2. Here we shall further discuss important aspects of the results of our validation analyses.

The effect of relaxing the soft-bounds

Figs. S5 and S6 show the effect of relaxing the soft bounds around the considered calibration points (for both clock models, and under any considered phylogenetic hypothesis). These results show that under the CIR model (Fig. S5) changes are observed when the soft bounds are relaxed, as expected. Softer bounds correspond to deeper divergence times on average, and an increased difference in the estimated age is observed for nodes of greater age. In addition, comparison of Fig. S5 A, B, C and D show that there is a compounding effect when different soft bound relaxation levels are used on different tree topologies. The tree in Fig. 1 (see Fig. S5A) shows greater levels of increase in the estimated divergence times when the soft bounds are relaxed (from 5% to 50%). On the other hand the tree in Fig. S4 show minimal increments in the estimated divergence times when the soft bounds are relaxed. However, even in the case of the nodes in Fig. 1 (Fig S5A), changing the relaxation level from 5% to 20% only causes minimal increments on the estimated divergence times. Relaxing the bounds from 20% to 50% (as expected) results in greater increments of the recovered nodal ages, but the differences are still small, and noticeable only for the deepest nodes in Fig. 1 – see Fig. S5. Indeed, even the case of the deepest node of interest (i.e. the one indicating the origin of the Metazoa) in the topology of Fig. 1, which is the node showing the largest overall increment when the bound is relaxed from 5% to 50% (see Fig S5), the estimated divergence time only increases ~18%. In contrast to the results under the CIR model (Fig.

S5), divergence times do not change considerably with increasing relaxation levels if the UGM model is used (Fig. S6). However, using this model the 95% highest posteriors intervals around the optimal divergence times are wider than those obtained under CIR (see Database S2). Overall, these results suggest our main results (Fig. 1 and main text) are robust to relaxation of the soft bounds, i.e. they have not been biased by the use of calibrations that are too strictly bound. Because results obtained using a soft bound relaxation level of 20% are not very different from those obtained using a relaxation level of 50%, all other validation analyses were performed using this intermediate (20%) soft bound relaxation level.

The effect of phylogenetic uncertainty

Fig. S7A and B show the effects of phylogenetic uncertainty on our results. These results are important because, given the uncertainty still pertaining to some aspect of metazoan phylogenetics (see methods), they illustrate that, for overlapping nodes, our results are effectively invariant with respect to phylogenetic uncertainty. That is, the age of the nodes of interest do not change dramatically when different tree topologies are used to anchor the molecular clock analyses. This result holds under both considered clock models. Accordingly, results of some validation analyses (e.g. the computationally-intensive Jackknife analysis) were performed only in the case of the topology used in Fig. 1.

The effect of calibration point choice

Fig. S8 shows the results of our 50% Calibrations-Jackknife analysis. This Figure demonstrates that even randomly deleting 50% of the calibration points in Table S4, on average, does not significantly change any of our estimated divergence times. Fig. S8 only shows the optimal divergence times compared against average jackknife values. Standard deviations around the jackknifed divergence times are reported in Database S2. We have also performed analyses without data to visualize the priors used in our analyses (not shown). The results of the prior analyses, and of our jackknife analyses, suggest that our set of calibration points do not bias the results. In addition, the jackknife analysis suggests that despite the wide distribution of our calibrations across the Phanerozoic, random subsamples of these calibrations consistently support the same set of molecular divergence times, and thus our calibration points reciprocally validate each other.

The effect of the prior root age

Fig S9A, B and C, illustrate the effect of changing the prior root age (from 1000 or 1600 MA). It is clear from this figure that changing the prior root age only has a minimal effect on the estimated divergence times, and only for the deepest nodes in our tree – e.g. the node marking the origin of the Metazoa. This result was not unexpected as it is obvious that nodes that are closer to the root of the dated topologies must be more strongly influenced by changes of the prior root age in comparison to nodes that are positioned more crownward in the trees. However, even in the case of the deepest considered node on the tree in Fig. S3 (in which the effect of changing the prior root age is more evident – see Fig S9C) the estimated divergence time only increases ~21% (from 858 to 1093 Ma) when the prior root age is increased from 1000 to 1600 Ma. We conclude that the prior root age we used to obtain our optimal divergence times (Fig. 1)

was adequate and should not have affected our results in ways that could have mislead our conclusions.

Molecular clock model

Fig. S10 shows that the divergence times we estimated, despite being obviously dependent on the relaxed molecular clock model used (CIR or UGM), do not change significantly when different clock models are used.

Overall, we can thus conclude that the results of our molecular clock analyses are robust to the variations of the considered parameters, leading us to conclude that the optimal divergence times (Fig. 1) reported and discussed in the main text are robust.

3. The Neoproterozoic Fossil Record

Results: classification of Ediacara macrofossils

1) Rangeomorpha: Rangeomorphs are a monophyletic clade of modular organisms composed of unique self-similar leaf-like structures termed frondlets. These frondlets consist of a repetitive branching pattern that is identical throughout at least three orders of branching. At least two separate branching architectures represent separate clades within the rangeomorphs: Charnia-type and Rangea-Type (*93*). In many species, modular units are acquired early in ontogeny and inflate in size with growth. The repeated branching of the rangeomorph frondlet results in a significant increase in surface area, which was necessary for osmotrophy.

Occurrence: Avalon to Nama: Mistaken Point Newfoundland Canada; Charnwood Forest England; Flinders Ranges Australia, Wernecke Mountains, northwestern Canada; Salient Mountain, British Columbia Canada; White Sea Russia; southern Namibia.

Ecology: Frondlets are assembled into various morphological architectures including carpet-like (benthic reclining) *Fractofusus*, radial cabbage-shaped *Bradgatia*, fence-shaped *Pectinifrons*, and upper tier fronds such as *Rangea*.

Taxa: *Avalofractus abaculus, Beothukis mistakensis, Bradgatia linfordensis, Charnia masoni, Charnia antecedens, Fractofusus misrai, Fractofusus andersoni, Frondophyllas grandis, Haspidophyllas flexibilis, Pectinifrons abyssalis, Rangea schneiderhoehni, Trepassia wardae*.

2) Erniettomorpha: Erniettomorphs are a monophyletic clade of modular organisms in which the modules are smooth, unbranched, and cylindrical in shape. Several taxa are multi-foliate, meaning three or more identical leaf-like petaloids composed of modular tubes are arranged around a central axis. Tubes typically alternate from side to side along the central midline, implying that they are not truly bilaterally symmetrical. Growth results from sequentially adding modular segments that are approximately the same size and shape.

Occurrence: White Sea to Nama: Flinders Ranges, Australia; White Sea, Russia; Mackenzie Mts, Canada; Podolia, Ukraine; south-western North America; southern Namibia;

Ecology: Examples include the benthic carpet-like *Phyllozoon*, the bag-shaped *Ernietta*, Three-veined *Pteridinium* and multifoliate frond *Swartpuntia*.

Taxa: *Ernietta plateauensis, Nasepia altae, Palaeoplatoda segmentata, Phyllozoon hanseni, Pteridinium simplex, Swartpuntia germsi, Valdainia plumosa*.

3) Dickinsoniomorpha: Dickinsoniomorphs are a clade of organisms composed of smooth, featureless tubes with a definitive anterior-posterior differentiation. Several specimens are associated with concentric grooves believed to represent shrinkage of specimens resulting from muscular contraction or loss of an internal hydrological skeleton. Rare specimens are associated with trackways suggesting active mobility. Tubular architecture is similar in many respects to Erniettomorph construction, however Erniettomorphs lack concentric shrinkage, trace fossils, and a clear anterior-posterior differentiation. Furthermore, Dickinsoniomorphs lack a multi-foliate construction.

Occurrence: White Sea: Flinders Range, Australia; White Sea, Russia; Podolia, Ukraine; Mackenzie Mountains, Canada.

Ecology: All Dickinsoniomorphs are benthic reclining mats.

Taxa: *Andiva ivantsovi, Dickinsonia brachina, Dickinsonia costata, Dickinsonia lissa, Dickinsonia rex, Dickinsonia tenuis, Epibaion axiferus, Windermeria aitkeni, Yorgia waggoneri*.

4) Arboreomorpha: Arboreomorphs are a clade of fronds with bifoliate petaloids consisting of parallel primary branches which diverge from the central stalk at acute to right angles (45°–90°) and end at an outer margin. The branches are all joined together and possibly attached to a dorsal sheet. Primary branches are composed of teardrop-shaped secondary branches which are at right angle to the primary branches. The central stalk is large and prominent.

Occurrence: Avalon to Nama: Mistaken Point Newfoundland Canada; Charnwood Forest England; Flinders Ranges Australia, White Sea Russia; Wernecke Mountains, northwestern Canada.

Ecology: all Arboreomorphs are fronds.

Taxa: *Charniodiscus arboreus, Charniodiscus concentricus, Charniodiscus longus, Charniodiscus oppositus, Charniodiscus procerus, Charniodiscus spinosus, Khatyspytia grandis, Vaizitsinia sophia*. ***note:** Some have allied Burgess Shale fossil *Thaumaptilon* with *Charniodiscus* based on the similarities in the sheet-like frond morphology, although *Thaumaptilon* branching has been interpreted to house zooids.

5) Triradialomorpha: Triradialomorphs (Trilobozoa?) are a monophyletic clade characterized by three plains of symmetry (*Anfesta*; *Triforillonia*) or by the spiral rotation of three independent arm-like structures (*Tribrachidium*, *Albumares*). Each branch is typically composed of smaller branching structures.

Occurrence: Avalon to White Sea: Mistaken Point Newfoundland Canada; Flinders Ranges Australia, White Sea Russia; Podolia, Ukraine; Uttar Pradesh, India.

Ecology: All Triradialomorphs are benthic reclining.

Taxa: *Albumares brunsae, Anfesta stankovskii, Pomoria corolliformis, Skinnera brooksi, Tribrachidium heraldicum, Triforillonia costellae*. ***note**: it may be that certain forms like *Eoandromeda* (which have 8 spiral arms) might fit within this category, although the unbranched tubular arms are distinct from known Triradialomorphs.

6) Kimberellomorpha: Oval-shaped, bilaterally symmetrical fossils composed of several morphologically distinct and concentrically-arranges zones. Outermost zone is typically smooth and crenulated, while innermost region is bordered by thin transverse wrinkles and contains a deep longitudinal invagination in the center. The anterior end is narrower and appears to house a retractable, arrow-shaped structure presumed to be responsible for the fan-shaped scratch marks (i.e. *Radulichnus*) sometimes associated with *Kimberella*.

Occurrence: White Sea: Flinders Ranges, Australia; White Sea, Russia; Uttar Pradesh, India.

Ecology: Kimberellomorphs are motile grazers.

Taxa: *Kimberella quadrata, Solza margarita*.

7) Bilaterialomorpha: This group is most likely a clade. Bilaterialomorphs consist of segmented forms with distinct bilateral symmetry along their length and a differentiated anterior-posterior region. These taxa have distinct headshield-like anterior region followed by a repeatedly segmented posterior region. Segments may appear to represent independent structures unattached to one another, although several taxa clearly demonstrate a membranous outline around the segments. Furthermore, the segmentation pattern across the midline can sometimes appear as alternating rather than opposing, and segments, when present, typically taper in size posteriorly. The extent to which these characters can be attributed to preservational artifacts is difficult to isolate.

Occurrence: White Sea: Flinders Ranges, Australia; White Sea, Russia.

Ecology: All Bilaterialomorphs are benthic reclining.

Taxa: *Archaeaspinus fedonkini, Cyanorus singularis, Ivovicia regulosa, Kharakhtia nessovi, Lossina lissetskii, Marywadea ovata, Onega stepanovi, Paravendia janae, Parvancorina minchami, Parvancorina saggita, Spriggina floundersi, Temnoxa molluscula, Vendia rachiata, Vendia sokolovi*.

8) Tetraradialomorpha: *Conomedusites* is the only known Tetraradialomorph and consists of a four-lobed radial body.

Occurrence: White Sea: Flinders Ranges, Australia; White Sea, Russia.

Ecology: *Conomedusites* is benthic reclining.

Taxa: *Conomedusites lobatus*.

9) Pentaradialomorpha: Pentaradialomorphs are represented by a single taxon (*Arkarura adami*) consisting of a small circular disc with a central star-shaped structure constructed from five equidistant arms that extend from the center to reach the raised outer rim of the disc.

Occurrence: White Sea: Flinders Ranges, Australia

Ecology: *Arkarura* is benthic reclining.

Taxa: *Arkarua adami*.

10) Sponges: A paraphyletic assemblage of conical to globular fossils with circular exhalant canals (oscula?). Some specimens of *Palaeophragmodictya* exhibit a likely spicular mesh although no known spicules have been found in association with Ediacaran fossils. Conical forms like *Thectardis* adhere to a specific length to width (diameter of the

oscula) ratio > 1.6 in order to avoid recycling by hydrodynamically expelling water away from the sponge, while *Ausia* has rows of large incurrent pores (ostium?).

Occurrence: Avalon to Nama: Mistaken Point Newfoundland Canada; Flinders Ranges, Australia; southern Namibia.

Ecology: Poriferan fossils are epifaunal (*Thectardis*) or benthic reclining (*Palaeophragmodictya*).

Taxa: *Ausia fenestrate, Palaeophragmodictya reticulate, Rugoconites enigmatis, Rugoconites tenuirugosus, Thectardis avalonensis*.

Valid Problematica: Taxa that we believe are valid but do not fit into any larger-scale groupings.

Taxa: *Armillifera parva, Beltanelliformis brunsae, Bomakellia kelleri, Bronicella podolica, Chondroplon bilobatum, Corumbella werneri, Eoporpita medusa, Funisia dorothea Hadrynichorde catalenensis, Hadryniscala avalonica, Hiemalora stellaris, Inaria karli, Lomosovis malus, Mawsonites spriggi, Nemiana simplex, Ovascutum concentricum, Palaeopascichnus delicates, Paracharina dengyingensis, Parviscopa bonavistensis, Primocandelabrum hemialoranum, Pseudovendia charnwoodensis, Somatohelix sinuosus , Ventogyrus chistyakovi*, *Eoandromeda octobrachiata, Yangtziramulus zhangi, Yelovichnus gracillis.*

Removed: Fossils we opted to remove from the analysis because they were exceedingly rare (one or two known specimens), poorly or incorrectly described in the primary literature, have been synonymized, or represented parts (typically holdfasts) of other organisms.

Taxa: *Anabylia improvisa; Archangelia valdaica; Askinica; Aspidella costata; Aspidella hatyspytia; Aspidella terranovica; Baikalina sessilis; Barmia lobatus; Beltanella gilesi; Beltanelloides sorichevae; Blackbrookia oaksi; Bonata septata; Brachina delicate; Charnia wardi; Charnia grandis; Cyclomedusa davidi; Cyclomedusa radiata; Cyclomedusa gigantea; Cyclomedusa plana; Cyclomedusa minima; Cyclomedusa delicata; Ediacaria flindersi; Elasenia aseevae; Elasenia uralica; Evmiaksia aksionovi; Garania petali; Gehlingia dibrachida; Glaessneria imperfecta; Irridinitus multiradiatus; Ivesheadia lobata; Jampolium wyrzhykoowskii; Kaisalia levis; Kaisalia mensae; Khatyspytia grandis; Kubisia glabra; Madigania annulata; Medusinites asteroides; Medusinites paliji; Medusinites patellaris; Mialsemia semichatovi; Nadalina yukonensis; Namiana bakeevi; Nimbia dniesteri; Nimbia occlusa; Nimbia paula; Orthogonium parallelum; Paliella patelliformis; Paramedusium africanum; Planomedusites patellaris; Platyopholinia pholata; Podolimirus mirus; Protodipleurosoma rugulosum; Protodipleurosoma wardi; Pseudovendia charnwoodensis; Ramellina pennata; Sekwia excentrica; Shepshedia palmata; Spriggia wadea; Stauinidia crucicula; Tateana inflata; Tirasiana cocardia; Tirasiana concentralis; Tirasiana coniformis; Tirasiana disciformis; Velancorina martina; Vendella haelenicae; Vendella sokolovi; Veprina undosa; Vladimissa missarzhevskii.*

Table S1.
First occurrences for all phyla and classes. The first-appearing genus (or representative genus if there are multiple coeval appearances) for each phylum and class is listed in the table below with the Period + Stage of appearance, the primary references, and PBDB reference ID number (if applicable).

Phylum	Class	*Genus*	First Occurrence	Source(s); PBDB Ref #
PORIFERA				
Demospongiae			**Cam 2 [Meis/Tom]**	
	class stem	*Choia*	Cam 2 [Meis/Tom]	Xiao et al. 2005; 32708
(Subclass)	Tetractinomorpha	*Geodia*	Cam 3 [Atd]	Reitner & Worheide 2002 (*102*)
(Subclass)	Ceractinomorpha	*Hamptonia*	Cam 3 [Atd]	Steiner et al. 2005; 29233
Homoscleromorpha			**Carb [early]**	
	Homoscleromorpha[1]		Carb [early]	Reitner & Worheide 2002 (*102*)
Hexactinellida			**Cam 2 [Meis/Tom]**	
	class stem	*Hunanospongia*	Cam 2/3 [Meis-Atd]	Steiner et al. 1993; 32714
(Subclass)	Amphidiscophora	*Larispongia*	Ord [Trem]	Carrera 1998; 18978
(Subclass)	Hexasterophora	*Calcihexactina*	Cam 2/3 [Meis-Atd]	Li et al. 2007 (*76*)
		Protospongia	Cam 2 [Meis/Tom]	Xiao et al. 2005; 32708
Calcarea			**Cam 2 [Meis/Tom]**	
	class stem	*Gravestockia*	Cam 3 [Atd]	Reitner 1992 (*103*)
	Heteractinida	*Eiffelia*	Cam 2 [Meis/Tom]	Bengtson et al. 1990; 13290
(Subclass)	Calcinea		Recent	
(Subclass)	Calcaronea	*Protoleucon*	Carb [Vise]	Sepkoski (*75*)
Archaeocyatha			**Cam 2 [Tom]**	
	Regulares	*Coscinocyathus*	Cam 2 [Tom]	Gandin, et al. 2007; 25805
	Irregulares	*Okulitchicyathus*	Cam 2 [Tom]	Rozanov et al. 1969; 13330
	Cribricyathea	*Leibaella*	Cam 3 [Atd]	Wood et al. 1993; 18191
CNIDARIA				
(stem class)	"Anabaritids" [2]	*Anabarites*	Cam 1 [N-D]	Kouchinsky et al. 2009 (*104*)
(stem class)	Hydroconozoa	*Hydroconus*	Cam 3 [Atd-Bot]	Kruse et al. 1996; 6600
Subphylum Anthazoa			**Cam 3 [Atd]**	
	class stem	*Arrowipora*	Cam 3	Fuller & Jenkins 2007; 26866
(Subclass)	Zoantharia	*Xianguangia*	Cam 3 [Atd]	Sepkoski (*75*)
(Subclass)	Alcyonarea	*Petilavenula*	Ord [Aren-Mori]	Cope 2005; 29486
Subphylum Medusozoa			**Cam 1 [N-D]**	
	class stem	*Cordubia*	Cam 1 [N-D]	Mayoral et al. 2004; 25892
	Scyphozoa		Recent	
	Conulata	*Carinachites*	Cam 1 [N-D]	Steiner et al. 2004; 29166
	Staurozoa		Recent	
	Cubozoa	unnamed	Cam 6/7 [Marj]	Cartwright et al. 2007 (*105*)
	Hydrozoa	*Cambrohydra*	Cam 3 [Atd]	Hu et al. 2005; 30233
CTENOPHORA				
Ctenophora			**Cam 3 [Atd]**	
	stem class	*Batofasiculus*	Cam 3 [Atd]	Hou et al. 2007; 33070
LOPHOTROCHOZOA				
Chaetognatha			**Cam 1 [N-D]**	

	"Protoconodonts"	*Protohertzina*	Cam 1 [N-D]	Li et al. 2007 (*76*); Landing et al. 1989; 29312
	class stem	*Protosaggitta*	Cam 3 [Atd]	Li et al. 2007 (*76*)
	Sagittoidea		Recent	
Rotifera			**Paleo [Eocene]**	
	Monogononta	*Notholca*	early Holocene	Swadling et al. 2001 (*106*)
	Digononta		Recent	
	Bdelloidea	*Habrotrocha*	Paleo [Eocene]	Waggoner & Poinar 1993 (*107*)
	Seisonidea		Recent	
Platyhelminthes			**Paleo [Eocene]**	
	Turbellaria	*Micropulaeosoma*	Paleo [Eocene]	Poinar 2003; 33073
	Monogenea		Recent	
	Trematoda		Recent	
	Cestoda		Recent	
Entoprocta			**Jur [Kim]**	
(Family)	Barentsiidae	*Barentsia*	Jur [Kim]	Todd & Taylor 1992 (*108*); Sepkoski (*75*)
Phoronida			**Cam 1**	
	class stem	*Eccentrotheca*	Cam 1	Landing et al. 1989 (*109*); Skovsted et al. 2008 (*110*)
	extant phoronids		Recent	
Brachiopoda			**Cam 1/2**	
	class stem	*Camenella*	Cam 1/2	Kouchinsky et al. 2011 (*8*); Skovsted et al. 2009 (*111*)
	stem Linguliformea[3]	*Mickwitzia*	Cam 3 [Atd]	Holmer & Popov 2007 (*112*)
	Lingulata	*Obolus*	Cam 2	Landing 1991; 430
	Paterinata	*Aldanotreta*	Cam 2	Kruse et al. 1995; 6607
	Craniata	*Fengzuella*	Cam 1	Steiner et al. 2007; 29183
	stem Rhyncholiformea[4]	*Salanygolina*	Cam 3 [Bot]	Holmer et al. 2009 (*113*)
	Chileata	*Kotujella*	Cam 3 [Atd]	Sepkoski (*75*)
	Obolellata	*Nochoriella*	Cam 2 [Tom]	Gregoryeva 1983; 900
	Kutorginata	*Khasagtina*	Cam 2 [Tom]	Ushatinskaya 1987; 876
	Strophomenata	*Billingsella*	Cam 3 [Bot]	Sepkoski (*75*); 751
	Rhynchonellata	*Wangyuia*	Cam 3 [Atd]	Hu et al. 2005; 30233
Bryozoa			**Cam 9**	
	Stenolaemata	*Pywackia*	Cam 9	Landing et al. 2010 (*114*)
	Gymnolaemata	*Callopora*	Ord [Aren]	Allen & Lester 1957; 8741
	Phylactolaemata		Recent	
Hyolitha			**Cam 1 [N-D]**	
	Hyolithamorpha	*Ovalitheca*	Cam 1 [N-D]	Khomentovsky & Karlova 1993; 13517
	Orthothecimorpha	*Loculitheca*	Cam 1 [N-D]	Khomentovsky & Karlova 1993; 13517
Mollusca			**Cam 1**	
	class stem	*Mobergella*	Cam 2	Li et al. 2007 (*76*); Rozanov et al. 1969; 13330
		Odontogriphus	Cam 5	Caron et al. 2006 (*115*)
	Halwaxiids	*Halkieria*	Cam 1	Landing et al. 1989; 29312
	Polyplacophora	*Ocruranus/Eohalobia*	Cam 1	Vendrasco et al. 2009; 32126
		Lopochites	Cam 1	Steiner et al. 2004; 29166
	Aplacophora	*Matthevia*	Cam 8	Sigwart & Sutton 2007 (*116*), Sepkoski (*75*)

		Acaenoplax	Sil [Wenlock]	Sutton et al. 2004 (*117*)
	Caudofoveata		Recent	
	Solenogastres		Recent	
	Rostroconcha	*Watsonella*	Cam 1	Landing et al. 1989; 29312
	Helcionelloida	*Helcionella*	Cam 1	Landing et al. 1989; 29312
	Tergomya	*Canopoconus*	Cam 1	Feng & Sun 2001; 15906
	Scaphapoda	*Rhytiodentalium*	Ord [Cara-mid]	Sepkoski (*75*)
	Bivalvia	*?Fordilla*	Cam 2 [N. Scotia]	Landing 1991; 430
		Pojetaia	Cam 3	Parkaev 2004, 13185
	Gastropoda	*Chippewaella*	Cam 7	Gunderson 1993; 566
		? Aldanella	Cam 1	Landing et al. 1989; 29312
	Paragastropoda	*Yuwenia*	Cam 3	Elicki 1994; 13333
	Cephalopoda	*Nectocaris pteryx*	Cam 5	Smith & Caron 2010 (*118*)
		Plectronoceras	Cam 9	Mutvei et al. 2007 (*119*)
	Stenothecoida	*Manikai*	Cam 1	Missarzhevsky 1989 (*120*)
		Stenothecoides	Cam 2	Brasier et al. 1996 (*121*)
	Tentaculita	*Tentaculites*	Ord [Trem]	Fisher & Young 1955; 26506
Coeloscleritophora[5]			**Cam 1**	
	chancellorids	*Chancelloria*	Cam 1 [Fortunian]	Kouchinsky et al. 2011 (*8*)
	siphonogonuchitids	*Spingonuchites*	Cam 1 [Fortunian]	Kouchinsky et al. 2011 (*8*)
		Drepanochites	Cam 2 [China]	Li et al. 2007 (*76*)
	engimatic sclerites	*Zhiiginites*	Cam 1	Conway Morris and Menge 1991; 506
	enigmatic tubular fossils		Cam 2	Li et al. 2007 (*76*)
Sipuncula			**Cam 3 [Atd]**	
	class stem	*Archaeogolfingia*	Cam 3 [Atd]	Huang et al. 2004 (*122*)
	Phascolosomida		Recent	
	Sipunculida		Recent	
Annelida			**Cam 3 [Atd]**	
	class stem	*Maotianchaeta*	Cam 3 [Atd]	Li et al. 2007 (*76*)
	Machaeridia	*Plumulites*	Ord [Trem]	Vinther et al. 2008 (*123*)
	Polychaeta	*Phragmochaeta*	Cam 3 [Atd]	Conway Morris & Peel 2010 (*124*)
	Echiura	*Coprinoscolex*	Carb [Mazon]	Jones & Thompson 1977 (*125*)
	Myzostomiida	*Myzostomites*	Ord [late]	Warn 1974 (*126*)
	Oligochaeta	*Pronaidites*	Carb [Kas/Gze]	Wills 1993 (*127*)
	Hirudinea	*Burejospermum*	Jur [Toar-Plie]	Jansson et al. 2008 (*128*)
Nemertea			**Carb [Serp-l]**	
	class stem	*Archisymplectes*	Carb [Serp-l]	Schram 1973 (*129*)
	Anolpla		Recent	
	Enopla		Recent	
ECDYSOZOA				
Priapulida			**Cam 2 [Tom]**	
	Palaeoscolecida	*Maotianshania*	Cam 2 [Tom]	Sun and Hou 1987; 419
	Priapulimorpha	*Ancalagon*	Cam 5 [Burgess]	Caron & Jackson 2008; 28283
	Halicryptomorpha		Recent	
	Seticoronaria		Recent	
Nematomorpha			**Cam 3**	
	class stem	*Cricocosmia*	Cam 3 [Chengjiang]	Hou & Sun, 1988; 847

	Nectonematoidea		Recent	
	Gordioidea		Recent	
Loricifera			**Cam 3**	
	class stem	*Sirilorica*	Cam 3 [Sirius Passet]	Peel 2010 (*130*)
Nematoda			**Cret [Barr]**	
	class stem	*Heleidomermis*	Cret [Barr]	Poinar et al. 1994 (*131*)
	Adenophorea		Recent	
	Secernentea		Recent	
Panarthropoda				
phylum indet.	stem arthropod traces	*Rusophycus*	Cam 2 [Tom]	Edgecombe 2010 (*79*)
unranked stem	Cambrian lobopods	*Luolishania*	Cam 3	e.g. Chen & Zhou 1997 (*132*)
Tardigrada			**Cam 5? [Siberia]**	
	class stem	unnamed tardigrade	Cam 5? [Siberia]	Muller et al. 1995 (*133*)
	Heterotardigrada		Recent	
	Mesotardigrada		Recent	
	Eutardigrada	*Milnesium*	Cret (Turo)	Bertolani & Grimaldi 2000 (*134*)
Lobopodia			**Cam 3**	
	class stem	*Microdictyon*	Cam 3	Hinz 1987; 15995; Kouchinsky et al. 2011 (*8*)
		Hadranax	Cam 3	Budd and Peel 1998; 546
	gilled lobopods	*Kerygmachela*	Cam 3	Budd 1993; 30407
Euarthropoda			**Cam 3**	
	class stem	*Fuxianhuia*	Cam 3	Hou and Bergstrom 1997 (*135*)
		Perspicaris	Cam 3	Steiner et al. 1993; 32714
		Tamisiocaris	Cam 3	Daley and Peel 2010 (*136*)
	Lamellipedia	*Naraoia*	Cam 3 [Atd]	Steiner et al. 2005; 29233
		Retifacies	Cam 3	Hou and Bergstrom 1997 (*135*)
		Kuamaia	Cam 3	Hou and Bergstrom 1997 (*135*)
		Xandarella	Cam 3	Hou and Bergstrom 1997 (*135*)
		Fallotaspis	Cam 3 [Atd-l]	Hollingsworth 1999; 3887
		Kwanyinaspis	Cam 3	Zhang and Shu 2005 (*137*)
Subphylum Chelicerata				
	class stem	*Sanctacaris*	Cam 5 [Burgess]	Dunlop and Selden 1998 (*138*)
	Pycnogonida	*Cambropycnogon*	Cam 8 [Maent]	Waloszek & Dunlop 2002 (*139*)
	Megacheira	*Haikoucaris*	Cam 3 [Atd]	Chen et al. 2004 (*140*)
	Merostomata	*Paleomerus*	Cam 3 [Atd]	Jensen 1990; 858
	Xiphosura	unnamed specimen	Ord [Trem]	Van Roy et al. 2010 (*141*)
	Arachnida	land scorpions	Sil [early]	Sepkoski (*75*)
Subphylum Indet.				
	Thylacocephala	*Isoxys*	Cam 3	Hu et al. 2007 (*142*); Vannier et al. 2006 (*143*)
Subphylum Crustacea				
	class stem	*Kunmingella*	Cam 3	Hou et al. 2010 (*144*); Steiner et al. 2005; 29233
		Marrella	Cam 5 [Burgess]	
		Cambropachycope	Cam 8	Waloszek & Muller 1990 (*145*)
	crown stem	*Pectocaris*	Cam 3 [Atd]	Hou et al. 2004 (*146*)
		Yicaris	Cam 3 [Atd]	Zhang et al. 2007 (*147*)
	Remipedia	*Tesnusocaris* [6] **	Carb [Pen-lower]	Brooks 1955 (*148*)

	Cephalocarida	*Dala*	Cam 8 [Maent]	Muller 1983; 860
	Branchiopoda	*Rehbachiella*	Cam 8 [Maent]	Walossek 1995 (*149*)
	Maxillopoda	*Priscansermarinus*	Cam 5 [Burgess]	
		Heymonsicambria	Cam 8/9 [Maent]	Walsozek & Muller 1994 (*150*)
	Ostracoda	*Kimsella*	Ord [Trem]	Williams et al. 2008 (*151*)
	Malacostraca	*Proboscicaris*	Cam 5 [Solvan]	Chlupac and Kordule 2002; 57206
Subphylum Hexapoda				
	Insecta	*Leverhulmia*	Dev [Emsi]	Fayers and Trewin 2005 (*152*)
	Collembola	*Rhyniella*	Dev [Emsi]	Greenslade & Whalley 1986 (*153*)
DEUTEROSTOMIA				
Vetulicolia			**Cam 3 [Atd]**	
	Vetulicolata	*Pomatrum*	Cam 3 [Atd]	Aldridge et al. 2007 (*154*)
	Heteromorphida	*Heteromorphus*	Cam 3 [Atd]	Aldridge et al. 2007 (*154*)
		Banffia	Cam 5 [Burgess]	Caron 2005 (*155*)
unranked stem	"Cambroernids"	*Eldonia*	Cam 3 [Atd]	Zhu et al. 2002 (*156*)
		Herpetogaster	Cam 5 [Burgess]	Caron et al. 2010 (*157*)
Hemichordata			**Cam 3 [Atd-Bot]**	
	Graptolithina	*Chaunograptus*	Cam 5 [Burgess]	Caron and Jackson 2008; 28283
	Pterobranchia	*Galeaplumosus*	Cam 3 [Atd-Bot]	Hou et al. 2011 (*158*)
	Enteropneusta	*Ottoia tenuis*	Cam 5 [Burgess]	
		Megaderaion	Jur [Sine]	Arduini et al. 1981 (*159*)
Echinodermata			**Cam 3**	
	class stem	*Ventulocystis*	Cam 3 [Chengjiang]	Li et al. 2007 (*76*)
		echinoderm plates	Cam 3	Kouchinsky et al. 2011 (*8*)
Subphylum Homalozoa	Stylophora	*Ceratocystis*	Cam 5	Zamora 2010 (*160*); Fatka and Kordule 2001; 19350
	Homoiostelea	*Castericystis*	Cam 6 [Marj]	Ubaghs and Robison 1986; 32653
	Homostelea	*Asturicystis*	Cam 5?	Fatka and Kordule 2001; 19350
		undescribed form	Cam 5	Zamora 2010 (*160*)
	Ctenocystoidea	*Ctenosystis*	Cam 5	Sepkoski (*75*)
		undescribed form	Cam 5	Zamora 2010 (*160*)
	Cincta	*Protocinctus*	Cam 5	Rahman and Zamora 2009 (*161*)
Subphylum Blastazoa	Eocrinoidea	*Alanisicystis*	Cam 4 [Bot]	Ubaghs and Vizcaino 1990; 544
		Gogia	Cam 4/5	Zamora 2010 (*160*); Durham 1978; 32669
	Rhombifera	*Cuniculocystis*	Ord [Aren-l]	Sepkoski (*75*)
	Diploporita	*? Lichenoides*	Mid Cam	Chlupac 1993; 25868
		Sinocystis	Ord [Trem]	Bruton et al. 2004; 19028
	Parablastoidea	*Blastoidocrinus*	Ord [Aren]	Sepkoski (*75*)
	Blastoidea	*Decaschisma*	Sil [Wenl-l]	Frest et al. 1999; 4379
	Coronoidea	*Cupulocorona*	Ord [Ashgill-l]	Sepkoski (*75*)
Subphylum Indet.	Edrioasteroidea	*Cambraster*	Cam 5 [lMid]	Zamora et al. 2007; 30458
		Stromatocystites	Cam 3/4 [Bot]	Chulpac 1993; 25868
	Helioplacoidea	*Helioplacus*	Cam 3/4 [Atd-Bot]	Wilbur 2006; 30495
	Ophiocistoidea	*Volchovia*	Ord [Aren-u]	Sepkoski (*75*)
	Cyclocystoidea	*Cyclosystoidea*	Ord Blackriveran	Koleta et al. 1987; 6707
	Camptostromoidea	*Camptostroma*	Cam 3/4	Sprinkle 1973; 22459; Sepkoski
Subphylum Crinozoa	class stem	*Echmatocrinus*	Mid Cam	Sepkoski (*75*)

	Crinoidea	*Hybocrinus*	Ord [Aren]	Sepkoski (*75*)
	Paracrinoidea	*Malocysites*	Ord [Llde]	Kobluk 1981; 26898
Subphylum Asterozoa	Somasteroida	*Apullaster*	Ord [Trem-u]	Sepkoski (*75*)
	Asteroidea	*Eriaster*	Ord [Trem]	Blake and Guensberg 2005; 28538
	Ophiuroidea	*Pradesura*	Ord [Aren-l]	Sepkoski (*75*)
Subphylum Echinozoa	Echinoidea	*Neobothriocidaris*	Ord [Llvi]	Kolata et al. 1987; 6707; Sepkoski (*75*)
	Holothuroidea	*Thuroholia*	Ord [Cara]	Gutschick 1954; 31864
Urochordata			**Cam 3**	
	class stem	*Shankouclava*	Cam 3 [Chengjiang]	Chen et al. 2003 (*162*)
	Ascidiacea	*Permosoma*	Perm [Leon]	Sepkoski (*75*)
	Thaliacea		Recent	
	Appendicularia		Recent	
	Sorberacea		Recent	
Cephalochordata			**Cam 3**	
	class stem	*Cathaymyrus*	Cam 3 [Chengjiang]	Shu et al. 1996 (*163*)
Craniata			**Cam 3 [Atd]**	
	Cephalaspidomorphi	*unnamed*	Ord [Cara]	Sepkoski (*75*)
		Trematapsis	Sil [Wenl]	Mark-Kurik 1969; 6155
	Pteraspidomorphi	*Arandaspis*	Ord [Aren]	Ritchie & Gilbert-Tomlinson 1977; 30365
	Agnatha	*Haikouichthys*	Cam 3 [Atd]	Zhang and Hou 2004 (*164*)
		various agnathans	Cam 3 [Chengjiang]	Li et al. 2007 (*76*)
		Anatolepis	Cam 9 [upper]	Smith et al. 2001 (*165*)
	Chondrichthyes	*Areyonga*	Ord [Llvi]	Young 1997; 30377

Notes

[1] Homoscleromorpha has recently been elevated to class rank; see (*166*).

[2] The affinities of the 'Anabaratids' are uncertain; we treat this grouping as a cnidarian-grade.

[3] *Mickwitzia* is a stem brachiopod, but may have Linguliformea affinities

[4] *Salanygolina*, also a stem brachiopod, shows affinities with the Rhyncholiformea

[5] Coeloscleritophora: halwaxiids form an accepted clade and have thus been removed from Coeloscleritophora. The phylogenetic affinities of remaining taxa remain uncertain, and thus they have been treated as a paraphyletic (but morphologically disparate) group.

[6] *Tesnusocaris* is very unlikely to be stem Remipedia – see (*167*); as this is the only fossil taxon known, we have left this in our compilation pending further analyses

Table S2.
Tally of first occurrences of phyla and classes per geologic Period across the Phanerozoic.
Classes were additionally categorized according to presence of readily fossilizable hard parts (Hard) or as predominantly soft-bodied (Soft).
F.O., first occurences; **E**, Early; **M**, Middle; **L**, Late; **R**, Recent; **T**, total first occurrences for each Period;
C, cumulative total occurrences.

	Ediacaran					Cambrian					Ordovician					Silurian				
	E	**M**	**L**	**T**	**C**	**E**	**M**	**L**	**T**	**C**	**E**	**M**	**L**	**T**	**C**	**E**	**M**	**L**	**T**	**C**
Phyla																				
Phyla F.O.'s	0	0	2	2	2	23	1	1	25	27	0	0	0	0	27	0	0	0	0	27
Hard																				
Class F.O.'s	0	0	0	0	0	47	10	1	58	58	13	3	3	19	77	0	1	0	1	78
Soft																				
Class F.O.'s	0	0	0	0	0	29	6	4	39	39	2	0	3	5	44	1	0	0	1	45
Total																				
Class F.O.'s	0	0	0	0	0	76	16	5	97	97	15	3	6	24	121	1	1	0	2	123

	Devonian					Carboniferous					Permian					Triassic				
	E	**M**	**L**	**T**	**C**	**E**	**M**	**L**	**T**	**C**	**E**	**M**	**L**	**T**	**C**	**E**	**M**	**L**	**T**	**C**
Phyla																				
Phyla F.O.'s	0	0	0	0	27	3	0	0	3	30	0	0	0	0	30	0	0	0	0	30
Hard																				
Class F.O.'s	0	0	0	0	78	1	0	0	1	79	0	0	0	0	79	0	0	0	0	79
Soft																				
Class F.O.'s	2	0	0	2	47	3	0	3	6	53	1	0	0	1	54	0	0	0	0	54
Total																				
Class F.O.'s	2	0	0	2	125	4	0	3	7	132	1	0	0	1	133	0	0	0	0	133

	Jurassic					Cretaceous					Paleogene					Neogene				
	E	M	L	T	C	E	M	L	T	C	E	M	L	T	C	E	M	L	T	C
Phyla																				
Phyla F.O.'s	0	0	1	1	31	0	0	0	0	31	0	2	0	2	33	0	0	0	0	33
Hard																				
Class F.O.'s	0	0	0	0	79	0	0	0	0	79	0	0	0	0	79	0	0	0	0	79
Soft																				
Class F.O.'s	0	0	2	2	56	0	0	1	1	57	0	2	0	2	59	0	0	0	0	59
Total																				
Class F.O.'s	0	0	2	2	135	0	0	1	1	136	0	2	0	2	138	0	0	0	0	138

	Quarternary		
	R	T	C
Phyla			
Phyla F.O.'s	0	0	33
Hard			
Class F.O.'s	1	1	80
Soft			
Class F.O.'s	28	28	87
Total			
Class F.O.'s	29	29	167

Table S3.
Cambrian-resolution of first occurrences.
Cambrian first occurrence tallies resolved to the new stratigraphic framework, including hard- and soft-part classes (see Table S2), and class-level stem lineages (see Methods). **F.O.**, first occurrence; **T**, total occurrences.

	Cambrian										
	Early				Middle			Late			
Stage #	**1**	**2**	**3**	**4**	**5**	**6**	**7**	**8**	**9**	**10**	**T**
Phyla											
Phyla F.O.'s	6	5	12	0	1	0	0	0	1	0	25
Hard											
Class F.O.'s	15	14	17	1	8	1	1	0	1	0	58
stem class F.O.'s	6	5	9	1	6	1	0	0	0	0	28
Soft											
Class F.O.'s	2	3	24	0	5	1	0	4	0	0	39
stem class F.O.'s	2	3	13	0	2	0	0	0	0	0	20
Total											
Phyla F.O.'s	6	5	12	0	1	0	0	0	1	0	25
Class F.O.'s	17	17	41	1	13	2	1	4	1	0	97
stem class F.O.'s	8	8	22	1	8	1	0	0	0	0	48
Cumulative Total											
Phyla F.O.'s	6	11	23	23	24	24	24	24	25	25	
Class F.O.'s	17	34	75	76	89	91	92	96	97	97	
stem class F.O.'s	8	16	38	39	47	48	48	48	48	48	

Table S4.
Molecular clock calibration points.

Taxon 1	Taxon 2	Upper limit	Lower limit	Source
Dendraster	Encope	-1	50	Peterson et al., 2004
Dendraster	Eucidaris	-1	255	Peterson et al., 2004
Dendraster	Asterina	-1	480	Peterson et al., 2004
Dendraster	Antedon	525	485	Peterson et al., 2008
Dendraster	Saccoglossus	565	-1	Peterson et al., 2008; Liu et al., 2010*
M_edulis	M_californianus	-1	20	Peterson et al., 2004
M_edulis	Modiolus	-1	325	Peterson et al., 2004
M_edulis	Nucula	-1	485	Peterson et al., 2004
Haliotis	Crepidula	-1	500	Peterson and Butterfield, 2005
M_edulis	Crepidula	548	530	Peterson et al., 2008**
Lestes	Enallagma	-1	120	Peterson et al., 2004
Drosophila	Aedes	295	235	Peterson et al., 2004; Benton and Donoghue, 2007
Anopheles	Enallagma	-1	325	Peterson et al., 2004
Priapulus	Drosophila	-1	522	Benton and Donoghue, 2007***
Drosophila	Daphnia	-1	500	Walossek, 1995****
Daphnia	Rhipicephalus	-1	515	Rota-Stabelli et al., 2010; Maloof et al., 2010*****
Anolis	Gallus	299	259	Benton and Donoghue, 2007
Gallus	Homo	330	312	Benton and Donoghue, 2007
Xenopus	Homo	350	330	Benton and Donoghue, 2007
Homo	Monodelphis	138	124	Benton and Donoghue, 2007
Rattus	Homo	100	61	Benton and Donoghue, 2007
Homo	Danio	421	416	Benton and Donoghue, 2007
Danio	Tetraodon	165	149	Benton and Donoghue, 2007
Geodia	Verongula	713	-1	Peterson et al., 2008; Sperling et al., 2010

* Same justification as in (*14*) for the earliest putative bilaterian trace fossils providing a maximum on the origin of Ambulacraria, but shifted 10 Ma earlier due to the discovery of trace fossils in the Mistaken Point Formation by (*42*).
** Maximum age shifted to 548 Ma to accommodate the formal possibility that some undescribed forms in the Nama Group, Namibia, which hosts the earliest biomineralizing fossils, may represent conchiferan molluscs.
*** (*168*) provides a minimum for the divergence between nematodes and arthropods, but the same minimum can be applied to the divergence between arthropods and priapulids. Age for the middle Tommotian adjusted slightly based on new ages in (*169*).
**** The Orsten fossil *Rehbachiella* is a likely branchiopod crustacean, providing a minimum age estimate for this divergence.

*****As trilobites are likely stem-mandibulates (*71*), the first appearance of trilobites sets a minimum for this node. Trilobites first appear in the Atdabanian, and we have adopted a conservative estimate of 515 for the Atdabanian-Botomian boundary based on the chronology presented in (*169*). The fossil *Yicaris* (*147*) from the Lower Cambrian of China also provides another example of Lower Cambrian (Atdabanian) pancrustaceans.

Table S5.
Higher-level groupings of Ediacaran Organisms: This proposed classification utilizes morphological and implied behavioral data such as branching or segment architecture, body symmetry, associated trace fossils, and growth parameters in order to subdivide the Ediacara biota into distinct clades. See methods for additional details.
A = Avalon assemblage; **WS** = White Sea assemblage; **N** = Nama assemblage

Clades	Genus	Species	First Occ	Last Occ
Rangeomorpha			**A**	**N**
	Avalofractus	*abaculus*	A	A
	Beothukis	*mistakensis*	A	WS
	Bradgatia	*linfordensis*	A	WS
	Charnia	*masoni*	A	N
	Charnia	*antecedens*	A	WS
	Fractofusus	*misrai*	A	A
	Fractofusus	*andersoni*	A	A
	Frondophyllas	*grandis*	A	A
	Haspidophyllas	*flexibilis*	A	A
	Pectinifrons	*abyssalis*	A	A
	Rangea	*schneiderhoehni*	WS	N
	Trepassia	*wardae*	A	A
Erniettomorpha			**WS**	**N**
	Ernietta	*plateauensis*	N	N
	Nasepia	*altae*	N	N
	Palaeoplatoda	*segmentata*	WS	WS
	Phyllozoon	*hanseni*	WS	WS
	Pteridinium	*simplex*	WS	N
	Swartpuntia	*germsi*	WS	N
	Valdainia	*plumosa*	WS	WS
Dickinsoniomorpha			**WS**	**WS**
	Andiva	*ivantsovi*	WS	WS
	Dickinsonia	*brachina*	WS	WS
	Dickinsonia	*costata*	WS	WS
	Dickinsonia	*lissa*	WS	WS
	Dickinsonia	*rex*	WS	WS
	Dickinsonia	*tenuis*	WS	WS
	Epibaion	*axiferus*	WS	WS
	Windermeria	*aitkeni*	WS	WS
	Yorgia	*waggoneri*	WS	WS

Arboreomorpha			**A**	**N**
	Charniodiscus	*arboreus*	A	WS
	Charniodiscus	*concentricus*	A	WS
	Charniodiscus	*longus*	WS	WS
	Charniodiscus	*oppositus*	WS	WS
	Charniodiscus	*procerus*	A	WS
	Charniodiscus	*spinosus*	A	A
	Khatyspytia	*grandis*	N	N
	Vaizitsinia	*sophia*	WS	WS
Triradialomorpha			**A**	**WS**
	Albumares	*brunsae*	WS	WS
	Anfesta	*stankovskii*	WS	WS
	Pomoria	*corolliformis*	WS	WS
	Skinnera	*brooksi*	WS	WS
	Tribrachidium	*heraldicum*	WS	WS
	Triforillonia	*costellae*	A	A
Kimberellomorpha			**WS**	**WS**
	Kimberella	*quadrata*	WS	WS
	Solza	*margarita*	WS	WS

Likely Clades	**Genus**	**Species**	**First Occ**	**Last Occ**
Bilateralomorpha			**WS**	**WS**
	Archaeaspinus	*fedonkini*	WS	WS
	Cyanorus	*singularis*	WS	WS
	Ivovicia	*regulosa*	WS	WS
	Kharakhtia	*nessovi*	WS	WS
	Lossina	*lissetskii*	WS	WS
	Marywadea	*ovata*	WS	WS
	Onega	*stepanovi*	WS	WS
	Paravendia	*janae*	WS	WS
	Parvancorina	*minchami*	WS	WS
	Parvancorina	*saggita*	WS	WS
	Spriggina	*floundersi*	WS	WS
	Temnoxa	*molluscula*	WS	WS
	Vendia	*rachiata*	WS	WS
	Vendia	*sokolovi*	WS	WS
Tetraradialomorpha			**WS**	**WS**
	Conomedusites	*lobatus*	WS	WS

Pentaradialomorpha			**WS**	**WS**
	Arkarua	*adami*	WS	WS

Sponges			**A**	**N**
	Ausia	*fenestrata*	WS	N
	Palaeophragmodictya	*reticulata*	WS	WS
	Rugoconites	*enigmatis*	WS	WS
	Rugoconites	*tenuirugosus*	WS	WS
	Thectardis	*avalonensis*	A	A

Valid			**A**	**N**
	Armillifera	*parva*	WS	WS
	Beltanelliformis	*brunsae*	WS	N
	Bomakellia	*kelleri*	WS	WS
	Bronicella	*podolica*	WS	WS
	Chondroplon	*bilobatum*	WS	WS
	Corumbella	*werneri*	N	N
	Eoandromeda	*octobrachiata*	D*	WS
	Eoporpita	*medusa*	WS	WS
	Funisia	*dorothea*	WS	WS
	Hadrynichorde	*catalenensis*	A	A
	Hadryniscala	*avalonica*	A	A
	Hiemalora	*stellaris*	A	N
	Inaria	*karli*	WS	WS
	Lomosovis	*malus*	WS	WS
	Mawsonites	*spriggi*	WS	WS
	Nemiana	*simplex*	WS	WS
	Ovatoscutum	*concentricum*	WS	WS
	Palaeopascichnus	*delicatus*	A	WS
	Paracharina	*dengyingensis*	WS	WS
	Parviscopa	*bonavistensis*	A	A
	Primocandelabrum	*hemialoranum*	A	A
	Somatohelix	*sinuosus*	WS	WS
	Ventogyrus	*chistyakovi*	WS	WS
	Yangtziramulus	*zhangi*	N	N
	Yelovichnus	*gracillis*	WS	WS

Removed	**Genus**	**Species**		
	Anabylia	*improvisa*		
	Archangelia	*valdaica*		

	Askinica	*sp.*		
	Aspidella	*costata*		
	Aspidella	*hatyspytia*		
	Aspidella	*terranovica*		
	Baikalina	*sessilis*		
	Barmia	*lobatus*		
	Beltanella	*gilesi*		
	Beltanelloides	*sorichevae*		
	Blackbrookia	*oaksi*		
	Bonata	*septata*		
	Brachina	*delicata*		
	Charnia	*wardi*		
	Charnia	*grandis*		
	Cyclomedusa	*davidi*		
	Cyclomedusa	*radiata*		
	Cyclomedusa	*gigantea*		
	Cyclomedusa	*plana*		
	Cyclomedusa	*minima*		
	Cyclomedusa	*delicata*		
	Ediacaria	*flindersi*		
	Elasenia	*aseevae*		
	Elasenia	*uralica*		
	Evmiaksia	*aksionovi*		
	Garania	*petali*		
	Gehlingia	*dibrachida*		
	Glaessneria	*imperfecta*		
	Irridinitus	*multiradiatus*		
	Ivesheadia	*lobata*		
	Jampolium	*wyrzhykoowskii*		
	Kaisalia	*levis*		
	Kaisalia	*mensae*		
	Khatyspytia	*grandis*		
	Kubisia	*glabra*		
	Madigania	*annulata*		
	Medusinites	*asteroides*		
	Medusinites	*paliji*		
	Medusinites	*patellaris*		
	Mialsemia	*semichatovi*		

	Nadalina	*yukonensis*		
	Namiana	*bakeevi*		
	Nimbia	*dniesteri*		
	Nimbia	*occlusa*		
	Nimbia	*paula*		
	Orthogonium	*parallelum*		
	Paliella	*patelliformis*		
	Paramedusium	*africanum*		
	Planomedusites	*patellaris*		
	Platyopholinia	*pholata*		
	Podolimirus	*mirus*		
	Protodipleurosoma	*wardi*		
	Protodipleurosoma	*rugulosum*		
	Pseudovendia	*charnwoodensis*		
	Ramellina	*pennata*		
	Sekwia	*excentrica*		
	Shepshedia	*palmata*		
	Spriggia	*wadea*		
	Stauinidia	*crucicula*		
	Tateana	*inflata*		
	Tirasiana	*cocardia*		
	Tirasiana	*disciformis*		
	Tirasiana	*coniformis*		
	Tirasiana	*concentralis*		
	Velancorina	*martina*		
	Vendella	*haelenicae*		
	Vendella	*sokolovi*		
	Vendella	*larini*		
	Vendomia	*menneri*		
	Veprina	*undosa*		
	Vladimissa	*missarzhevskii*		

Table S6.
Summary of Ediacaran clades by biostratigraphic zone. The first appearance of a clade is indicated by **XX**; clade presence by **X**. The number of genera first appearing in each assemblage is shown, as well as the standing generic diversity.

First occurrence	Avalon	White Sea	Nama
CLADES/Gen first Occ	18	53	5
Gen total	18	59	12
Arboreomorphs	xx	x	x
Rangeomorphs	xx	x	x
Sponges	xx	x	x
Triradialomorphs	xx	x	-
Bilateralomorphs	-	xx	-
Erniettomorphs	-	xx	x
Kimberellomorph	-	xx	-
Pentaradialomorphs	-	xx	-
Dickinsoniomorph	-	xx	-
Tetraradialomorphs	-	xx	-

Figure S1. Phylogenetic tree derived from the analyses of our new data set. Analyses performed using MrBayes and two unlinked GTR + G models, see Methods for details.

Figure S2. Chronogram derived dating Fig. S1. Molecular clock analyses performed using Phylobayes, see Methods for settings.

Figure S3. Chronogram derived dating a modification of Fig. 1 in which the sponge lineages and the Placozoa are arranged according to Sperling et al. (2009), see Methods for settings.

Figure S4. Chronogram derived dating a modification of Fig. 1 in which the sponge lineages and the Placozoa are arranged according to Philippe et al. (2009), see Methods for settings.

Figure S5. The effect of relaxing the soft bound on the estimated divergence times. In Blue: Dates obtained using a soft bound relaxation level of 5%. In Red: Dates obtained using a soft bound relaxation level of 10%. In Green: Dates obtained using a soft bound relaxation level of 20%. In Purple: Dates obtained using a soft bound relaxation level of 50%. Fixed parameters (all panels): molecular clock model (CIR) and root prior age 1000 Ma (SD = 100 Ma). (A) Dates recovered using the topology of Fig. 1. (B) Dates recovered using the topology of Fig. S1 and S2. (C) Dates recovered using the topology of Fig. S3. (D) Dates recovered using the topology of Fig. S4. On the X axis nodes from Fig.1(Panel A), Fig. S1 and S2 (Panel B), Fig. S3 (Panel C) and Fig. S4 (Panel D) ordered according to their age. On the Y axis: Nodes age.

Figure S6. The effect of relaxing the soft bound on the estimated divergence times. In Blue: Dates obtained using a soft bound relaxation level of 5%. In Red: Dates obtained using a soft bound relaxation level of 10%. In Green: Dates obtained using a soft bound relaxation level of 20%. In Purple: Dates obtained using a soft bound relaxation level of 50%. Fixed parameters (all panels): molecular clock model (UGM) and root prior age 1000 Ma (SD = 100 Ma). (A) Dates recovered using the topology of Fig. 1. (B) Dates recovered using the topology of Fig. S1 (see also S2). (C) Dates recovered using the topology of Fig. S3. (D) Dates recovered using the topology of Fig. S4. On the X axis nodes from Fig.1(Panel A), Fig. S1 and S2 (Panel B), Fig. S3 (Panel C) and Fig. S4 (Panel D) ordered according to their age. On the Y axis: Nodes age.

Figure S7. The effect of phylogenetic uncertainty on node age. In Blue: Dates obtained using the topology of Fig. 1. In Green: Dates obtained using the topology in Fig. S2. In Red: Dates obtained using the topology in Fig. S3. In Purple: Dates obtained using the topology in Fig. S4. (A) Fixed parameters: Root age, 1000 Ma (SD = 100 Ma), molecular clock model used (CIR), soft bound relaxation level (20%). (B) Fixed parameters: Root age, 1000 Ma (SD = 100 Ma), molecular clock model used (UGM), soft bound relaxation Level (20%). On the X axis: nodes from Database S2 that are common to all three considered tree topologies ordered according to their age. On the Y axis: Nodes age.

Figure S8. Comparison of optimal dates with corresponding values obtained from a 50-replicates, Jackknife analysis in which, for each replicate, 50% of the calibration points in Table S4 were deleted. In Blue: optimal dates. In Red: Jackknifed estimates. Fixed parameters: Molecular clock model (CIR), tree topology (Fig. 1), soft bound relaxation level (20%), root age prior (1000 MA, SD = 100 Ma). On the X axis nodes from the tree in Fig. 1 (see also Database S2) ordered according to their age. On the Y axis: Nodes age.

Figure S9. Effect of the Prior root age on the estimated divergence times. In Blue divergence times obtained using a prior root age of 1000 Ma (SD = 100 Ma). In Red estimated divergence times obtained using a prior root age of 1600 Ma (SD = 400 Ma). Fixed parameters: molecular clock model (CIR), and soft bound relaxation level (20%). (A) Tree topology (Fig. 1), (B) Tree topology Fig (S1 see also S2), (C) Tree topology (Fig. S3). (D) Tree topology (Fig. S4). . On the X axis nodes from Fig.1(Panel A), Fig. S1 and S2 (Panel B), Fig. S3 (Panel C) and Fig. S4 (Panel D) ordered according to their age. On the Y axis: Nodes age.

Figure S10. The effect of molecular clock model used on the estimated divergence times. In Blue: Dates obtained using the CIR model. In Red: dates obtained using the UGM model. Fixed Parameters (All panels): Root age of 1000 Ma (SD = 100 Ma), soft bound relaxation Level (20%). Other Fixed Parameters (A) Tree topology (Fig. 1). (B) Tree topology (Fig. S2). (C) Tree topology (Fig. S3). (D) Tree topology (Fig. S4). On the X axis nodes from Fig.1(Panel A), Fig. S1 and S2 (Panel B), Fig. S3 (Panel C) and Fig. S4 (Panel D) ordered according to their age. On the Y axis: Nodes age.

Fig S1

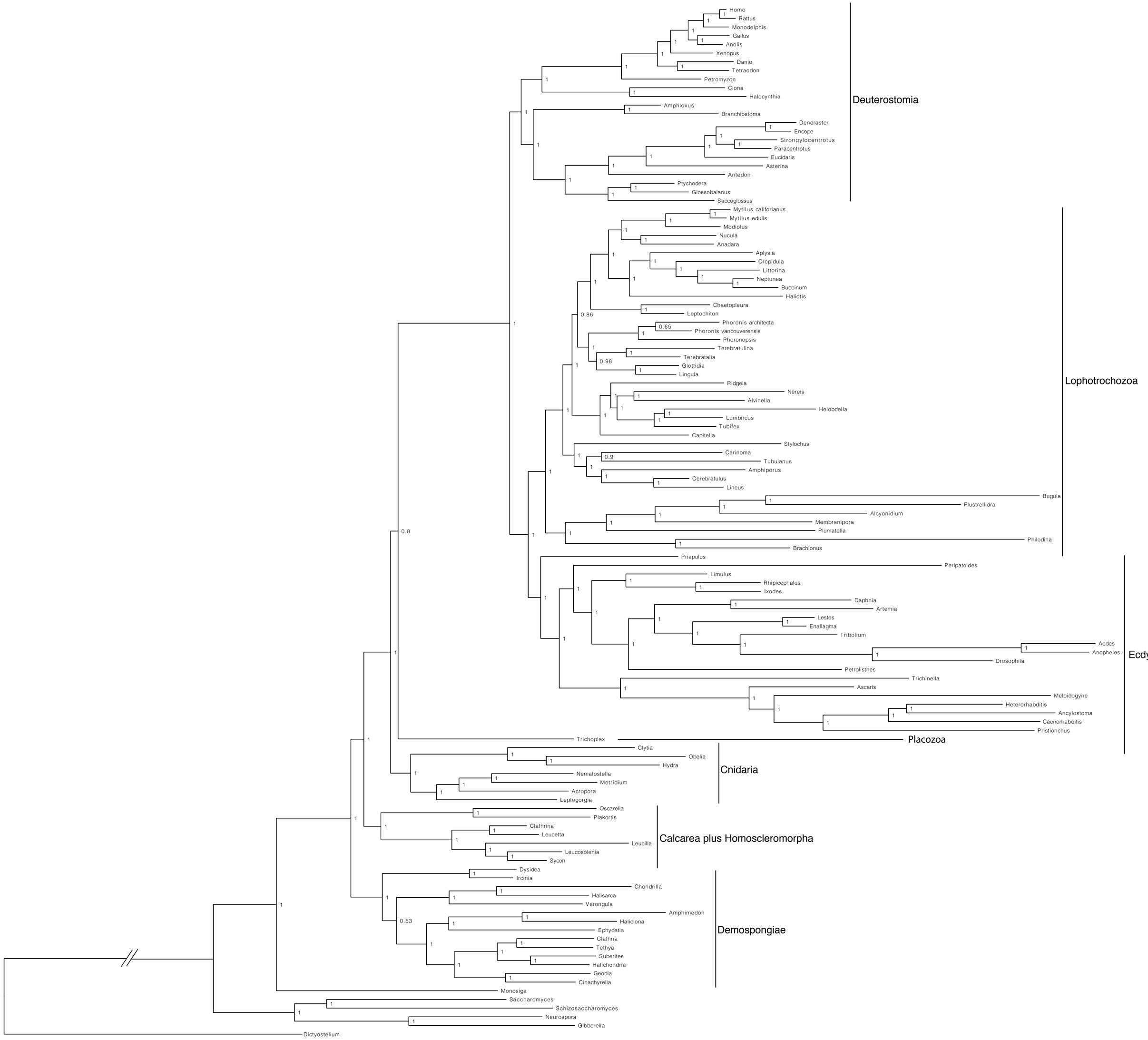
Homo
Rattus
Monodelphis
Gallus
Anolis
Xenopus
Danio
Tetraodon
Petromyzon
Ciona
Halocynthia
Amphioxus
Branchiostoma
Dendraster
Encope
Strongylocentrotus
Paracentrotus
Eucidaris
Asterina
Antedon
Ptychodera
Glossobalanus
Saccoglossus
Deuterostomia
Mytilus californianus
Mytilus edulis
Modiolus
Nucula
Anadara
Aplysia
Crepidula
Littorina
Neptunea
Buccinum
Haliotis
Chaetopleura
Leptochiton
Phoronis architecta
Phoronis vancouverensis
Phoronopsis
Terebratulina
Terebratalia
Glottidia
Lingula
Ridgeia
Nereis
Alvinella
Helobdella
Lumbricus
Tubifex
Capitella
Stylochus
Carinoma
Tubulanus
Amphiporus
Cerebratulus
Lineus
Lophotrochozoa
Bugula
Flustrellidra
Alcyonidium
Membranipora
Plumatella
Philodina
Brachionus
Priapulus
Peripatoides
Limulus
Rhipicephalus
Ixodes
Daphnia
Artemia
Lestes
Enallagma
Tribolium
Aedes
Anopheles
Drosophila
Petrolisthes
Trichinella
Ascaris
Meloidogyne
Heterorhabditis
Ancylostoma
Caenorhabditis
Pristionchus
Ecdysozoa
Trichoplax
Placozoa
Clytia
Obelia
Hydra
Nematostella
Metridium
Acropora
Leptogorgia
Cnidaria
Oscarella
Plakortis
Clathrina
Leucetta
Leucilla
Leucosolenia
Sycon
Calcarea plus Homoscleromorpha
Dysidea
Ircinia
Chondrilla
Halisarca
Verongula
Amphimedon
Haliclona
Ephydatia
Clathria
Tethya
Suberites
Halichondria
Geodia
Cinachyrella
Demospongiae
Monosiga
Saccharomyces
Schizosaccharomyces
Neurospora
Gibberella
Dictyostelium
1
0.8
0.86
0.65
0.98
0.9
0.53

Fig. S2

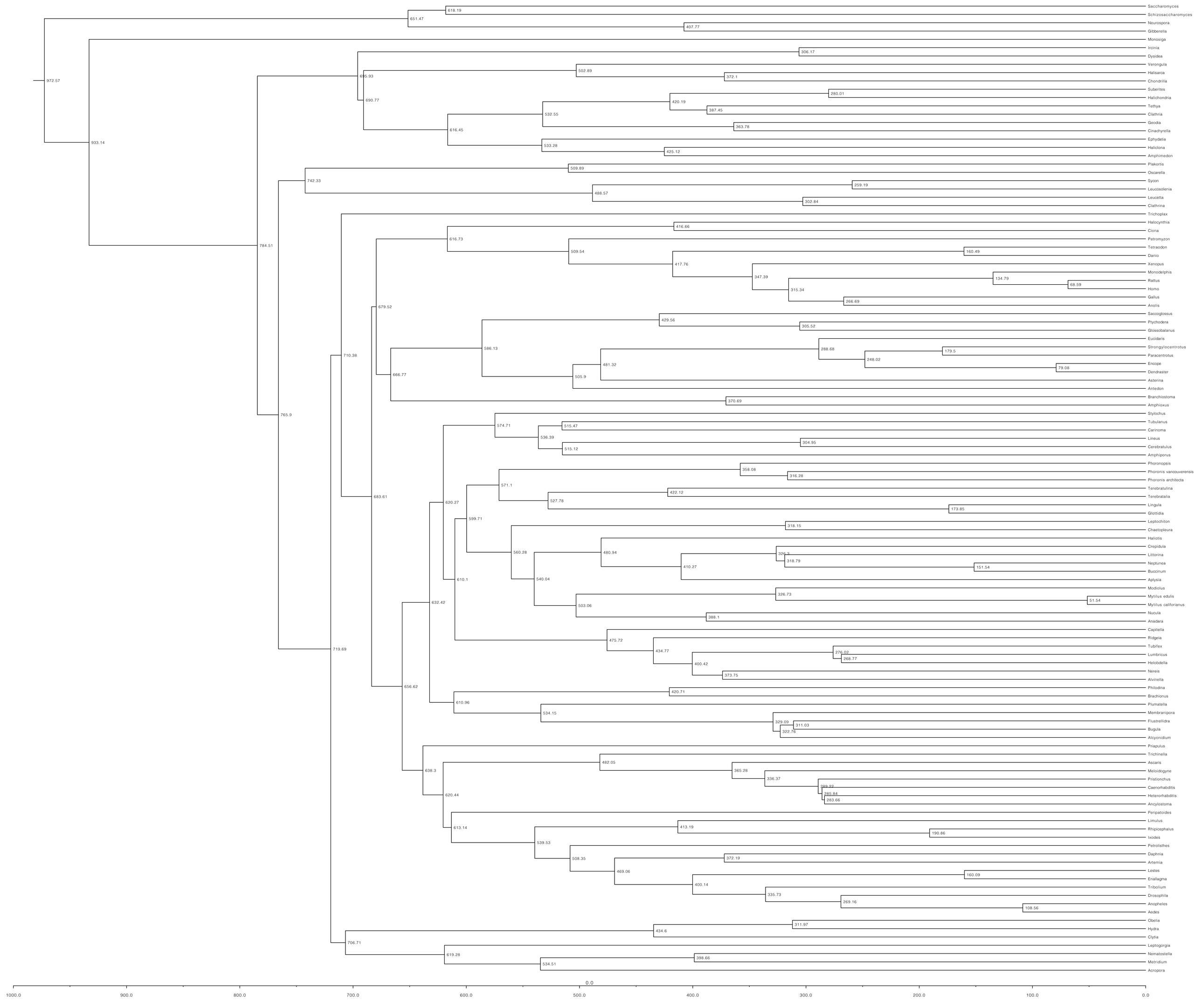
Saccharomyces
Schizosaccharomyces
Neurospora
Gibberella
Monosiga
Ircinia
Dysidea
Verongula
Halisarca
Chondrilla
Suberites
Halichondria
Tethya
Clathria
Geodia
Cinachyrella
Ephydatia
Haliclona
Amphimedon
Plakortis
Oscarella
Sycon
Leucosolenia
Leucetta
Clathrina
Trichoplax
Halocynthia
Ciona
Petromyzon
Tetraodon
Danio
Xenopus
Monodelphis
Rattus
Homo
Gallus
Anolis
Saccoglossus
Ptychodera
Glossobalanus
Eucidaris
Strongylocentrotus
Paracentrotus
Encope
Dendraster
Asterina
Antedon
Branchiostoma
Amphioxus
Stylochus
Tubulanus
Carinoma
Lineus
Cerebratulus
Amphiporus
Phoronopsis
Phoronis vancouverensis
Phoronis architecta
Terebratulina
Terebratalia
Lingula
Glottidia
Leptochiton
Chaetopleura
Haliotis
Crepidula
Littorina
Neptunea
Buccinum
Aplysia
Modiolus
Mytilus edulis
Mytilus californianus
Nucula
Anadara
Capitella
Ridgeia
Tubifex
Lumbricus
Helobdella
Nereis
Alvinella
Philodina
Brachionus
Plumatella
Membranipora
Flustrellidra
Bugula
Alcyonidium
Priapulus
Trichinella
Ascaris
Meloidogyne
Pristionchus
Caenorhabditis
Heterorhabditis
Ancylostoma
Peripatoides
Limulus
Rhipicephalus
Ixodes
Petrolisthes
Daphnia
Artemia
Lestes
Enallagma
Tribolium
Drosophila
Anopheles
Aedes
Obelia
Hydra
Clytia
Leptogorgia
Nematostella
Metridium
Acropora
618.19
651.47
407.77
306.17
502.89
372.1
635.93
690.77
280.01
420.19
387.45
532.55
363.78
616.45
533.28
425.12
972.57
933.14
509.89
742.33
259.19
488.57
302.84
416.66
616.73
509.54
160.49
417.76
347.39
134.79
68.59
315.34
266.69
784.51
679.52
429.56
305.52
586.13
288.68
179.5
248.02
79.08
481.32
505.9
666.77
370.69
710.38
765.9
574.71
515.47
536.39
304.95
515.12
358.08
316.28
571.1
422.12
527.78
173.85
620.27
599.71
318.15
560.28
480.94
326.3
318.79
410.27
151.54
610.1
540.04
326.73
51.54
632.42
503.06
388.1
475.72
434.77
276.02
268.77
400.42
373.75
683.61
656.62
420.71
610.96
534.15
329.09
311.03
322.76
638.3
482.05
365.28
336.37
289.22
285.84
283.66
620.44
613.14
413.19
190.86
539.53
508.35
372.19
469.06
160.09
400.14
335.73
269.16
108.56
719.69
311.97
434.6
706.71
619.28
398.66
534.51
1000.0
900.0
800.0
700.0
600.0
500.0
400.0
300.0
200.0
100.0
0.0
0.0

Fig. S3

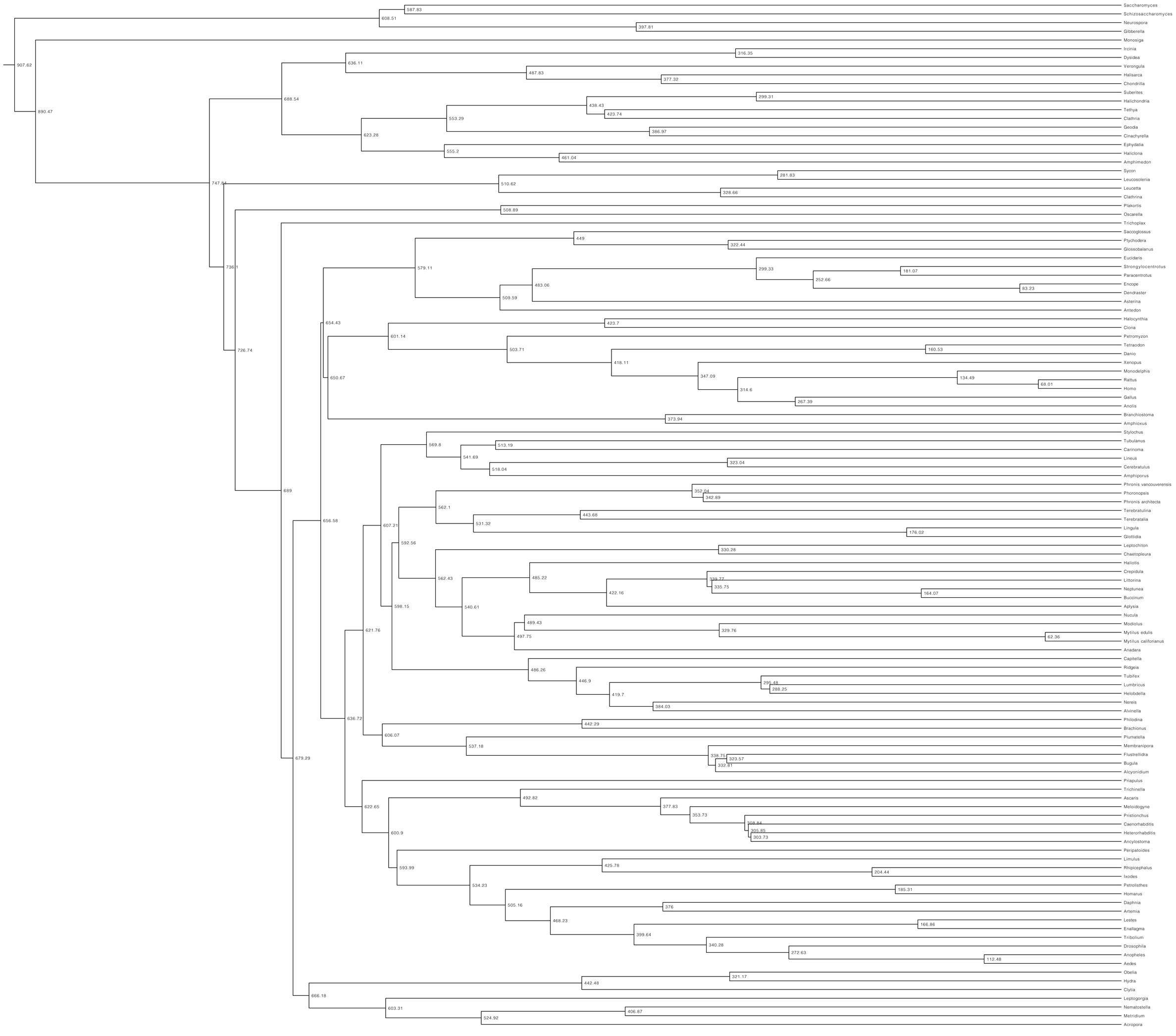
Saccharomyces
Schizosaccharomyces
Neurospora
Gibberella
Monosiga
Ircinia
Dysidea
Verongula
Halisarca
Chondrilla
Suberites
Halichondria
Tethya
Clathria
Geodia
Cinachyrella
Ephydatia
Haliclona
Amphimedon
Sycon
Leucosolenia
Leucetta
Clathrina
Plakortis
Oscarella
Trichoplax
Saccoglossus
Ptychodera
Glossobalanus
Eucidaris
Strongylocentrotus
Paracentrotus
Encope
Dendraster
Asterina
Antedon
Halocynthia
Ciona
Petromyzon
Tetraodon
Danio
Xenopus
Monodelphis
Rattus
Homo
Gallus
Anolis
Branchiostoma
Amphioxus
Stylochus
Tubulanus
Carinoma
Lineus
Cerebratulus
Amphiporus
Phronis vancouverensis
Phoronopsis
Phronis architecta
Terebratulina
Terebratalia
Lingula
Glottidia
Leptochiton
Chaetopleura
Haliotis
Crepidula
Littorina
Neptunea
Buccinum
Aplysia
Nucula
Modiolus
Mytilus edulis
Mytilus californianus
Anadara
Capitella
Ridgeia
Tubifex
Lumbricus
Helobdella
Nereis
Alvinella
Philodina
Brachionus
Plumatella
Membranipora
Flustrellidra
Bugula
Alcyonidium
Priapulus
Trichinella
Ascaris
Meloidogyne
Pristionchus
Caenorhabditis
Heterorhabditis
Ancylostoma
Peripatoides
Limulus
Rhipicephalus
Ixodes
Petrolisthes
Homarus
Daphnia
Artemia
Lestes
Enallagma
Tribolium
Drosophila
Anopheles
Aedes
Obelia
Hydra
Clytia
Leptogorgia
Nematostella
Metridium
Acropora
907.62
890.47
747.64
736.1
726.74
689
656.58
679.29
666.18
636.11
487.83
377.32
688.54
623.28
553.29
438.43
423.74
386.97
299.31
555.2
461.04
510.62
281.83
328.66
508.89
449
322.44
579.11
483.06
509.59
299.33
181.07
252.66
83.23
654.43
601.14
503.71
418.11
347.09
314.6
267.39
423.7
160.53
134.49
68.01
650.67
373.94
569.8
513.19
541.69
518.04
323.04
352.04
342.89
562.1
531.32
443.68
176.02
607.21
592.56
598.15
562.43
540.61
485.22
422.16
339.77
335.75
164.07
330.28
489.43
497.75
329.76
62.36
621.76
636.72
606.07
537.18
442.29
338.75
323.57
332.81
486.26
446.9
419.7
295.48
288.25
384.03
622.65
600.9
492.82
377.83
353.73
308.84
305.85
303.73
593.99
534.23
505.16
468.23
425.78
204.44
185.31
376
399.64
166.86
340.28
272.63
112.48
442.48
321.17
603.31
524.92
406.87
0.0
900.0
800.0
700.0
600.0
500.0
400.0
300.0
200.0
100.0
0.0

Fig.S4

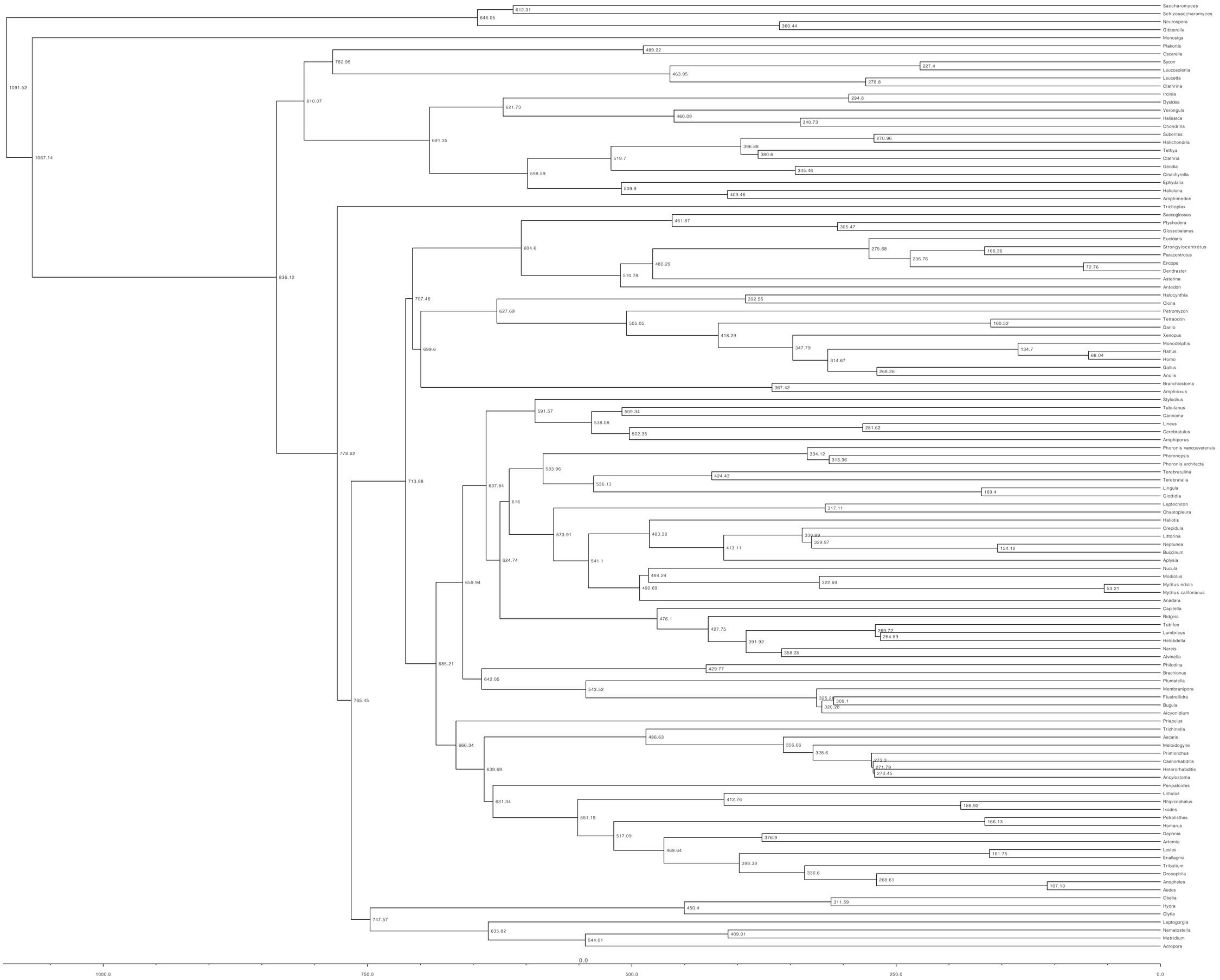
Saccharomyces
Schizosaccharomyces
Neurospora
Gibberella
Monosiga
Plakortis
Oscarella
Sycon
Leucosolenia
Leucetta
Clathrina
Ircinia
Dysidea
Verongula
Halisarca
Chondrilla
Suberites
Halichondria
Tethya
Clathria
Geodia
Cinachyrella
Ephydatia
Haliclona
Amphimedon
Trichoplax
Saccoglossus
Ptychodera
Glossobalanus
Eucidaris
Strongylocentrotus
Paracentrotus
Encope
Dendraster
Asterina
Antedon
Halocynthia
Ciona
Petromyzon
Tetraodon
Danio
Xenopus
Monodelphis
Rattus
Homo
Gallus
Anolis
Branchiostoma
Amphioxus
Stylochus
Tubulanus
Carinoma
Lineus
Cerebratulus
Amphiporus
Phoronis vancouverensis
Phoronopsis
Phoronis architecta
Terebratulina
Terebratalia
Lingula
Glottidia
Leptochiton
Chaetopleura
Haliotis
Crepidula
Littorina
Neptunea
Buccinum
Aplysia
Nucula
Modiolus
Mytilus edulis
Mytilus californianus
Anadara
Capitella
Ridgeia
Tubifex
Lumbricus
Helobdella
Nereis
Alvinella
Philodina
Brachionus
Plumatella
Membranipora
Flustrellidra
Bugula
Alcyonidium
Priapulus
Trichinella
Ascaris
Meloidogyne
Pristionchus
Caenorhabditis
Heterorhabditis
Ancylostoma
Peripatoides
Limulus
Rhipicephalus
Ixodes
Petrolisthes
Homarus
Daphnia
Artemia
Lestes
Enallagma
Tribolium
Drosophila
Anopheles
Aedes
Obelia
Hydra
Clytia
Leptogorgia
Nematostella
Metridium
Acropora
1091.52
646.05
612.31
360.44
1067.14
782.95
489.22
463.95
227.4
278.8
810.07
621.73
294.8
460.09
340.73
691.35
396.88
270.96
380.6
519.7
345.46
598.59
509.9
409.46
836.12
604.6
461.87
305.47
510.78
480.29
275.68
166.36
236.76
72.76
707.46
627.69
392.55
505.05
160.52
418.29
699.6
347.79
134.7
68.04
314.67
268.26
367.42
778.62
591.57
509.34
538.08
281.62
502.35
713.98
583.96
334.12
313.36
424.43
536.13
169.4
637.84
616
317.11
573.91
483.38
338.89
329.97
413.11
154.12
624.74
541.1
484.24
322.69
53.21
492.69
659.94
476.1
427.75
269.72
264.89
391.92
358.35
685.21
429.77
642.05
543.52
325.26
309.1
320.28
765.45
666.34
486.63
356.66
328.6
273.3
271.79
270.45
639.69
631.34
412.76
188.92
551.19
166.13
517.09
376.9
469.64
161.75
398.38
336.6
268.61
107.13
747.57
311.59
450.4
635.82
409.01
544.01
0.0
1000.0
750.0
500.0
250.0
0.0

Fig. S5

Nodes age

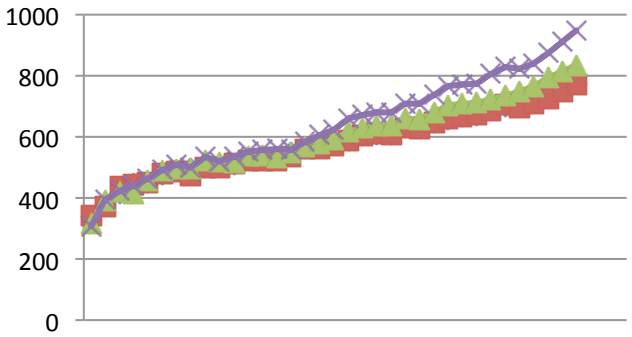

(A)

Nodes age

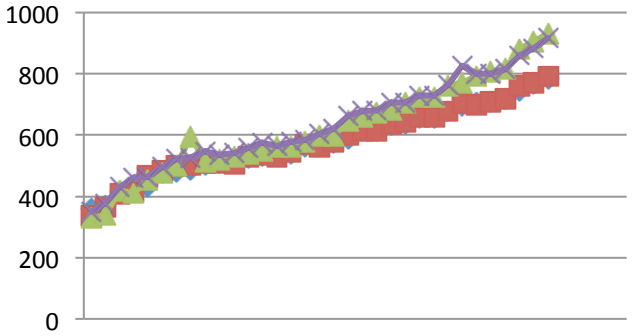

(B)

Nodes age

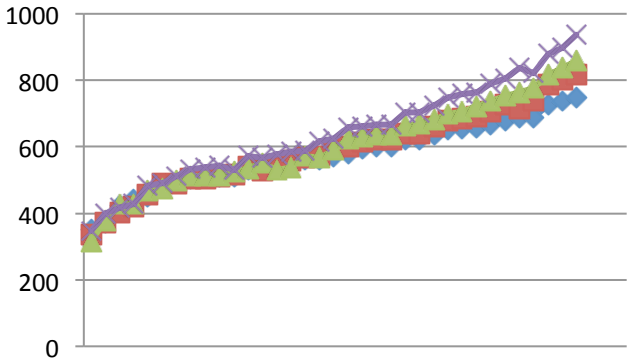

(C)

Nodes age

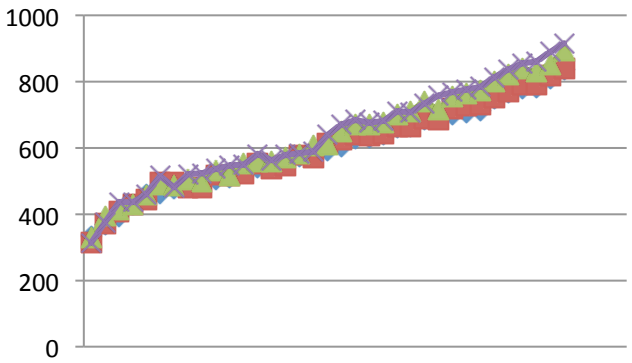

(D)

Fig. S6

Nodes age

(A)

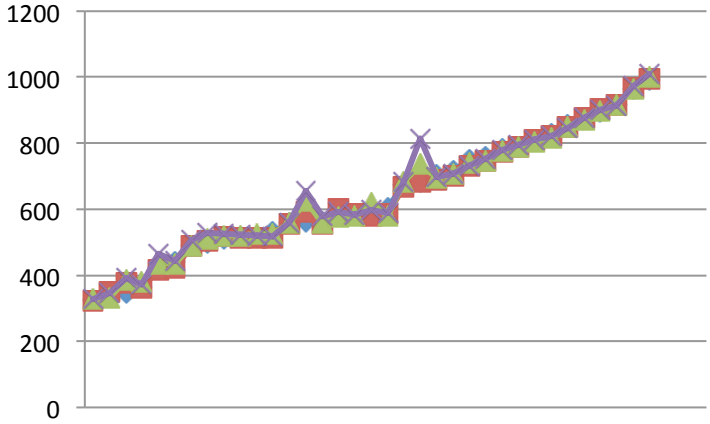

Nodes age

(B)

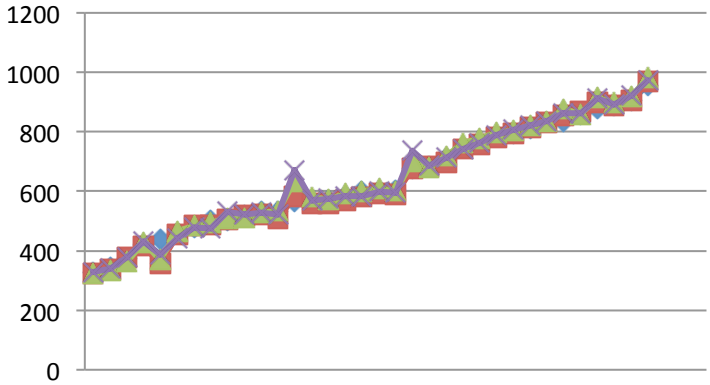

Nodes age

(C)

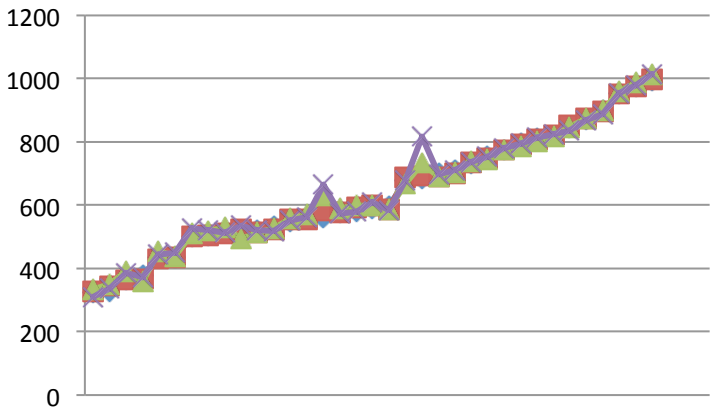

Nodes age

(D
)

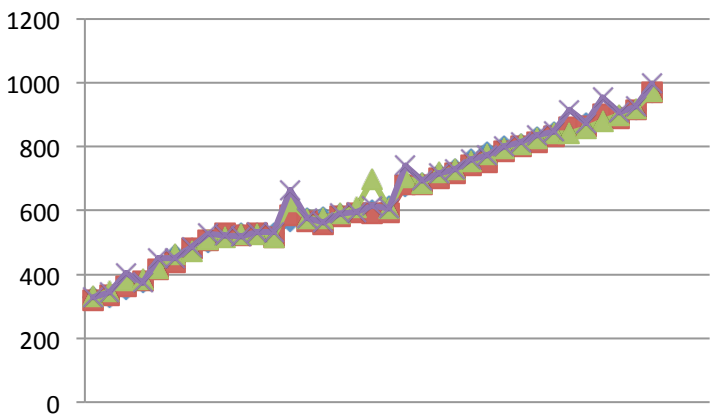

Fig. S7

Nodes age

(A)

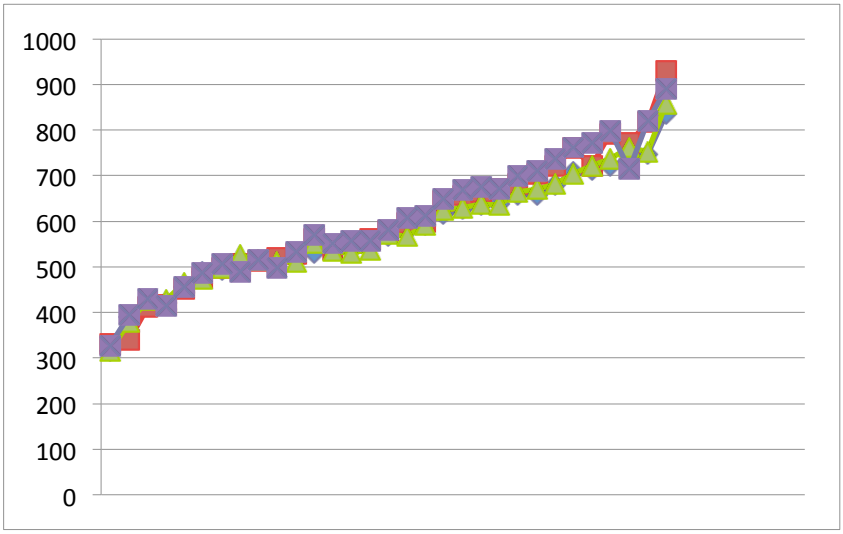

Nodes age

(B)

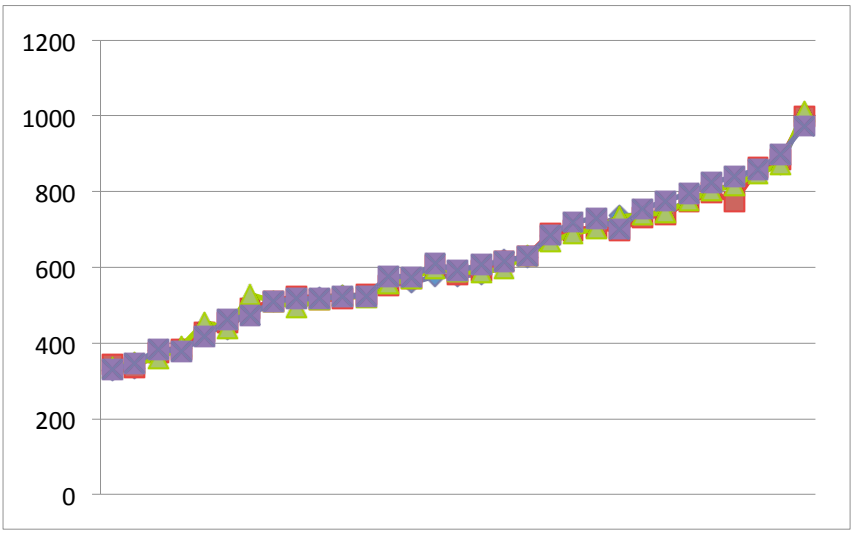

Fig. S8

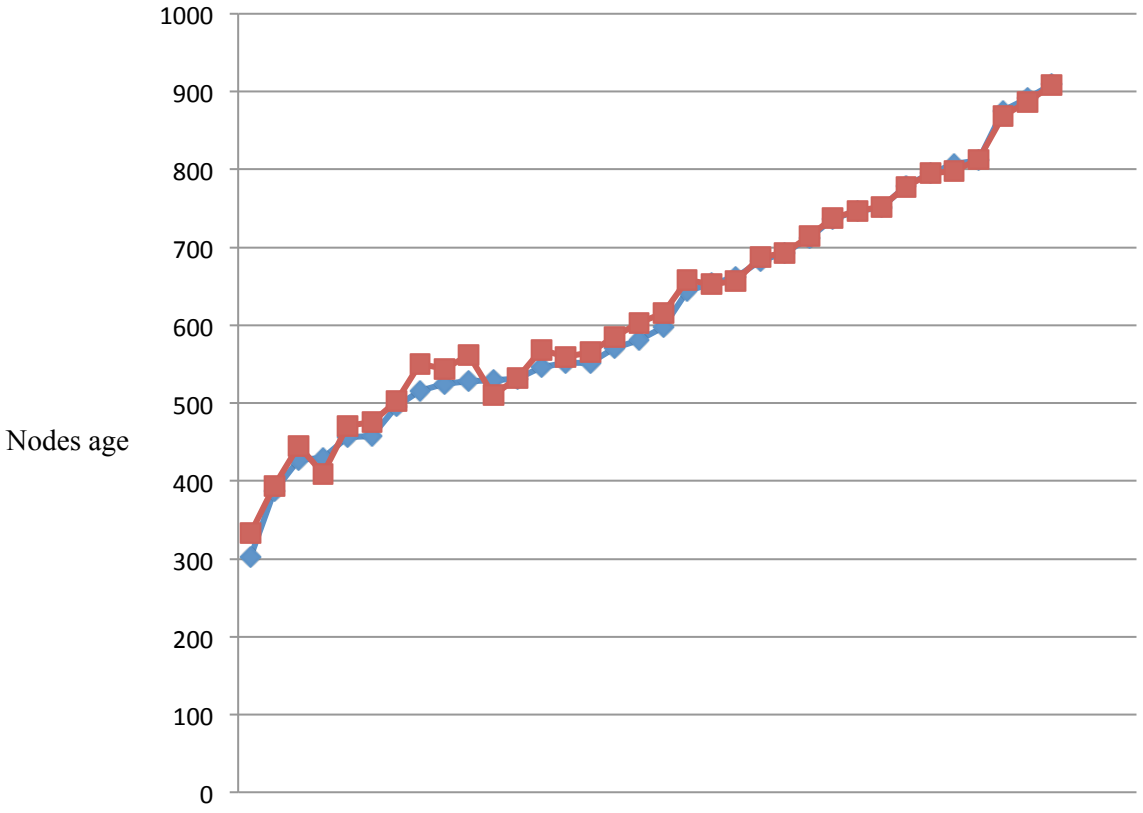

Fig. S9

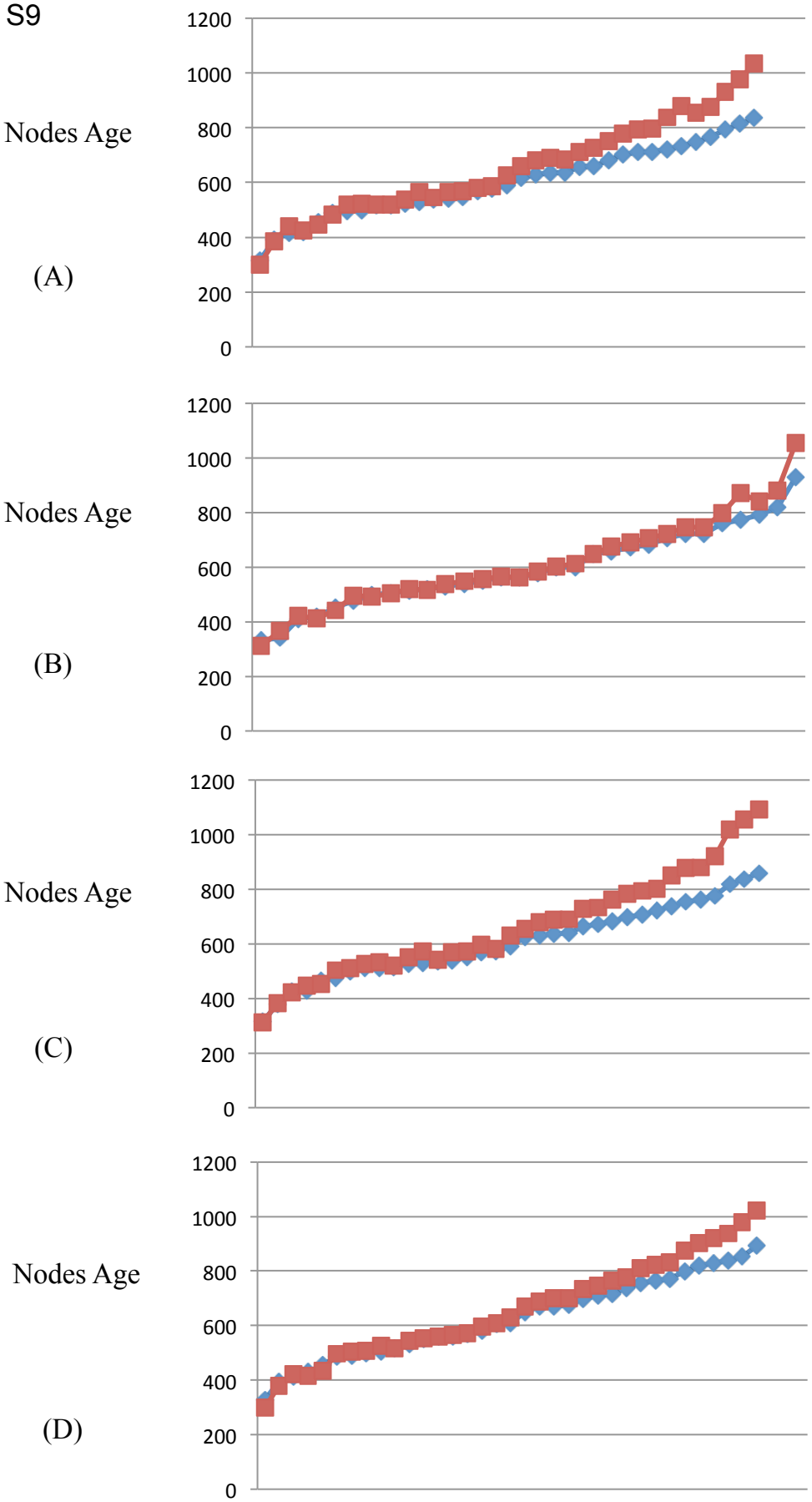
Nodes Age
1200
1000
800
600
400
200
0
(A)
Nodes Age
1200
1000
800
600
400
200
0
(B)
Nodes Age
1200
1000
800
600
400
200
0
(C)
Nodes Age
1200
1000
800
600
400
200
0
(D)

Fig. S10

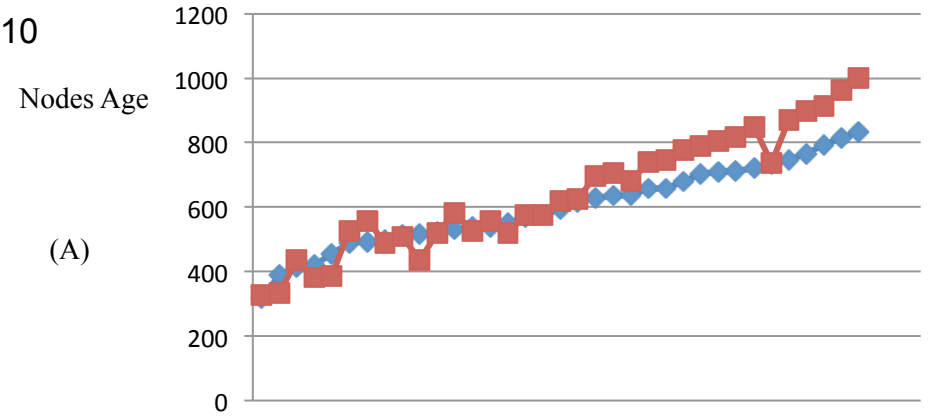
Nodes Age
1200
1000
800
600
400
200
0

(A)

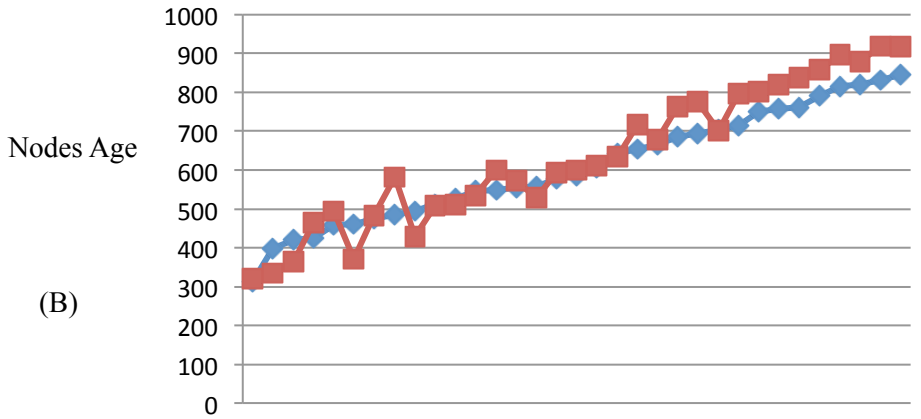
Nodes Age
1000
900
800
700
600
500
400
300
200
100
0

(B)

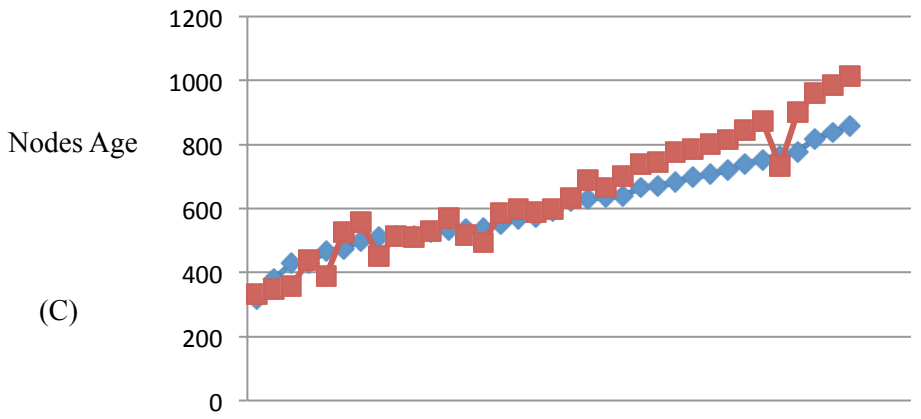
Nodes Age
1200
1000
800
600
400
200
0

(C)

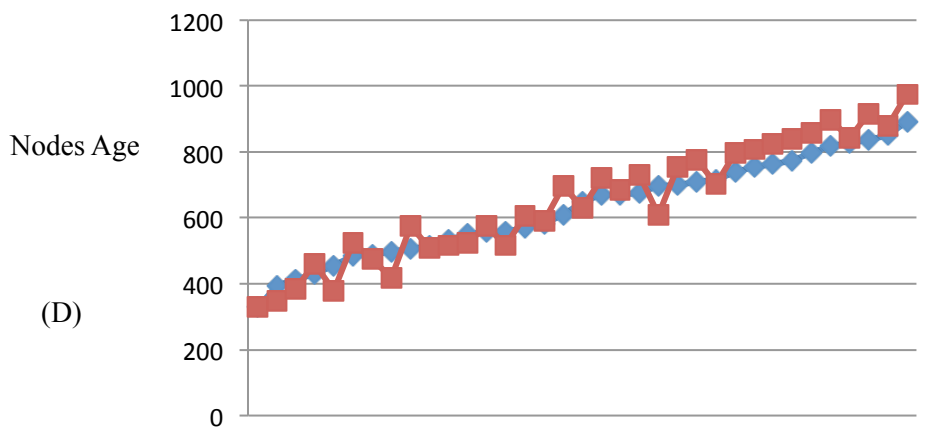
Nodes Age
1200
1000
800
600
400
200
0

(D)

Captions for Databases S1-S4

Database S1. "DatabaseS1.nex"
Combined amino acid and nucleotide alignment used for this study in Nexus format.

Database S2. "DatabaseS2.xls"
Results of the Molecular clock analyses

Database S3. mRNA nexus file "DatabaseS3.nex"
Nexus file of 131 representative transcription factors and signaling ligands from 8 metazoan taxa and two hypothetical outgroups. Note that no attempt was made to code these genes for actual metazoan near-relatives as our only goal was to highlight what had evolved before the last common ancestor of all living animal taxa. Genes were assembled from various sources and then searched in the trace archives for species of each of the phyla considered using reciprocal blast, and any resulting hits then aligned and confirmed by phylogenetic analysis using the default settings in MacVector (v. 10.0.2).

Database S4. miRNA nexus file "DatabaseS4.nex"
Nexus file of all 139 known microRNA gene families shared by at least two of the 21 analyzed metazoan taxa.

References and Notes

1. C. Darwin, *On the Origin of Species by means of Natural Selection* (John Murray, London, 1859).

2. A. H. Knoll, S. B. Carroll, Early animal evolution: Emerging views from comparative biology and geology. *Science* **284**, 2129 (1999).

3. J. W. Valentine, D. Jablonski, D. H. Erwin, Fossils, molecules and embryos: New perspectives on the Cambrian explosion. *Development* **126**, 851 (1999).

4. S. A. Bowring *et al*., Geochronologic constraints of the chronostratigraphic framework of the Neoproterozoic Huqf Supergroup, Sultanate of Oman. *Am. J. Sci.* **307**, 1097 (2007).

5. E. Landing, Precambrian-Cambrian boundary global stratotype ratified and a new perspective of Cambrian time. *Geology* **22**, 179 (1994).

6. S. Jensen, M. L. Droser, J. G. Gehling, in *Neoproterozoic Geobiology and Paleobiology,* S. Xiao, A. J. Kaufman, Eds. (Springer, Berlin, 2006), pp. 115–157.

7. A. C. Maloof *et al*., The earliest Cambrian record of animals and ocean geochemical change. *Geol. Soc. Am. Bull.* **122**, 1731 (2010).

8. A. Kouchinsky *et al*., Chronology of early Cambrian biomineralization. *Geol. Mag.* 1 (2011).

9. S. M. Porter, Closing the phosphotization window: Testing for the influence of taphonomic megabias on the pattern of small shelly fossil decline. *Palaios* **19**, 178 (2004).

10. D. H. Erwin, J. W. Valentine, J. J. Sepkoski Jr., A comparative study of diversification events: The early Paleozoic versus the Mesozoic. *Evolution* **41**, 1177 (1987).

11. G. E. Budd, S. Jensen, A critical reappraisal of the fossil record of the bilaterian phyla. *Biol. Rev. Camb. Philos. Soc.* **75**, 253 (2000).

12. B. Runnegar, A molecular-clock date for the origin of the animal phyla. *Lethaia* **15**, 199 (1982).

13. K. J. Peterson *et al*., Estimating metazoan divergence times with a molecular clock. *Proc. Natl. Acad. Sci. U.S.A.* **101**, 6536 (2004).

14. K. J. Peterson, J. A. Cotton, J. G. Gehling, D. Pisani, The Ediacaran emergence of bilaterians: Congruence between the genetic and the geological fossil records. *Philos. Trans. R. Soc. Lond. B Biol. Sci.* **363**, 1435 (2008).

15. H. Philippe *et al*., Phylogenomics revives traditional views on deep animal relationships. *Curr. Biol.* **19**, 706 (2009).

16. K. M. Halanych, The new view of animal phylogeny. *Annu. Rev. Ecol. Syst.* **35**, 229 (2004).

17. E. A. Sperling, K. J. Peterson, D. Pisani, Phylogenetic-signal dissection of nuclear housekeeping genes supports the paraphyly of sponges and the monophyly of Eumetazoa. *Mol. Biol. Evol.* **26**, 2261 (2009).

18. J. Baguñà, M. Riutort, The dawn of bilaterian animals: The case of acoelomorph flatworms. *Bioessays* **26**, 1046 (2004).

19. A. Hejnol, M. Q. Martindale, Acoel development supports a simple planula-like urbilaterian. *Philos. Trans. R. Soc. Lond. B Biol. Sci.* **363**, 1493 (2008).

20. H. Philippe *et al*., Acoelomorph flatworms are deuterostomes related to *Xenoturbella*. *Nature* **470**, 255 (2011).

21. G. D. Love *et al*., Fossil steroids record the appearance of Demospongiae during the Cryogenian period. *Nature* **457**, 718 (2009).

22. A. C. Maloof *et al*., Probable animal body-fossils from pre-Marinoan limestones, South Australia. *Nat. Geosci.* **3**, 653 (2010).

23. N. H. Putnam *et al*., Sea anemone genome reveals ancestral eumetazoan gene repertoire and genomic organization. *Science* **317**, 86 (2007).

24. A. H. Knoll, The multiple origins of complex multicellularity. *Annu. Rev. Earth Planet. Sci.* **39**, 217 (2011).

25. S. H. Xiao, Y. Zhang, A. H. Knoll, Three-dimensional preservation of algae and animal embryos in a Neoproterozoic phosphorite. *Nature* **391**, 553 (1998).

26. J. Y. Chen *et al*., Small bilaterian fossils from 40 to 55 million years before the cambrian. *Science* **305**, 218 (2004).

27. P. A. Cohen, A. H. Knoll, R. B. Kodner, Large spinose microfossils in Ediacaran rocks as resting stages of early animals. *Proc. Natl. Acad. Sci. U.S.A.* **106**, 6519 (2009).

28. J. W. Hagadorn *et al*., Cellular and subcellular structure of neoproterozoic animal embryos. *Science* **314**, 291 (2006).

29. S. H. Xiao, M. Laflamme, On the eve of animal radiation: Phylogeny, ecology and evolution of the Ediacara biota. *Trends Ecol. Evol.* **24**, 31 (2009).

30. A. Seilacher, Vendozoa: Organismic construction in the Proterozoic biosphere. *Lethaia* **22**, 229 (1989).

31. J. G. Gehling, The case for Ediacaran fossil roots to the metazoan tree. *Mem. Geol. Soc. India* **20**, 181 (1991).

32. B. M. Waggoner, The ediacaran biotas in space and time. *Integr. Comp. Biol.* **43**, 104 (2003).

33. G. M. Narbonne, Modular construction of early Ediacaran complex life forms. *Science* **305**, 1141 (2004).

34. E. A. Sperling, K. J. Peterson, M. Laflamme, Rangeomorphs, *Thectardis* (Porifera?) and dissolved organic carbon in the Ediacaran oceans. *Geobiology* **9**, 24 (2011).

35. A. M. Bush, R. K. Bambach, D. H. Erwin, in *Quantifying the Evolution of Early Life*, M. Laflamme, J. D. Schiffbauer, S. Q. Dornbos, Eds. (Springer Science, 2011), pp. 111–133.

36. S. Bengtson, Y. Zhao, Predatorial borings in late precambrian mineralized exoskeletons. *Science* **257**, 367 (1992).

37. J. E. Amthor *et al*., Extinction of *Cloudina* and *Namacalathus* at the Precambrian-Cambrian boundary in Oman. *Geology* **31**, 431 (2003).

38. G. M. Narbonne, The Ediacara Biota: Neoproterozoic origin of animals and their ecosystems. *Annu. Rev. Earth Planet. Sci.* **33**, 421 (2005).

39. A. Y. Ivantsov, New reconstruction of *Kimberella*, problematic Vendian metazoan. *Paleontol. J.* **43**, 601 (2009).

40. M. A. Fedonkin, A. Simonetta, A. Y. Ivantsov, in *The Rise and Fall of the Ediacaran Biota*, P. Vickers-Rich, P. Komarower, Eds. (Geological Society, London, 2007), pp. 157–179.

41. E. A. Sperling, J. Vinther, A placozoan affinity for *Dickinsonia* and the evolution of late Proterozoic metazoan feeding modes. *Evol. Dev.* **12**, 201 (2010).

42. A. G. Liu, D. McIlroy, M. D. Brasier, First evidence for locomotion in the Ediacara biota from the 565 Ma Mistaken Point Formation, Newfoundland. *Geology* **38**, 123 (2010). m

43. S. Jensen, M. L. Droser, J. G. Gehling, Trace fossil preservation and the early evolution of animals. *Palaeogeogr. Palaeoclimatol. Palaeoecol.* **220**, 19 (2005).

44. J. W. Valentine, D. H. Erwin, in *Development as an Evolutionary Process*, R. A. Raff, Ed. (Liss, New York, 1987).

45. J. P. Grotzinger, D. A. Fike, W. W. Fischer, Enigmatic origin of the largest-known carbon isotope excursion in Earth's history. *Nat. Geosci.* **4**, 285 (2011).

46. G. Shields-Zhou, L. Och, The case for a Neoproterozoic oxygenation event: Geochemical evidence and biological consequences. *GSA Today* **21**, 4 (2011).

47. D. A. Fike, J. P. Grotzinger, L. M. Pratt, R. E. Summons, Oxidation of the Ediacaran ocean. *Nature* **444**, 744 (2006).

48. C. Scott *et al*., Tracing the stepwise oxygenation of the Proterozoic ocean. *Nature* **452**, 456 (2008).

49. D. E. Canfield, S. W. Poulton, G. M. Narbonne, Late-Neoproterozoic deep-ocean oxygenation and the rise of animal life. *Science* **315**, 92 (2007).

50. B. Runnegar, Oxygen requirements, biology and phylogenetic significance of the late Precambrian worm *Dickinsonia*, and the evolution of burrowing habitat. *Alcheringa* **6**, 223 (1982).

51. D. H. Erwin, Early origin of the bilaterian developmental toolkit. *Philos. Trans. R. Soc. Lond. B Biol. Sci.* **364**, 2253 (2009).

52. A. Sebé-Pedrós, A. de Mendoza, B. F. Lang, B. M. Degnan, I. Ruiz-Trillo, Unexpected repertoire of metazoan transcription factors in the unicellular holozoan *Capsaspora owczarzaki*. *Mol. Biol. Evol.* **28**, 1241 (2011).

53. G. S. Richards, B. M. Degnan, The dawn of developmental signaling in the metazoa. *Cold Spring Harb. Symp. Quant. Biol.* **74**, 81 (2009).

54. M. Srivastava *et al*., The *Amphimedon queenslandica* genome and the evolution of animal complexity. *Nature* **466**, 720 (2010).

55. J. F. Ryan *et al*., The cnidarian-bilaterian ancestor possessed at least 56 homeoboxes: Evidence from the starlet sea anemone, *Nematostella vetensis*. *Genome Biol.* **7**, R64 (2006).

56. E. H. Davidson, D. H. Erwin, Gene regulatory networks and the evolution of animal body plans. *Science* **311**, 796 (2006).

57. E. H. Davidson, D. H. Erwin, An integrated view of precambrian eumetazoan evolution. *Cold Spring Harb. Symp. Quant. Biol.* **74**, 65 (2009).

58. E. H. Davidson, D. H. Erwin, Evolutionary innovation and stability in animal gene networks. *J. Exp. Zool. B Mol. Dev. Evol.* **314B**, 182 (2010).

59. E. V. Makeyev, T. Maniatis, Multilevel regulation of gene expression by microRNAs. *Science* **319**, 1789 (2008).

60. K. J. Peterson, M. R. Dietrich, M. A. McPeek, MicroRNAs and metazoan macroevolution: Insights into canalization, complexity, and the Cambrian explosion. *Bioessays* **31**, 736 (2009).

61. C. R. Marshall, J. W. Valentine, The importance of preadapted genomes in the origin of the animal bodyplans and the Cambrian explosion. *Evolution* **64**, 1189 (2010).

62. A. Kalsotra, T. A. Cooper, Functional consequences of developmentally regulated alternative splicing. *Nat. Rev. Genet.* **12**, 715 (2011).

63. D. H. Erwin, J. W. Valentine, *The Cambrian Explosion: The Construction of Animal Biodiversity* (Roberts, Greenwood, CO, 2012).

64. N. J. Butterfield, Plankton ecology and the Proterozoic-Phanerozoic transition. *Paleobiology* **23**, 247 (1997).

65. J. B. Losos, Adaptive radiation, ecological opportunity, and evolutionary determinism. American Society of Naturalists E. O. Wilson award address. *Am. Nat.* **175**, 623 (2010).

66. C. G. Jones, J. H. Lawton, M. Shachak, Positive and negative effects of organisms as physical ecosystem engineers. *Ecology* **78**, 1946 (1997).

67. J. P. Wright, C. G. Jones, The concept of organisms as ecosystem engineers ten years on: Progress, limitations, and challenges. *Bioscience* **56**, 203 (2006).

68. D. H. Erwin, Macroevolution of ecosystem engineering, niche construction and diversity. *Trends Ecol. Evol.* **23**, 304 (2008).

69. A. M. Lohrer, S. F. Thrush, M. M. Gibbs, Bioturbators enhance ecosystem function through complex biogeochemical interactions. *Nature* **431**, 1092 (2004).

70. S. Bengtson, Origins and early evolution of predation. *Paleontol. Soc. Pap.* **8**, 289 (2002).

71. O. Rota-Stabelli *et al*., A congruent solution to arthropod phylogeny: Phylogenomics, microRNAs and morphology support monophyletic Mandibulata. *Proc. R. Soc. B* **278**, 298 (2011).

72. L. I. Campbell *et al*., MicroRNAs and phylogenomics resolve the relationships of Tardigrada and suggest that velvet worms are the sister group of Arthropoda. *Proc. Natl. Acad. Sci. U.S.A.* **108**, 15920 (2011).

73. H. Szaniawski, New evidence for the protoconodont origin of chaetognaths. *Acta Palaeontol. Pol.* **47**, 409 (2002).

74. J. J. Sepkoski Jr., *A Compendium of Fossil Marine Animal Families* (Milwaukee Public Museum Contributions in Biology and Geology, ed. 2, 1992), vol. 83, pp. 1–156.

75. J. J. Sepkoski Jr., A compendium of fossil marine animal genera. *Bull. Am. Paleontol.* **363**, 1 (2002).

76. G. X. Li *et al*., Early Cambrian metazoan fossil record of South China: Generic diversity and radiation patterns. *Palaeogeogr. Palaeoclimatol. Palaeoecol.* **254**, 229 (2007).

77. L. E. Babcock, S. C. Peng, Cambrian chronostratigraphy: Current state and future plans. *Palaeogeogr. Palaeoclimatol. Palaeoecol.* **254**, 62 (2007).

78. M. Y. Zhu, L. E. Babcock, S. C. Peng, Advances in Cambrian stratigraphy and paleontology: Integrating correlation techniques, paleobiology, taphonomy and paleoenvironmental reconstruction. *Paleoworld* **15**, 217 (2006).

79. G. D. Edgecombe, Arthropod phylogeny: an overview from the perspectives of morphology, molecular data and the fossil record. *Arthropod Struct. Dev.* **39**, 74 (2010).

80. E. A. Sperling, D. Pisani, K. J. Peterson, Molecular paleobiological insights into the origin of the Brachiopoda. *Evol. Dev.* **13**, 290 (2011).

81. J. Mallatt, C. W. Craig, M. J. Yoder, Nearly complete rRNA genes assembled from across the metazoan animals: Effects of more taxa, a structure-based alignment, and paired-sites evolutionary models on phylogeny reconstruction. *Mol. Phylogenet. Evol.* **55**, 1 (2010).

82. E. A. Sperling, D. Pisani, K. J. Peterson, in *The Rise and Fall of the Ediacaran Biota*, P. Vickers-Rich, P. Komarower, Eds. (Geological Society, London, Special Publications, 2007), vol. 286, pp. 355–368.

83. F. Ronquist, J. P. Huelsenbeck, MrBayes 3: Bayesian phylogenetic inference under mixed models. *Bioinformatics* **19**, 1572 (2003).

84. http://mrbayes.csit.fsu.edu/wiki/index.php/Main_Page

85. H. Philippe *et al*., Resolving difficult phylogenetic questions: Why more sequences are not enough. *PLoS Biol.* **9**, e1000602 (2011).

86. E. A. Sperling, J. M. Robinson, D. Pisani, K. J. Peterson, Where's the glass? Biomarkers, molecular clocks, and microRNAs suggest a 200-Myr missing Precambrian fossil record of siliceous sponge spicules. *Geobiology* **8**, 24 (2010).

87. K. S. Pick *et al*., Improved phylogenomic taxon sampling noticeably affects nonbilaterian relationships. *Mol. Biol. Evol.* **27**, 1983 (2010).

88. N. Lartillot, T. Lepage, S. Blanquart, PhyloBayes 3: A Bayesian software package for phylogenetic reconstruction and molecular dating. *Bioinformatics* **25**, 2286 (2009).

89. T. Lepage, D. Bryant, H. Philippe, N. Lartillot, A general comparison of relaxed molecular clock models. *Mol. Biol. Evol.* **24**, 2669 (2007).

90. A. J. Drummond, S. Y. W. Ho, M. J. Phillips, A. Rambaut, Relaxed phylogenetics and dating with confidence. *PLoS Biol.* **4**, e88 (2006).

91. J. Inoue, P. C. Donoghue, Z. Yang, The impact of the representation of fossil calibrations on Bayesian estimation of species divergence times. *Syst. Biol.* **59**, 74 (2010).

92. A. Seilacher, Vendobionta and Psammocorallia: Lost constructions of Precambrian evolution. *J. Geol. Soc. London* **149**, 607 (1992).

93. M. Laflamme, G. M. Narbonne, Ediacaran Fronds. *Palaeogeogr. Palaeoclimatol. Palaeoecol.* **258**, 162 (2008).

94. M. A. Fedonkin *et al*., *The Rise of Animals: Evolution and Diversification of the Kingdom Animalia* (John Hopkins Press, Baltimore, 2007).

95. B. Shen, L. Dong, S. Xiao, M. Kowalewski, The Avalon explosion: Evolution of Ediacara morphospace. *Science* **319**, 81 (2008).

96. H. J. Hofmann, S. J. O'Brien, A. F. King, Ediacaran biota on Bonavista Peninsula, Newfoundland, Canada. *J. Paleontol.* **82**, 1 (2008).

97. D. V. Grazhdankin, Patterns of distribution in the Ediacaran biotas: Facies versus biogeography and evolution. *Paleobiology* **30**, 203 (2004).

98. R. Richter, Die ältesten Fossilien Sud-Afrikas. *Senckenberg lethaea* **36**, 243 (1955).

99. H. D. Pflug, Systematik der jung-präikambrischen Petalonamae. *Paläontologische Zeitschrift* **46**, 56 (1970).

100. M. F. Glaessner, in W. A. Berggren *et al*., *Introduction, Fossilization (taphonomy) Biogeography and Biostratigraphy*, Part A of R. C. Moore, Ed., *Treatise on Invertebrate Paleontology* (Geological Society of America, New York, and University of Kansas, Lawrence, 1979).

101. M. A. Fedonkin, in *The Vendian System*, vol. 1., *Paleontology*, B. S. Sokolov, A. B. Iwanowski, Eds. (Springer, New York, 1990), pp. 7–120, 132–137.

102. J. Reitner, G. Worheide, in *Systema Porifera: A Guide to the Classification of Sponges*, J. N. A. Hooper, R. W. M. Van Soest, Eds. (Kluwer Academic/Plenum, New York, 2002), pp. 52–68.

103. J. Reitner, Coralline spongien: Der versuch einer phylogenetisch-taxonomischen analyse. *Berl. Geowiss. Abh. Reihe E (Paläobiol.)* **1**, 1 (1992).

104. A. Kouchinsky, S. Bengtson, W. Feng, R. Kutygin, A. Val'kov, The Lower Cambrian fossil anabaritids: Affinities, ocurrences and systematics. *J. Syst. Palaeontology* **7**, 241 (2009).

105. P. Cartwright *et al*., Exceptionally preserved jellyfishes from the Middle Cambrian. *PLoS ONE* **2**, e1121 (2007).

106. K. Swadling, H. J. G. Dartnall, J. A. E. Gibson, É. Saulnier-Talbot, W. F. Vincent, Fossil rotifers and the early colonization of an Antarctic lake. *Quat. Res.* **55**, 380 (2001).

107. B. M. Waggoner, G. O. Poinar, Jr., Fossil habrotrochid rotifers in Dominican amber. *Cell. Mol. Life Sci.* **49**, 354 (1993).

108. J. A. Todd, P. D. Taylor, The first fossil entoproct. *Naturwissenschaften* **79**, 311 (1992).

109. E. Landing, P. M. Myrow, A. P. Benus, G. M. Narbonne, The Placentian series: Appearance of the oldest skeletalized faunas in southeastern Newfoundland. *J. Paleontol.* **63**, 739 (1989).

110. C. B. Skovsted, G. A. Brock, J. R. Paterson, L. E. Holmer, G. E. Budd, The scleritome of *Eccentrotheca* from the Lower Cambrian of South Australia: Lophophorate affinities and implications for tommotid phylogeny. *Geology* **36**, 171 (2008).

111. C. B. Skovsted, U. Balthasar, G. A. Brock, J. R. Paterson, The tommotiid Camenella reticulosa from the early Cambrian of South Australia: Morphology, scleritome reconstruction, and phylogeny. *Acta Palaeontol. Pol.* **54**, 525 (2009).

112. L. E. Holmer, L. E. Popov, in *Treatise on Invertebrate Paleontology*, Part H, *Brachiopoda, Revised*, A. Williams, S. J. Carlson, C. H. C. Brunton, Eds. (Geological Society of America, Univ. of Kansas, Boulder, Lawrence, 2007), pp. 2580–2590.

113. L. E. Holmer, S. P. Stolk, C. B. Skovsted, U. Balthasar, L. Popov, The enigmatic Early Cambrian *Salanygolina*–a stem group of rhynchonelliform chileate brachiopods? *Palaeontology* **52**, 1 (2009).

114. E. Landing, A. English, J. D. Keppie, Cambrian origin of all skeletonized metazoan phyla–discovery of Earth's oldest bryozoans (Upper Cambrian, southern Mexico). *Geology* **38**, 547 (2010).

115. J. B. Caron, A. Scheltema, C. Schander, D. Rudkin, A soft-bodied mollusc with radula from the Middle Cambrian Burgess Shale. *Nature* **442**, 159 (2006).

116. J. D. Sigwart, M. D. Sutton, Deep molluscan phylogeny: Synthesis of palaeontological and neontological data. *Philos. Trans. R. Soc. Lond. B Biol. Sci.* **274**, 2413 (2007).

117. M. D. Sutton, D. E. G. Briggs, D. J. Siveter, D. J. Siveter, Computer reconstruction and analysis of the vermiform mollusc *Acaenoplax hayae* from the Herefordshire Lagerstätte (Silurian, England), and implications for molluscan phylogeny. *Palaeontology* **47**, 293 (2004).

118. M. R. Smith, J. B. Caron, Primitive soft-bodied cephalopods from the Cambrian. *Nature* **465**, 469 (2010).

119. H. Mutvei, Y.-B. Zhang, E. Dunca, Late Cambrian plectronocerid nautiloids and their role in cephalopod evolution. *Palaeontology* **50**, 1327 (2007).

120. V. V. Missarzhevsky, The oldest skeletal fossils and stratigraphy of the Precambrian-Cambrian boundary beds. *Trans. Geol. Inst. Russ. Acad. Sci.* **443**, 1 (1989).

121. M. D. Brasier, G. Shields, V. N. Kuleshov, E. A. Zhegallo, Integrated chemo- and biostratigraphic calibration of early animal evolution: Neoproterozoic-early Cambrian of southwest Mongolia. *Geol. Mag.* **133**, 445 (1996).

122. D.-Y. Huang, J.-Y. Chen, J. Vannier, J. I. Saiz Salinas, Early Cambrian sipunculan worms from southwest China. *Philos. Trans. R. Soc. Lond. B Biol. Sci.* **271**, 1671 (2004).

123. J. Vinther, P. Van Roy, D. E. G. Briggs, Machaeridians are Palaeozoic armoured annelids. *Nature* **451**, 185 (2008).

124. S. Conway Morris, J. S. Peel, New palaeoscolecidan worms from the Lower Cambrian: Sirius Passet, Latham Shale and Kinzers Shale. *Acta Palaeontol. Pol.* **55**, 141 (2010).

125. D. Jones, I. Thompson, Echiura from the Pennsylvanian Essex Fauna of northern Illinois. *Lethaia* **10**, 317 (1977).

126. J. Warn, Presumed Myzostomid infestation of an Ordovician crinoid. *J. Paleontol.* **48**, 506 (1974).

127. M. A. Wills, in *The Fossil Record 2*, M. J. Benton, Ed. (Chapman and Hall, London, 1993), chap. 15, p. 271.

128. I.-M. Jansson, S. McLoughlin, V. Vadja, Early Jurassic annelid cocoons from eastern Australia. *Alcheringa* **32**, 285 (2008).

129. F. D. Schram, Pseudocoelomates and a nemertine from the Illinois Pennsylvanian. *J. Paleontol.* **47**, 985 (1973).

130. J. S. Peel, A corset-like fossil from the Cambrian Sirius Passet Lagerstatte of North Greenland and its implications for cycloneuralian evolution. *J. Paleontol.* **84**, 332 (2010).

131. G. O. Poinar, Jr., A. Acra, F. Acra, Earliest fossil nematode (Mermithidae) in Cretaceous Lebanese amber. *Fundam. Appl. Nematol.* **17**, 475 (1994).

132. J.-Y. Chen, G.-Q. Zhou, Biology of the Chengjiang fauna. *Bull. Nat. Mus. Nat. Sci.* **10**, 11 (1997).

133. K. J. Müller, D. Walossek, A. Zakharov, 'Orsten' type phosphatized softintegument preservation and a new record from the Middle Cambrian Kuonamka Formation in Siberia. *N. Jb. Geol. Palaeontol. Abh.* **191**, 101 (1995).

134. R. Bertolani, D. Grimaldi, in *Studies on Fossils in Amber, with Particular Reference to the Cretaceous of New Jersey*, D. Grimaldi, Ed. (Backhuys, Leiden, 2000), pp. 103–110.

135. X. G. Hou, J. Bergstrom, Arthropods of the Lower Cambrian Chengjiang fauna, Southwest China. *Fossils Strata* **45**, 116 (1997).

136. A. C. Daley, J. S. Peel, A possible anomalocaridid from the Cambrian Sirius Passet Lagerstatte, North Greenland. *J. Paleontol.* **84**, 352 (2010).

137. X. L. Zhang, D. G. Shu, A new arthropod from the Chengjiang lagerstatte, Early Cambrian, southern China. *Alcheringa* **29**, 185 (2005).

138. J. A. Dunlop, P. A. Selden, in *Arthropod Relationships, Systematics Association Special Volume 55*, R. A. Fortey, R. Thomas, Eds. (Chapman and Hall, London, 1998), pp. 221–235.

139. D. Waloszek, J. A. Dunlop, A larval sea spider (Arthropoda: Pycnogonida) from the Upper Cambrian 'Orsten' of Sweden, and the phylogenetic position of pycnogonids. *Palaeontology* **45**, 421 (2002).

140. J. Chen, D. Waloszek, A. Maas, A new 'great appendage' arthropod from the Lower Cambrian of China and homology of chelicerate chelicerae and raptorial antero-ventral appendages. *Lethaia* **37**, 3 (2004).

141. P. Van Roy *et al*., Ordovician faunas of Burgess Shale type. *Nature* **465**, 215 (2010).

142. S. Hu *et al*., Diverse pelagic predators from the Chengjiang Lagerstatte and the establishment of modern-style pelagic ecosystems in the early Cambrian. *Palaeogeogr. Palaeoclimatol. Palaeoecol.* **254**, 307 (2007).

143. J. Vannier *et al*., The Early Cambrian origin of the thylacocephalan arthropods. *Acta Palaeontol. Pol.* **51**, 201 (2006).

144. X. G. Hou *et al*., Soft-part anatomy of the Early Cambrian bivalved arthropods *Kunyangella* and *Kunmingella*: Significance for the phylogenetic relationships of Bradoriida. *Philos. Trans. R. Soc. Lond. B Biol. Sci.* **277**, 1835 (2010).

145. D. Waloszek, K. J. Muller, Upper Cambrian stem-lineage crustaceans and their bearing upon the monophyletic origin of Crustacea and the position of Agnostus. *Lethaia* **23**, 409 (1990).

146. X.-G. Hou, J. Bergstrom, G.-H. Hu, The Lower Cambrian crustacean *Pectocaris* from the Chengjiang Biota, Yunnan, China. *J. Paleontol.* **78**, 700 (2004).

147. X. G. Zhang, D. J. Siveter, D. Waloszek, A. Maas, An epipodite-bearing crown-group crustacean from the Lower Cambrian. *Nature* **449**, 595 (2007).

148. H. K. Brooks, A crustacean from the Tesnus Formation (Pennsylvanian) of Texas. *J. Paleontol.* **29**, 852 (1955).

149. D. Walossek, The Upper Cambrian *Rehbachiella*, its larval development, morphology and significance for the phylogeny of Branchiopoda and Crustacea. *Hydrobiologia* **298**, 1 (1995).

150. D. Walossek, J. Repetski, K. J. Muller, An exceptionally preserved parasitic arthropod, *Heymonsicambria taylori* n. sp. (Arthropoda incertae cedis: Pentastomida), from Cambrian-Ordovician boundary beds of Newfoundland, Canada. *Can. J. Earth Sci.* **31**, 1664 (1994).

151. M. Williams *et al*., The earliest ostracodes: The geological evidence. *Palaeobiodivers. Palaeoenviron.* **88**, 11 (2008).

152. S. R. Fayers, N. H. Trewin, A hexapod from the Early Devonian Windyfield Chert, Rhynie, Scotland. *Palaeontology* **48**, 1117 (2005).

153. P. Greenslade, P. E. S. Whalley, in: *Second International Seminar on Apterygota*, R. Dallai, ed. (University of Siena, Siena, 1986), pp. 319-323.

154. R. J. Aldridge, H. O. U. Xian-Guang, D. A. V. I. D. J. Siveter, D. E. R. E. K. J. Siveter, S. A. R. A. H. E. Gabbott, The systematics and phylogenetic relationships of vetulicolians. *Palaeontology* **50**, 131 (2007).

155. J. B. Caron, *Banfifia constricta*, a putative vetulicolid from the Middle Cambrian Burgess Shale. *Trans. R. Soc. Edinb. Earth Sci.* **96**, 95 (2005).

156. M. Zhu, Y. Zhao, J. Chen, Revision of the Cambrian discoidal animals *Stellostomites eumorphus* and *Pararotadiscus guizhouensis* from South China. *Geobios* **35**, 165 (2002).

157. J. B. Caron, S. Conway Morris, D. Shu, Tentaculate fossils from the Cambrian of Canada (British Columbia) and China (Yunnan) interpreted as primitive deuterostomes. *PLoS ONE* **5**, e9586 (2010).

158. X. G. Hou *et al*., An early Cambrian hemichordate zooid. *Curr. Biol.* **21**, 612 (2011).

159. P. Arduini, G. Pinna, G. Teruzzi, *Megaderaion sinemuriense* n.g. n.sp., a new fossil enteropneust of the Sinemurian of Osteno in Lombardy. *Atti Soc. It. Sci. Nat. Museo Milano* **122**, 462 (1981).

160. S. Zamora, Middle Cambrian echinoderms from north Spain show echinoderms diversified earlier in Gondwana. *Geology* **38**, 507 (2010).

161. I. A. Rahman, S. Zamora, The oldest cinctan carpoid (stem-group Echinodermata), and the evolution of the water vascular system. *Zool. J. Linn. Soc.* **157**, 420 (2009).

162. J.-Y. Chen *et al*., The first tunicate from the Early Cambrian of South China. *Proc. Natl. Acad. Sci. U.S.A.* **100**, 8314 (2003).

163. D. G. Shu, S. C. Morris, X. L. Zhang, A *Pikaia*-like chordate from the Lower Cambrian of China. *Nature* **384**, 157 (1996).

164. X.-G. Zhang, X.-G. Hou, Evidence for a single median fin-fold and tail in the Lower Cambrian vertebrate, *Haikouichthys ercaicunensis*. *J. Evol. Biol.* **17**, 1162 (2004).

165. M. P. Smith, I. J. Sansom, K. D. Cochrane, in *Major Events in Early vertebrate Evolution—Palaeontology, Phylogeny, Genetics, and Development*, P. E. Ahlberg, Ed. (Systematics Association Special Volume, London, 2001), vol. 61, pp. 67–84.

166. E. Gazave *et al*., No longer Demospongiae: Homoscleromorpha formal nomination as a fourth class of Porifera. *Hydrobiologia* (2011).

167. M. T. Neiber *et al*.; Global Biodiversity and Phylogenetic Evaluation of Remipedia, Global biodiversity and phylogenetic evaluation of remipedia (crustacea). *PLoS ONE* **6**, e19627 (2011).

168. M. J. Benton, P. C. J. Donoghue, Paleontological evidence to date the tree of life. *Mol. Biol. Evol.* **24**, 26 (2007).

169. A. C. Maloof *et al*., Constraints on early Cambrian carbon cycling from the duration of the Nemakit-Daldynian-Tommotian boundary Delta 13C shift, Morocco. *Geology* **38**, 623 (2010).